2005

Spray Cooling For Land, Sea, Air And Space Based Applications, A Fluid Managment System For Multiple Nozzle Spray Cooling And A Guide To High Heat Flux Heater Design

Brian Glassman
University of Central Florida

SPRAY COOLING FOR LAND, SEA, AIR AND SPACE BASED APPLICATIONS, A FLUID MANAGEMENT SYSTEM FOR MULTIPLE NOZZLE SPRAY COOLING AND A GUIDE TO HIGH HEAT FLUX HEATER DESIGN

By

BRIAN SCOTT GLASSMAN
B.S. Florida Institute of Technology, 2001
Melbourne Florida U.S.A

A thesis submitted in partial fulfillment of the requirements
for the degree of Master of Science
in the Department of Mechanical Material and Aerospace Engineering
in the College of Engineering and Computer Science
at the University of Central Florida
Orlando, Florida

Spring Term
2005

ABSTRACT

This thesis is divided into four distinct chapters all linked by the topic of spray cooling. Chapter one gives a detailed categorization of future and current spray cooling applications, and reviews the major advantages and disadvantages that spray cooling has over other high heat flux cooling techniques.

Chapter two outlines the developmental goals of spray cooling, which are to *increase the output of a current system* and to *enable new technologies to be technically feasible*. Furthermore, this chapter outlines in detail the impact that land, air, sea, and space environments have on the cooling system and what technologies could be enabled in each environment with the aid of spray cooling. In particular, the heat exchanger, condenser and radiator are analyzed in their corresponding environments.

Chapter three presents an experimental investigation of a fluid management system for a large area multiple nozzle spray cooler. A fluid management or suction system was used to control the liquid film layer thickness needed for effective heat transfer. An array of sixteen pressure atomized spray nozzles along with an imbedded fluid suction system was constructed. Two surfaces were spray tested one being a clear grooved Plexiglas plate used for visualization and the other being a bottom heated grooved 4.5 x 4.5 cm^2 copper plate used to determine the heat flux. The suction system utilized an array of thin copper tubes to extract excess liquid from the cooled surface. Pure water was ejected from two spray nozzle configurations at flow rates of 0.7 L/min to 1 L/min per nozzle. It was found that the fluid management system provided fluid removal efficiencies of 98% with a 4-nozzle array, and 90% with the full 16-nozzle array for the downward spraying orientation. The corresponding heat fluxes for the 16 nozzle

configuration were found with and without the aid of the fluid management system. It was found that the fluid management system increased heat fluxes on the average of 30 W/cm^2 at similar values of superheat. Unfortunately, the effectiveness of this array at removing heat at full levels of suction is approximately 50% & 40% of a single nozzle at respective 10°C & 15°C values of superheat. The heat transfer data more closely resembled convective pooling boiling. Thus, it was concluded that the poor heat transfer was due to flooding occurring which made the heat transfer mechanism mainly forced convective boiling and not spray cooling.

Finally, Chapter four gives a detailed guide for the design and construction of a high heat flux heater for experimental uses where accurate measurements of surface temperatures and heat fluxes are extremely important. The heater designs presented allow for different testing applications; however, an emphasis is placed on heaters designed for use with spray cooling.

I dedicate my thesis to my mother and father, Linda and Andy whose patience, nurturing and regard for education held me on a steady course. I want to thank my sister Stephanie whose antics always kept me thinking of ways to outsmart her. I also want to thank my Grandmother Irene and Grandma Sally for their unconditional love and emotional support. I want to acknowledge my Aunt Nancy for her wise encouragement and advice. Finally, I want to remember my Poppa Frank whose love and enthusiasm for engineering was passed down to me with unending patience at his basement workbench.

ACKNOWLEDGMENTS

I would first like to thank my advisor, Dr. Louis Chow, for his exceptional mentorship and his boundless dedication to his graduate students. Much of the research done in this thesis would not have occurred if it was not for the exposure he has given me in his field of expertise. Dr. Chow also inspired me to surpass the normal amount of work required for a master's thesis. I hope that the extra material presented here would be beneficial to the future development of high heat flux cooling systems and their possible applications.

This research was sponsored by the Propulsion Directorate of the Air Force Research Laboratory (AFRL), Wright Patterson Air Force Base, Ohio. I wish to thank Dr. Kirk Yerkes and Mr. Brian Donovan of AFRL, Huseyin Bostanci of RTI and my friend Rodolfo Hutchinson for their advice and help associated with this research.

TABLE OF CONTENTS

LIST OF FIGURES

LIST OF TABLES

LIST OF SYMBOLS AND NOMENCALTURE

1D	One Dimensional
AC	Alternating Current
A_{out}	Outside Area of the Heater (cm^2)
A_h	Top Pedestal Heater Area (cm^2)
atm	Atmospheric Pressure (atm)
D	Diameter of Heater Cartridge (in)
E_{in}	Electrical Input (W)
$E_{in\_electrical}$	Electrical Energy Input (W)
Eff_{suc}	Effectiveness of Suction System
E_{cooled}	Energy Absorbed by Spray Cooling (W)
E_{loss}	Energy Loss to the Shell of the Heater (W)
k	Thermal Conductivity (W/m-K)
k_{inter}	Interpolated Value of Thermal Conductivity (W/cm-K)
HEDS	Human Exploration & Development of Space Project
HEL	High Energy Laser
HVAC	Heating Ventilation & Air Conditioning
I	Amperage
ITO	Indium Tin Oxide Heater
in-Hg	Pressure, Inches of Mercury, (0.491 Psi)
L	Length of Heater Cartridge (in)
min	Minutes
PID	Proportional Integral Derivative Controller

Psi	Pressure (lbs/in^2)
q''	Heat Flux (W/cm^2)
$\dot{Q}_{cooling}$	Heat Flux due to Cooling (W/cm^2)
$\dot{Q}_{Loss}$	Heat flux due to Losses in the System (W/cm^2)
R	Electrical Resistance (Ohms)
SCFB	Subcooled Flow Boiling
SBL	Space Based Laser
T^*	Up Stream Temperature (°C)
T_s	Radiator Surface Temperature (°C)
T_w	Cooled Surface Temperature (°C)
T.C.	Thermocouple
$T_{b1\text{-}b3}$	T.C. Temperature Differences of Right Side 1-3 (°C)
$T_{1\text{-}3}$	T.C. Temperature Differences of Left Side 1-3 (°C)
TES	Thermal Energy Storage
TFR	Thick Film Resistors
V	Voltage (V)
W	Power (Watts)
X	Distance (cm)
$X_{1\text{-}2}$	Distance Between T.C.1 and T.C. 2 (10.16mm)
$X_{1\text{-}3}$	Distance Between T.C.1 and T.C. 3 (17.78mm)
$X_{2\text{-}3}$	Distance Between T.C.2 and T.C. 3 (7.62 mm)
$X_{1\text{-}w}$	Distance T.C. is from the Cooled Surface (6.08 mm)

$\dot{V}olume_{edges}$	Volume Flow Rate Over the Edges of the Spray Cooler (L/min)
Ω	Resistance, (Ohms)
ρ	Density (kg/m^3)
ρ^*	Up Stream Density (kg/m3)
ε	Emissivity
σ	Stefan-Boltzmann constant ($5.67E^{-4}$ $W/cm^2\text{-}K^4$)
ΔT	Temp. Difference between Ambient Air and the Rejection Equipment

1. CATERGORIZATION AND BENEFITS OF SPRAY COOLING

1.1 Introduction to Chapter

Chapter one of this masters' thesis provides a categorization for all current and future spray cooling applications and additionally gives short examples from each category. It also gives a quick overview of other cooling technologies and then compares the advantages & disadvantages of spray cooling to other high heat flux cooling technologies, in particular subcooled flow boiling. Finally, this chapter closes by presenting some odd applications of spray cooling.

1.2 Categorization of Spray Cooling

Spray cooling is a term that is used very loosely and applies to many different types of applications ranging from the medical, industrial, agricultural, electronics and HVAC industries. In doing this categorization the author hopes to reduce the ambiguity about current applications for spray cooling by showing how they relate to one another.

Spray cooling can be broken down into two very general categories; that of cooling a gas, to lower the temperature of that gas, or that of spray cooling an object to remove heat from it. The first involves spraying a mist of liquid, usually water, into a stream of gas, usually air. If the gas is of a sufficient temperature, the mist of liquid will then evaporate taking heat away from that gas; consequently dropping its temperature. This process is commonly used in HVAC systems as well as other industrial processes,

involving regulation of a gases temperature. Spray cooling of gasses is not the focus of this thesis, therefore will not be considered further.

The second category of spray cooling is that of removing heat from an object or surface and can be further divided into two the subcategories: cooling applications with surface temperatures *above* Leidenfrost point of the coolant and ones with surface temperatures *below* the Leidenfrost point of the coolant.

The *Leidenfrost point* is defined as the minimum temperature of a surface at which a respective liquid will fully form a vapor film, insulating that liquid from the surface. At one atmosphere the Leidenfrost point for water is 250°C [1]. This can simply be observed for water as the minimum temperature for a surface for which a droplet, if placed on the surface, will then bead up and dance around [1].

Applications for spray cooling surfaces *above* the coolant's *Leidenfrost point* are mostly materials processing, more specifically metal quenching and material tempering [2]. Spray cooling in these applications is primarily comprised of open loop system. These spray cooling systems are applied to areas on the order of many square meters and main goal is to temper the metal being processed by cooling it at a specific rate. Specific spray nozzles have been designed for this purpose by companies such as Spray Systems Co. of Wheaton, Illinois. The main reason these applications are open loop is that large amounts of vapor are created. Consequently, it is much more economical to allow those vapors to escape to the atmosphere than to operate a system to recondense these vapors back into liquid. Spray cooling *above* the coolants Leidenfrost point is not the focus of this thesis and will not be considered further.

Applications for spray cooling *below* the coolant's Leidenfrost point are the main focus of the author's research and application for this will be elaborated on in chapter 2. *Note*: Spray cooling would be called forced liquid convection if the cooled surface temperature was not above the boiling point of the sprayed liquid. Thus to take advantage of spray cooling the target application must have a surface temperatures above the boiling point of that fluid. Fortunately, the boiling point of the fluid can be adjusted by operating at different system pressures [3].

1.3 Cooling Systems Quick Overview

Simply the definition of spray cooling can be defined as the follows: *Spray cooling is a phase change method of cooling that utilizes a spray of liquid on the cooled surface to greatly increase effectiveness of heat transfer* [4]. Spray cooling is not the only cooling technique but it is one well suited to cooling with extremely high heat fluxes. Heat flux is defined as: *The amount of heat energy per unit time passing through a given area.* To give some perspective on heat flux table 1 was created. *Disclaimer:* The values in table 1 are to be taken as rough estimates. Furthermore, some of these values have no unrestricted publication to back them, however the author knows through his reading and interactions with military personnel that the given heat fluxes are possible.

Table 1: Heat Flux Comparison for Cooling Technology as of 2003

Name	Heat Flux (W/cm2)	Name	Heat Flux (W/cm2)
Sun Light on Earth	0.14	Cray Super Computer CPU	70 - 120
Light Bulb (40-100W)	1	Acetylene Torch	100
Burn a Person in one Second	5	Aircraft Electronics	150
Propane Torch	10	Slab Lasers	>50
Nuclear Reactor	10 -70	High Power Laser Diodes	<400
Car Engine	30-60	High Power Microwave	<700
Intel Pentium 4 CPU	15 -30	Power Converters IGBT, MOSFETs	<900
Shuttle Re-Entry	<60	Surface of the Sun	6,500

There are many different types of cooling systems available in the market today. When selecting a cooling system factors such as: maximum heat flux, heat loads, temperature requirements, reliability, power consumption, complexity, maturity of the technology, operational environments, and cost must be full considered for each particular application. This in itself may be a difficult task and depended upon the restriction set on the cooling system.

Table 2 shows comparative cooling technology's heat fluxes and heat transfer coefficients. The author would like to mention, *that table 2 is meant as an rough reference* for these cooling technologies and that there may be particular publications that list values outside of what are listed on the table.

Table 2: Cooling Techniques and Respective Heat Fluxes and Heat Transfer Coefficients

Mechanism	Name of Cooling Technology or Method	Heater Transfer Coefficient ($W/cm^2 K$)	Highest Recorded Heat Flux (W/cm^2)	Reference
Single Phase	Free Air Convection Finned Heat sink	0.005 -0.05	15	[5] [1]
Single Phase	Forced Air Convection (*Heat Sink with a Fan*)	0.001 - 0.01	40	[5] [1]
Single Phase	Natural Convection with FC's (*single phase*)	0.05-0.08	>80	[5] [1]
Single Phase	Natural Convection with water (single phase)	0.08-0.1	5-90	[1]
Two Phase	Heat Pipes			
Single Phase	Microchannel		1000	
Electrical	Peliter Coolers	-NA-	70	
Electrical	Quantum Tunnel Cooling	-NA-	200	
Two Phase	Subcooled Flow	2	120	
Two / One Phase	Subcooled Flow Boiling			
Two Phase	Microchannel Boiling	10-20		
Two Phase	Spray Cooling	20-40	1200	[6]
Two Phase	Two Phase Jet Impingement	20	1000	

From table 2 one can see that spray cooling has a very high associated heat transfer coefficient and heat flux. This put spray cooling in the category of a "high heat flux cooling systems." As for low heat flux applications, it mostly does not make sense to select a spray cooling system. This mainly is due to the myriad of cheaper, more established, less complex, and more reliable lower heat flux cooling systems already on the market [7]. None the less, spray cooling must compete with other high heat flux cooling technologies. Subcooled flow boiling (SCFB) on table 2 is listed as both a two and one phase cooling technique. To clarify, SCFB utilizes boiling to generate vapor

which greatly increase transfer heat but then the vapor quickly condense in the subcooled bulk coolant. Thus the heat rejection equipment is a single phase heat exchanger.

1.4 Advantages and Disadvantages of Spray Cooling

From tables 2 one can see that spray cooling has very high heat fluxes when compared to other cooling technologies. Only jet impingement, microchannel cooling and subcooled flow boiling (SCFB) can achieve similar heat fluxes. Nevertheless, spray cooling has a few major advantages over many of the other high heat flux cooling techniques. The first major advantage that spray cooling will allow for is a uniform temperature across the cooled surface, i.e. isothermal. *Isothermal surfaces* enable many cooling application to operate very effectively, for example this was demonstrated for a laser diodes array by M.R. Pais in 1994 [8] [9]. To date, large area isothermal spray cooling has not been proven in a spray cooling publication for square surface areas larger than 5cm by 5cm. Despite the lack of publications, the author knows of companies such as Rini Technologies of Orlando Florida which have currently proven the isothermal operation of spray cooling on large areas.

The second advantage spray cooling has over other high heat flux cooling techniques is that of its *lower associated flow rates*. Flow rates have a direct impact on closed loop system components, mainly on the sizes of the pumps and the associated tubing. In small scale cooling application, ones with low heat loads, the differences in pump size between SCFB, microchannel cooling and spray cooling can be ignored. Take for example a cooling system with a heat load of 250W; SCFB in this case would require a flow rate of 0.048 gallons/min with a 20°C coolant temperature rise; whereas, spray cooling, would require 0.008 gallons/min. The difference in pump size between the two

flowrates is neglectable, thus flowrates only make a minor impact on systems size at *low heat loads*.

Conversely at high heat loads, such as *2.5MW*, SCFB operating with a rejection difference of ΔT of 20°C would require 475 gallons/min; whereas, spray cooling would require 80 gallons/min. Here, the differences in pump sizes at such a high flowrates make an immense impact on overall cooling system size, weight, and power requirements. *Note: Appendix C shows the supporting calculation for both the low and high heat load examples.*

The final large advantage spray cooling has over other high heat flux cooling techniques is that of a higher heat rejection temperature. Closed loop spray cooling systems' utilize a condenser to reject heat; whereas, single phase jet impingement, single phase microchannel and SCFB utilizes a heat exchanger. The normal advantages of using a condenser in cooling system instead of an exchangers, is that of the condenser having a smaller associated size due to its higher heat rejection temperatures.

Take for example two cooling systems, one being a SCFB system operating with a coolant temperature rise of 40°C (ΔT), and the other being a spray cooling system. Both systems are required to maintain an array of laser diodes at 60°C. Say the SCFB system is required to maintain at least a 10°C subcooled temperature to meet the required heat fluxes across the laser diode array. The fluid exiting the SCFB would then have a temperature of 50°C, and the fluid entering the SCFB would be at 10°C, again that is assuming a 40°C rise in coolant temperature is achieved. The heat exchanger would then have to take the coolant at 50°C and cool it sensibly down to 10°C.

Now, the spray cooling system can utilize saturated liquid coolant at 50°C and produces vapor at 55°C, this assumes that at 5°C superheat between the coolant and the surface of the diodes are required to achieve the needed heat fluxes. The condenser would then take that 55°C vapor and condenses it back at a constant temperature process to 50°C saturated liquid. The difference seen between the heat exchanger of the SCFB system and the condenser of the spray cooled system would be the lower rejection temperature of the heat exchanger in relation to the higher isothermal temperature of the condenser. The lower rejection temperature directly means that the size of the heat exchanger in a SCFB would be greater than that of the corresponding condenser in a spray cooled system. Consequently, two phase cooling systems such as, two phase jet impingement, two phase microchannel cooling & spray cooling have smaller heat rejection equipment, namely condensers, when compared to the heat rejection equipment of a single phase or SCFB cooling systems.

Another minor advantage of a spray cooling systems would be the ability to turn the spray on and off. This ability was shown by the Intel group with their inkjet assisted spray cooler, which only applied coolant when needed to a microprocessor [10]. Spray cooling can also feasible be operate in an open loop mode, this is elaborated on in section 2.3.1 *Open vs. Closed Loop.* Finally, spray cooling systems operate well with a wide range of coolants, such as dielectric, which can be sprayed directly onto the electronic item being cooled [11] [4].

There are also some disadvantages to spray cooling systems; many of these disadvantages are being worked out by the two leading companies involved in spray cooling of electronics which are, Isothermal Systems Research Inc. of Clarkston

Washington and Rini Technologies, of Orlando Florida. Spray cooling directly on delicate electronic equipment is difficult due to the very small erosion effects of an impinging spray over time. Over time a coolant containing small bits of foreign material sprayed onto a surface will slowly erode that surface. These bits of foreign material can be the result of many of things inside of the systems, such as oxidation from the tubing; small bits of metal ground off a gear pump and so on... Step can be taken to reduce the corrosion effect such as using, high efficiency filters, and metal traps with inlayed natural magnets.

Another disadvantage as of now is with pressure atomized spray nozzles which require high machining tolerances and can be difficult to manufacture. Companies such as: Delavan of the U.K., Spray System Co. of Wheaton IL, and Hago of Mountainside NJ, produce high quality spray nozzles, however they all charge around $10-$20 per nozzles, which is only a disadvantage if extremely large quantities of spray nozzles are required. Moreover, pressure atomized nozzles are very sensitive to large amounts of coolant debris, which must be filtered out to prevent the spray nozzles from clogging. Vapor atomized spray nozzles are also produced by the same companies; however, they do not require such high machining tolerances and are less susceptible to clogging due to their larger diameters nozzle orifices.

Yet another disadvantage of spray cooling systems, especially large areas spray cooling and vapor atomized systems, are their system complexity, see *chapter 3* for system details on the author's large area spray cooling system. The complexity of the spray cooling system *may be its biggest disadvantage.*

The finally disadvantage spray cooling has is the lack of understanding about its operational characteristics in variable and microgravity environments. Up to this date only Baysinger & Yerkes have presented a paper on the effects microgravity has on the heat transfer characteristics of spray cooling [12]. To date there has only been one publication on the effects that extreme variable gravity has on a spray cooling systems. Rini concluded that a 5 G environment did not affect the heat transfer for a *single nozzle spray cooler*. However, a similar experiment must be conducted on a *large area spray cooling system*. This must be fully explored before a spray cooling systems can be placed on a variable or microgravity platform and can be considered a disadvantage till it is well understood, sections 2.3.3 *"Air Based Cooling Applications"* & 2.3.4 *"Space Based Cooling Application"* elaborate on this particular disadvantage [13].

1.5 Odd Applications of Spray Cooling

The author feels that it is important to note these unusual applications for two reasons: they are in commercial uses today, and that only new advances in spray cooling may better aid an unusual application. The author has mention in chapter 1 that it only makes sense to use spray cooling in application where high heat fluxes are needed; however these are the few exceptions, hence the title *Odd Applications*.

Another notable application of spray cooling with surface temperatures *above* the Leidenfrost point of the coolant is in the field of dermatology. Lasers have become an important tool in the field of dermatology and are used for a variety of reasons. One problem with the dermatologist's use of lasers was that of epidermal or skin damage cause by the excess heat created during the lasers uses. Using a cryogenic spray cooling system to intermittently cool the skin between light pulses dramatically reduced the

damage to the skin and allowed the dermatologist to increase the power per pulse. Moreover, spray cooling was used over cryogenic boiling because its high associated heat fluxes provided the fastest cooling time between laser pulses. In this particular application, spray cooling directly reduced skin damage & decrease treatment times for the patients [14] [15]

The oddest application of spray cooling the author has seen is that of cool off livestock, in particular pigs. Spray cooling is being used this case because it is the most monetarily economical way of cooling pigs in small enclosures. The human sweat glands are magnificent thermal cooling devices. On a hot day they allow us to shed excess heat, by releasing sweat on to the skin. That sweat then vaporizes into the atmosphere, and takes with it excess heat. Vaporization occurs even though the surface of the skin in this case is not at the boiling point of the water. This is due to the low vapor pressure associated with a dry atmosphere. In other words, vaporization will occur if the relative humidity of the air is below 100% and the temperature of the pigs' skin is above the dew point. The only catch is that the rate of vaporation or heat removal is dependent upon, the relative humidity and ambient temperatures. Unfortunately, pigs do not have sweet glands, so spraying them with a water mist cools them in the most economical way, aside from the old fashion mud puddle. So, simply put, spraying pigs in small enclosures with a fine mist of water is an easy way to keep them cool using the minimal amount of water.

1.6 Conclusion to Chapter

In conclusion, this chapter determined that spray cooling should be categorized into two main categories the *spray cooling of a gas* or the *spray cooling of an object or surface*. The second category of spray cooling, should then be subcategories into cooling applications with surface temperatures *above* Leidenfrost point of the coolant and ones with surface temperatures *below* the Leidenfrost point of the coolant.

This chapter also concluded that spray cooling is best used as a high heat flux cooling system. This was due the large number of cheaper, more established, less complex, and more reliable lower heat flux cooling systems already on the market.

Spray cooling has major advantages over other high heat flux cooling systems such as SCFB. These advantages are isothermal surface temperatures, lower flow rates at respectable heat loads, and higher rejection temperatures. High rejection temperatures allows for smaller condenser when compared to the heat exchanger of a single phase cooling system such as SCFB.

Spray cooling's current disadvantages are the high machining tolerance required by pressure atomized spray nozzles which are also susceptible to clogging if the coolant is not filtered of debris. However, this is not so important in a vapor atomized spray nozzle system. Another disadvantage is the system complexities associated with large area spray cooling. And the final disadvantage is the lack of understanding about how spray cooling behaves in a microgravity and variable gravity environment.

2. MOBLIE LAND, SEA, AIR AND SPACE BASED HIGH HEAT FLUX COOLING APPLICATIONS

2.1 Spray Cooling Developmental Goals

There is a multitude of applications for spray cooling and each one of them presents a unique set of requirements that the spray cooling system must meet. The bulk of these applications are simply tied to the removal of heat from electronic devices. All of the spray cooling applications in this section are categorized as one with surface temperatures being *below* the Leidenfrost point of the coolant.

There are two distinct funding parties interested in the development of the spray cooling for electronic systems: the military, and the commercial company. Each has a specific set of requirements that must be met in order for this cooling technology to enter practical uses. Regardless both have the same goals for the development of spray cooling which is *to increase the output of a current system,* or *to enable a new technology to be technically feasible.*

2.1.1 Spray Cooling to Increase Output

Microprocessors and high power electronic devices such as MOSFETs (Metal Oxide Semiconductor Field Effect Transistors), IGBTs (Insulated Gate Bipolar Transistors) and MCTs (MOS Controlled Thyristors) can create heat fluxes easily above 100W/cm^2 and probably beyond if the temperature is maintain within the operational

limits [16]. Increase in microprocessor's power densities are starting to approach the limits of forces air cooling, new cooling techniques are being explored to spread the heat, hence lowering the heat flux, or remove the heat directly [17] [18]. Cooling techniques such as heat pipes and single phase liquid cooling systems are expected to be next in line for cooling of higher heat density microprocessors [17]. Microprocessors for super computers have already exceeded the limits of single phase liquid cooling. Cary Inc. maker of supercomputers was first in applying spray cooling in its SV2 marketed super computer system [19].

Spray cooling in this case allows high heat density microprocessors to run at a higher clock speed than they would be otherwise able to do with conventional forced air cooling techniques [10]. An increase in clock speed directly increases the heat generation inside of the microchip. Increasing the clock speed requires that one maintain the microchip within operational temperatures (usually under 120°F). For this a higher heat flux cooling technique is required, such as spray cooling. Exactly the same is true for high power electronic devices, except instead of clock speed, power output increases, with the uses of higher heat flux cooling technologies. In both microchip and power devices more effective cooling techniques, as the ones shown in table 2 will increase the output of the current device in use. Combine this with new microchip packaging techniques and the microprocessor will be able to continue to develop unimpeded by thermal issues [5] [17].

2.1.2 Spray Cooling to Enable New Technologies to be Feasible

The second developmental goal of spray cooling is to enable new emerging technologies to become technically feasible. The main funding party behind this

developmental push is the military. Applications such as high energy lasers (HEL), high power radar systems and high power microwave systems are expected to be technically feasible for mobile platforms with the aid of spray cooling [12]. The cooling needs of most of these applications today can be accomplished by subcooled flow boiling. Unfortunately, the large system size and weight associated with subcooled flow boiling (SCFB) of large heat loads makes it extremely difficult to placed on any small land, air or space based platform. For terrestrial application SCFB can be directly applied but is strictly limited to fixed land or larger mobile land and sea platforms. Consequently spray cooling in particular *spray cooling of large areas* is being developed so that these advanced military systems can be placed on smaller and more mobile platforms. Up till now spray cooling has been awarded 4.1millon dollars in research money by SBIR & STTR, Appendix F shows the companies and topic numbers of each award.

2.2 Spray Cooling of High Energy Lasers

One such application for spray cooling in which it will serve as an enabling technology is that of high energy lasers systems (HEL) [6] [20]. The highest power lasers of the 1990's where the chemical lasers [21], however a new alternative laser technology, solid state lasers, is being developed due to the benefits it has over its chemical based brother [22]. So if the major benefits associated with solid state lasers are that they have much higher lasing densities, can be run off of electricity as apposed to chemicals, smaller system size for a respective power output, and they have no caustic working fluids. Solid state lasers have many other benefits when compared to chemical based laser but there are some major hurtles to overcome before they can produce power outputs comparable to chemical based lasers [23]. The one main hurtle which the author is

concerned with is the thermal densities created inside of the lasing materials, and power electronics.

High energy solid state laser can be broken up into its main heat generating components; the laser diodes, main laser gain material, and the power electronics [6] [8] [9]. Each component has a respective efficiency; which relates directly to the amount of waste heat generated from that component. Engineers are working to increase efficiencies and consequently reduce the waste heat generated by each component. Regardless there is going to be slight inefficiencies in even the best systems. Laser diodes are a vital component in a high energy solid state system [9].

Currently laser diodes have been operated at up to 50% even 65% electrical efficiencies [24] [9]. For example, take a 50% efficient laser diode array producing a power output of 40KW. This laser diode array would produce 20KW of waste heat that must be disposed of. Spreading the heat out over a larger area would allow standard OEM single phase cooling systems to be used but this means that more lasers diodes must be uses to achieve the desired power output. Again take for example the same laser diode array producing 20KW of waste heat. A standard OEM single phase cooling system providing heat fluxes of $100W/cm^2$ would require $200cm^2$ of surface area to cool the array properly.

However, for this component of the HEL system to fit on smaller more mobile platforms, the size of the laser diode array and its corresponding surface area must be reduced. This can be done by switching to cooling systems with higher achievable heat fluxes such as: spray cooling, SCFB, or microchannel cooling. Now, going back again to the laser diode array producing 20KW of waste heat, one can see that a cooling system

capable of heat fluxes up to 400W/cm^2 would reduce the required surface area to 50cm^2 [9]. Thus one can see that a *large area spray cooling system* would reduce the size and corresponding surface area of the laser diode array. For this reason effective high heat flux cooling systems are going to be needed to make small mobile HEL applications possible [6] [23] [12].

To prove this point even further say the previously mentioned laser diode's efficiency increases to 90%. That still means that a 40 KW laser diode array would produce 4KW of waste heat. However if the cooling system is still capable of cooling 20KW of waste heat one can then increase the output power. In this example, that would allow the 90% efficient laser diode array now to operate at 200KW; of course, that is assuming that cooling and the laser diodes are the only limiting factors.

2.3 Land, Air, Sea and Space Environments Impact on the Cooling System

Military planners have been looking at the strategic advantages of having high energy lasers, high power radar and high power microwave systems on wide range of mobile platforms [25]. But from and engineering standpoint the difficulties in cooling a land, air, sea, or space based systems can vary widely.

The author's review of the literature has found a *lack of attention paid to the cooling aspect of each of these environments*. So the author has elected to elaborate on the difficulties associated with the design of a cooling system in each of these environments. In particular, author wishes to elaborate on the radiator, condenser, and heat exchanger, since they would in most case be the most limiting component in the cooling system's design.

2.3.1 Mobile Land Based Cooling Applications and Open vs. Closed Loop

Fixed land based applications were the first proof of high powered laser technologies effectiveness. The high energy laser system test facility in White Sands New Mexico used their high energy chemical based laser to shoot down a Katyusha rocket and artillery shells in flight [23] [26] [27]. These tests validated HEL as an effective anti-missile defense system. Since then military planners quickly hoped to put HEL systems in multiple mobile land based platforms. Currently the HEL lasers are chemical based and take up a substantial amount of room, so they would be limited mainly to train and multiple semi-sized mobile size platforms. Consequently, the solid state laser has been identified as a key technology needed to move this defense system to smaller more mobile land based platforms such as tanks, and Humvees. The US Space and Missile Defense Command have already taken to this with their Humvees based ZEUS-HLONS systems [28], which explodes mines. Lawrence Livermore Labs have also shown interest in this move with their mockup HEL Humvee [29]. For HEL system make a seriously move to these smaller mobile land based platforms the cooling needs of the system must be fully assessed.

The cooling systems of all mobile land based platforms will be extremely dependent upon ambient air conditions. The cooling systems of all mobile land based platforms fundamentally have to reject heat generated from the operation of the main system. In doing this they can either be an open loop system, rejecting their coolant directly into the atmosphere, or a close loop systems rejecting their heat into the surrounding air. It is most impractical for a SCFB system to be open loop due to the extreme waste of coolant (Appendix C for proof calculations). This fact alone would

render all open loop single phase cooling systems uneconomical and infeasible for small mobile based platforms. Spray cooling can feasible be an open loop system because the latent heat of vaporation absorbs much more heat than a sensible temperature changes, thus the coolant flow rates are much lower. The latent heat of water is h_{fg} =2257 KJ/Liter where one kilogram equal one liter

$$\dot{Q} = \dot{m}(h_f + h_g) \qquad \text{(Eq 2.1)}$$

Assume at 1 MW heat load, mass flow rate can be found using Eq 2.1 to be 0.443Liter/s for 1 MW of heat, which is respectively 0.12 gallons/ MW-sec. Converting this figure to minutes gives 7.2 Gallons/MW-min. Hence a formula can be written which would give the volume of the coolant vaporized for an open loop spray cooling system at a respective power level of cooling and firing time.

$$(Power\ \ in\ \ MW)\left(7.2\frac{Gallon}{Min-MW}\right)(Firing\ \ Time\ \ in\ \ Mins) = Gallons\ \ Needed \qquad \text{(Eq. 2.2)}$$

The weight of the water coolant then can be found by multiplying the resultant by 10.142lbs/gallon. So for example, a light personal carrier retrofitted with a small HEL with a 0.4 MW cooling systems fired continuously or intermittently for a total time of 1 hour, will require 175 gallons of water weight at a total weight of 1,752 lbs. This is manageable but not at all optimized; a closed loop system would be far more conservative in weight. However, in the event that the closed loop system is compromised, say the condenser is fatally broken; a spray cooling system can still operate in an open loop mode as long as there is an adequate coolant supply.

After evaluating the open loop cooling systems one can then shift their attention to close loop cooling systems. As mentioned earlier land based close loop cooling systems have to reject heat to the surrounding air, which can vary greatly in temperature from one place to the next, and from one day to another. The effectiveness of a condenser, in a spray cooling system, or a heat exchanger in a SCBF system is directly affected by the ΔT or temperature difference between the heat rejection equipment and the ambient air. A larger ΔT would translate directly into a smaller condenser or heat exchanger. So a land based HEL cooling system operating in an 110°F (43°C) desert would have a much larger heat exchanger or condenser then a HEL cooling system operating in the cooler 50°F (10°C) mountainous region, assuming the air density was the same. Additionally air densities change with altitude; this will be mentioned in detail in the section *air based cooling application.* These variability means that a mobile cooling system like one being placed on the Humvee would have to be over designed to meet the needs of the more extreme environments. Again spray cooling advantage from section 1.4 is that it has a higher rejection temperature than that of SCFB. Condensers and heat exchangers surface area (and size) has an inverse dependent upon temperature. So for example a condenser with ΔT twice that of a heat exchanger will have half the surface area of the heat exchanger. Include this result with the smaller pump size requirements associated with the lower flow rates and one could safely say that a spray cooling system would weight less than a SCFB system, for the same cooling load. Regardless of the system used, the ambient temperature & density will have the greatest effect on the cooling system.

2.3.2 Mobile Sea Based Cooling Applications

Sea based applications for cooling of high power systems has a distinct advantage over that of land based system, which is the sea itself [30]. The sea, is a great heat sink, the surface temperature of the oceans on average very from 28.4°F (-2°C) to 91°F (33°C), from the polar to the equatorial regions respectively [31]. The temperature of the oceans also varies with depth; most importantly the density of water is 1000 times that of air, so the heat capacity of water per unit volume is tremendously greater then that of air. The amount of energy available in one cubic meter of water can be calculated by multiplying the density of the media by its constant pressure specific heat and one will get 1.174 KJ/m^3-K for air and 4180 KJ/m^3-K for water [1]. So water roughly can provide 3,500 times the cooling capacity as air per unit volume. So in comparison a sea based cooling applications will have much smaller heat exchanger or condenser then a similar capacity land based cooling system.

Sea based cooling systems should be a closed loop system; because if they were open loop they would have to uses sea water as a coolant. Sea water has a corrosive nature which is unfriendly to most metals and electronic components. Additionally sea water has relatively high amount minerals and flotsam which must be filtered out. Consequently, a heat exchanger or condenser will be employ to remove heat from the closed loop coolant and release it into the sea. From a thermal engineering standpoint one could say that it would be much easier to place a high power system like the HEL on a small PT boat then a similarly sized Humvee. Even if both are done, the boat will most likely have the advantage of having a more environmentally reliable system due to the lower temperature variation of the ocean from place to place.

2.3.3 Air Based Cooling Applications

Fifteen years ago the U.S. Airforce started developmental research into placing high power systems, like the HEL, on airplane platforms. Companies such as Boeing have used the tremendously large 747 jetliner as a flight platform to demonstrate the airborne use of the high energy chemical based laser system [32]. Current cooling challenges must be over come for solid state HEL, high powered radar and microwave systems to be placed on smaller more mobile air platforms. Recently the U.S. Airforce has been working with the Raytheon Company to produce a 100KW laser to be placed on an F-35 joint strike fighter jet platform [33] [34] [35]. Subcooled flow boiling is barely applicable on these smaller air platforms due mainly to the large size of the required exchangers [36]. Spray cooling with its high rejection temperature requires a condenser which is much smaller than that of SCFB system's heat exchanger. Consequently, the cooling system selected will depending upon the flight platform chosen and may have to operate in a variable gravity environment, operating at different altitudes, and at different airspeeds. Regardless of the cooling system chosen the altitude and flight speed will have a direct effect on the size of the heat exchanger or condenser in use.

The atmospheric temperatures of the earth vary greatly with altitude and location. The International Standard Atmosphere has created a general formula for average air temperature vs. altitude. A very rough rule of thumb is that the temperature of the atmosphere drops 10°C for every 1000 meters of altitude, and 5.5°F for every 1000 feet [31]. Additionally air density is dependent upon altitude (pressure) and local temperature. So the density of air on an average clear day over the equator at 5,000 ft is 1.054kg/m^3; whereas, 30,000 feet is 0.458 kg/m^3 [31] [37]. Fortunately, the variations of air densities

at higher altitudes are smaller than that of lower altitudes. Lower altitudes have temperature & pressure variation dependent upon their global locations and local weather conditions. At higher altitudes, such as 25,000 feet, the air temperature and densities vary slightly over the entire globe. Consequently, in designing a heat exchange or condenser to operate at these altitudes one must only consider variations in the air speed (which relates mass flow rate) of the aircraft. At lower altitudes design considerations for heat exchangers or condensers become much more complicated. At lower altitudes one must consider local air conditions (temperature, density) and variations in air speed (mass flow rate) of the aircraft, in the design process.

Supersonic velocities add a new complication in the design of the heat exchange or condenser. It would be unreasonable to place a HEL system on a supersonic aircraft, for instance a F-35, and not have it operate at supersonic speeds. Hence the design of any sub/supersonic aircraft must also take into account cooling at supersonic velocities. Mostly all condensers or heat exchangers assume flow passing over their internal surfaces at velocities much lower than the speed of sound. If velocities exceeded the speed of sound, internal shockwaves would form in the condenser or heat exchanger. The effects of these shockwaves could be devastating to the fragile finned design of most condensers or heat exchanges. One could account for this in the initial design but it would add a huge level of complexity which is not needed. As a result, mostly all condenser & heat exchangers operate at subsonic internal velocities. Subsonic fluid flows can be achieved in a supersonic aircraft by using a convergent divergent diffuser or a body diffuser as stated by Preston [38]. Preston comments on these diffusers in relation to their uses with turbine engines by saying, “generally convergent divergent diffusers are only suitable for

short burst of supersonic flight, less than mach 3." The other option is center body diffuser, which for which Preston states "this design is suited to sustained supersonic flight and therefore would be a better choice than the convergent divergent diffuser." The downside to body diffuser is they utilize tracking center cone which adds more moving parts to the design. Both diffuser designs can uses to reduce supersonic flows to subsonic flows for uses in condensers or heat exchangers.

Both the convergent divergent and body diffuser create normal or oblique shock waves which will directly increase the temperature of the incoming air. From compressible flow fluid dynamics the ratio of T/T^* can be calculated based on the Mach number. For examples an aircraft utilizing a convergent divergent diffuser at flying 16,000 feet and at a speed of M = 1.3, the corresponding ratio of T/T^* & ρ/ρ^* across a normal shock would be 1.19 & 1.515 respectively [37].

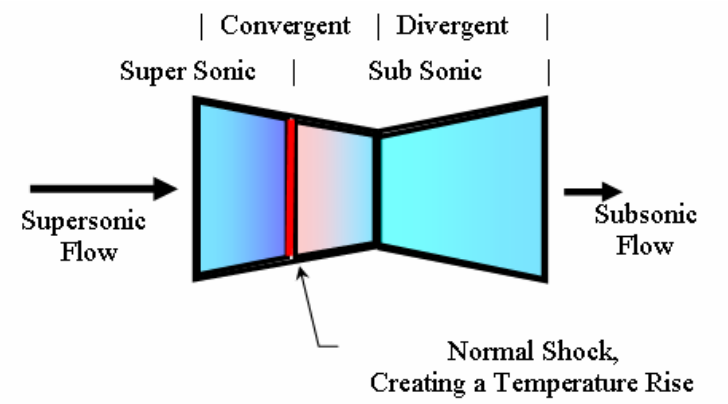

Figure 2.1: Convergent Divergent Intake Nozzle

NOAA's standard air temperature model would predict the air temperature and density at 16,000 feet to be -17°C (256K) and at a density of 0.742 kg/m³. If this air were to pass through the normal shock it would then rise to a temperature of 32°C (305K) and to a

density of 1.124 kg/m³. Obviously much more consideration must taken when design a cooling system operation on a super-sonic aircraft.

Consequently, the final design of a high heat flux cooling system for a flight platform is most dependent upon the size and flight characteristics of the airplane chosen, it is feasible to uses a SCFB system on a Boeing 747 with a 100KW HEL, but not a F-35. An F-35 (Joint Strike Fighter) must have a cooling system that can operate at supersonic speed, and can handle variable gravity environment; whereas, a Boeing 747 or C-130 does not have such requirement. Secondly, the design of the cooling system is depend upon the flight altitudes and global locations which relate directly differences in ambient air densities and temperatures. Finally in cooling applications where a full sizes heat exchanger or condenser can not be accommodated easily (F-35) a different cooling scenario or scheme can be chosen to reduce the heat rejection equipment's size. Such cooling scenarios are depicted in detail in the next section "space based cooling systems", since they lend themselves more to these types of environments.

2.3.4 Space Based Cooling Systems

Military planners have dreamed of utilizing a networks of space based high energy lasers as a defense net against inter-continental ballistic missiles (ICBM) attacks [25]. Space based laser (SBL) have advantages over air based laser platforms such as, larger coverage area due to their higher orbital altitudes, and much longer effective ranges due to the lack of atmospheric light losses and distortion [39] [21] [25]. For such a system to be implemented a myriad of problems must be overcome in present day, lasers, optics, power generation and cooling technologies [12]. Thus, high heat flux cooling

technologies has been identified as one of the enabling technological needs for future SBL & Human Exploration and Development of Space (HEDS) projects [40].

Space based cooling systems have a numerous number of factors limiting all facets of their design. A few of the major and most notable factors are power requirements, weight and size limitation, and reliability. Consequently, designing any space based cooling system most likely is tremendously more difficult than designing any similar land or air based system. All spaced based cooling systems can only transfer heat away from the system by radiative heat transfer, due to the lack of atmosphere at or pass orbital attitudes. Hence this section will concentrate on *possible space based high heat flux cooling technology* and *radiator size in relation to different types of cooling scenarios*.

Radiative heat transfer becomes effective at higher rejection temperatures because of the fourth order dependent upon the temperature term as seen below.

$$q''_{rad} = \varepsilon\sigma\left(T_s^4 - T_{space}^4\right) \qquad \text{(Eq. 2.3)}$$

Where ε is the emissivity of the surface in the range of $0 < \varepsilon < 1$, T_s is the surface temperature of the radiator, σ is the *Stefan-Boltzmann* constant being $5.67E^{-4}$ W/cm^2-K^4, T_{space} is about 5K if the object is shield from the sun and absorbs only interplanetary radiation [41] [1] [42]. One has a few options in the overall cooling scenario in which the space based cooling system will operate.

The feasible cooling scenarios for space based cooling systems are, *one that reject heat as quickly as possible back to space***,** *one that store a lot of the heat then slowly*

rejects the heat back to space, or *ones that store the heat then utilizes it to generate electricity while slowly rejecting it back into space*.

The first *scenario* of rejecting the heat as quickly as possible back into space, indicate that a very effective radiator will be require. Again the radiative heat transfer rate will be dependent upon Eq. 2.3. The following calculations will assume a radiator with solid walls, so that a two-phase flow can be keep within the radiator.

Table 3 : Radiator Surface Temperature vs. Heat Flux

Assuming a Perfect Radiating Body

Heat Flux (KW/m^2)	Surface Temp (◦C)
0.315	0
0.617	50
1.098	100
1.815	150
2.838	200
6.112	300
11.632	400
20.244	500
32.934	600
50.820	700
75.159	800

Table 2 shows the respective heat flux for a perfect radiation body ($\varepsilon = 1$), shielded from the suns ($T_{space} = 5K$) at various radiator surface temperatures. Using this table & Eq. 2.3 one can calculate the minimum *surface area* needed to *continuously* cool a 50KW heat source at a radiator surface temperature of 100°C to be $46m^2$. However, in reality the emissivity will be more around 0.9 so the area in this example is going to be 51 m^2. Increasing the radiator surface temperature to 200°C reduces the radiator's surface area to $18m^2$. Consequently, one can see that size and weight restrictions on a cooling

system continuously dissipating high heat loads will require it to have a radiator with high surface rejection temperatures [42]. Keep in mind that a thin walled radiator could radiate energy from both sides, so the actual size is depend upon chosen radiator configuration. Donabedian's *Spacecraft Thermal Control Handbook* has a very good analysis of radiator for cryogenic spaced based cooling applications [42].

The *second* cooling scenario could be that of storing the heat and then slowly rejecting it into space. Thermal energy storage can be achieved by storing heat in a sensible or a latent heat material. Latent heat storage utilize phase change materials (PCM) to absorbed heat (ex. from solid to liquid) and offers greater heat storage densities then that of sensible heat absorption. Conceivably, one could use thermal energy storage (TES) systems to store heat then release it slowly over a cool down period [43] [42]. This would lesson the heat dissipation requirement of the radiator which would allow it to be much smaller in surface area, and lower in rejection temperature. Take for example a cooling system dissipating a heat load of 50KW over 30 seconds, and then allowed 4 minute of post cooling. The cooling rate of the radiator would be found to be

$$\frac{(Cooling\ Power\ (KW))*(On\ Time\ (\text{sec.}))}{(Cooling\ Time\ (\text{sec.}) + On\ Time\ (\text{sec.}))} = Radative\ Cooling\ Load\ (KW) \qquad \text{(Eq 2.4)}$$

$$\frac{(50KW)*(30\,\text{sec})}{(240\,\text{sec} + 30\,\text{sec})} = 5.6KW \qquad \text{(Eq 2.5)}$$

The required surface area of a radiator rejecting 5.6KW of heat at 100°C, assuming an emissivity of 0.9 would then be

$$\frac{5.6KW}{1.098\frac{KW}{m^2}} * \frac{1}{0.9} = 5.7\,m^2 \qquad \text{(Eq 2.6)}$$

Thus the radiator surface area can be greatly reduced by storing the heat created during the operation of the main system in a temporary thermal energy storage device. Unfortunately, research in to the thermal energy storage field for space based application is relatively new and requires much more research [40: pg 149]. Donabedian's *Spacecraft Thermal Control Handbook* does a very good review of cryogenic thermal energy storage systems.

In the third cooling *scenario*, one could utilize the heat rejected by the cooling system to generate electricity. This can be considered a way of increasing the overall electrical efficiency of the system being cooled. Often it is quoted that available power for space based system is large limitation it operations [40: pg 21].

Recently a deep space probe launched in 1997 named Cassini-Huygens visited Saturn with three radioisotope thermoelectric generators onboard [44]. These thermoelectric generators utilized pressed oxide plutonium-238 fuel to generate heat which was utilized by thermoelectric elements to produce a maximum of 870 watts of electricity energy. It is reasonable to assume that a solid state based HEL system would require short periods of very high power consumption. This could be conceivability supplied by battery packs constantly being charged by radioisotope thermoelectric generators, or some other power generation source [40: pg 21]. Reclaiming the heat created during operation could be a way of reducing the recharge time need for the battery packs. However, for a system like this to be implemented, the extra weight and

system complexity aided would have to be offset by a decrease in recharge time and or a weight savings by reducing the size of the battery pack.

2.3.4.1 Conclusion to Space Radiators

In conclusion, the radiator will have a largest impact on the size of the space based cooling systems, due to the large surface areas associated with rejecting huge amounts of heat into space. A two-phase radiator's size will be most depended upon the type of cooling scenario chosen, and the radiators rejection temperature. HEDS summarizes two phase radiators as "Radiators that take advantage of two-phase working fluids are more efficient and are relatively lightweight, but are subject to two-phase flow instabilities, freezing, structural damage, damage by meteorites and other phenomena [40:pg 29]." Consequently, much more research must be done to make 2 phase radiators feasible.

Current single phase radiators are directly applicable however their large associated size and weight limit their applicability. Newly developed alternative single phase radiators present weight and sizes savings. Microgravity research for HEDS summarizes other radiative options as "Liquid-droplet radiators and liquid-sheet radiators are among the most promising technologies for achieving lightweight heat exchangers for space applications, and do not seem to be affected by microgravity." Unfortunately, cooling systems that utilizing single phase radiators can not take advantage of the benefits that two phase cooling systems would have; such as, higher rejection temperatures, lower associated flowrates.

2.3.4.2 Conclusion to Space Cooling Systems

Up till this point single phase (high Reynolds number) and solid state radiative cooling systems have only been used in space. The use of multiple phase cooling system has not been adopted due to the lack of understanding associated with two phase flows in a microgravity environment. NASA has recommended that one of the program objectives of the HEDS project will be to study multiphase flow systems in detail.

> In particular phase change systems are likely to be necessary for power production, propulsion, and life support. Unfortunately, relatively little is currently known about the effect of gravity on multiphase systems and processes. Multiphase flow and heat transfer technology is considered to be a critical technology for HEDS. Indeed it is expected to be mission-enabling, if properly developed and could lead to revolutionary changes in spacecraft hardware [40: Pg 180].

Cooling systems like, pool boiling, two phase microchannels, heat pipes, subcooled flow boiling, and spray cooling are expected to be candidates as cooling technologies to benefit from microgravity multiphase research. Additional cooling technologies such as single phase microchannel and quantum tunneling cooling could provide cooling solution but more research is needed to prove these cooling technologies to NASA.

2.4 Conclusion to Chapter

So in conclusion, this chapter outlines the developmental goals of spray cooling which are to *increase the output of a current system* and to *enable new technologies to be technically feasible*. Electronic devices such as IGBT, MOSFETs, MCTs and most importantly microprocessors would be listed underneath systems which would increase

their output powers or clock cycles with the aid of spray cooling. System such as: high energy lasers, high powered microwaves, and high power radar systems would be technically feasible for smaller mobile platforms with the aid of *large area spray cooling systems*. Both military and commercial companies are pushing to develop *large area spray cooling systems*, for their respective applications.

Furthermore this chapter outlines in detail the impact that land, air, sea, and space environments have on the cooling system, in particular on the heat exchanger, condenser and radiator.

Land based applications for large area spray cooling would enable HEL and high power microwave systems to be placed on smaller more mobile platforms such as Humvees and lightly armored vehicles. This is due to a spray cooling system having a lower coolant flow rates, isothermal surface temperatures, and smaller respective condenser sizes then a competing single phase cooling systems such as, SCFB.

Conversely, sea based applications for HEL, high power microwaves, and high power radar systems do not require spray cooling to be technically feasible, but would benefit from slightly smaller system sizes. All sea based cooling systems should not utilize sea water as an open loop fluid due to its corrosive nature. Finally heat exchangers or condensers for sea based systems would much smaller than a respective land or air based cooling system, due to the extremely high heat capacity of sea water.

Spray cooling systems would enable HEL, high power microwaves, and high power radar systems to be placed on smaller air platforms, such as the F-35. Considerations such as: flight altitude, flight speed, and global location must be accounted for when designing a heat exchanger or condenser for a subsonic aircraft.

Furthermore, a cooling system operating on supersonic aircraft must utilize a convergent divergent or body shaped diffusers to slow the income fluid flow to subsonic velocities. Additionally, the Mach number must be considered for a supersonic aircraft since it directly impacts the temperature and density of the air flowing through the condenser or heat exchanger. Finally, for a spray cooling system to be placed on a highly maneuverable aircraft it must be able to endure a variable gravity environment for extended periods of time.

Spray cooling is considered to be and enabling technology for future HEDS projects and for the HEL space based laser system. Much more research must be done to determine the effects microgravity has on multiple phase systems. Alternative cooling scenarios utilizing a thermal energy storage system would decrease the corresponding radiator surface area. Much more research is needed to determine the effects that space has on multiple phase radiators. Alternative lightweight single phase radiators for space present promise but must be research much more to validate their design.

3. MULTIPLE NOZZLE SPRAY COOLER

3.1 Introduction to Chapter and Literature Review

The advantages of two-phase cooling systems make them ideal for use in high heat flux cooling for aerospace and space based application [12]. The advantages like compactness, light overall system weights, and high heat flux dissipation lend themselves very well to cooling applications such as high energy lasers and high power electronics systems. Spray cooling and micro-channel cooling have presented themselves as the best solutions; however, spray cooling has advantages over micro-channels coolers such as isothermal surfaces temperatures, lower working fluid flow rates and smaller system size. It has been demonstrated that spray cooling can remove heat fluxes as high as 1000 W/cm^2 for single spray nozzle over an area of less than 2 cm^2 [4]. However, many applications require cooled areas on the order of tens of square centimeters. Spray cooling over larger areas ($20cm^2$) has been tested and it was found that flooding of the cooled surface occurs due to the lack of excess liquid drainage [45]. This flooding decreased the heat flux by 30% to 40%; therefore a fluid management system is needed to minimize the degradation in heat removal capabilities caused by flooding.

3.2 Design Problem

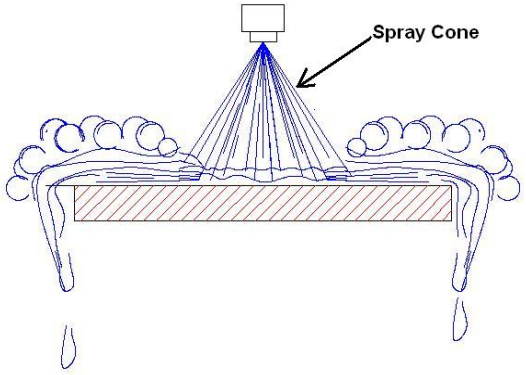

Figure 3.1: Single Spray Cone

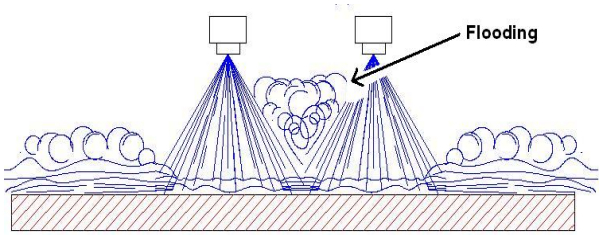

Figure 3.2: Multiple Spray Cone Interaction

The goal of this research is to design a scaleable pressure atomized spray cooler capable of cooling large areas, greater than 16.8 cm^2. The inherent problem with spray cooling large areas is the flooding of the cooled surface and the creation of unwanted temperature gradients across the cooled surfaces.

The main driving mechanism in spray cooling is the thin film, which is created just above the cooled surface [4] [45] [46]. In a single pressure atomized spray nozzle the liquid run off which is about 90% of the input is pushed away from the cooled surface via the momentum of the spray (Fig. 3.1), the other 10% is evaporated away [46] [47].

However, in large area spray cooling, multiple spray nozzles are used to cool the heated surface and their spray cones and run off liquid interact with each other [4]. If the

run off liquid is not removed from the cooled surface it will build up and flood the cooled surface; thereby destroying the thin film needed for effective spray cooling. Figure 3.2 shows a build up of liquid between the two spray cones. This build up would move the liquid/vapor phase change to a pool-boiling regime, which is unwanted and has lower associated heat flux than with spray cooling. The design problem presented in this paper is that of how one can control the flooding effect of a *Single Phase* multiple head spray nozzles and maximize the overall heat flux.

3.3 Design and Solution

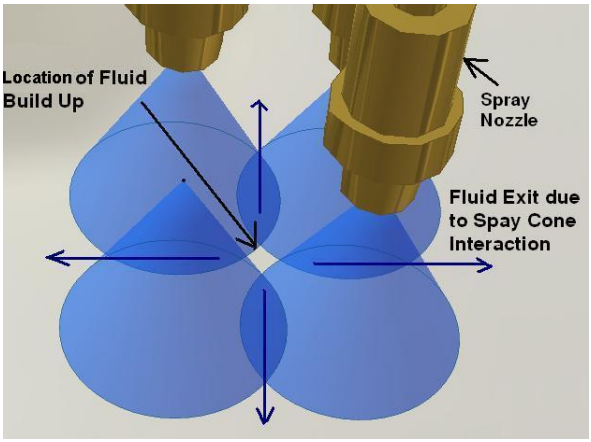

Figure 3.3: Fluid Build Up Points

In view of our design goals the author decided to construct and test 4 by 4 array of spray nozzles and create a system that could manage the excess fluid trapped between the adjacent spray cones. This system which Dr. Chow called the fluid management system utilizes an array of siphons to remove the excess liquid.

In a 2 by 2 array of spray nozzle it was observed that some of the excess fluid was being trapped between the spray cones, this can be seen in the top view of Fig. 3.3 and in

the side view in Fig. 3.2. Additionally, the spray cones interacted with each other; this can be seen in the darker areas of the spray cones in Fig. 3.3. The spray cone interaction forced the excess liquid to exit along the cooled surface in the direction as shown in Fig. 3.3.

In order to gain control over the build up of the excess fluid and its exit direction, two design features were implemented. First being the placement of siphon tubes at the flooding points and the second being an implementation of a grooved in the cooled copper plate. The grooves which are aligned in a grid pattern (Fig. 3.6) were used to directed excess liquid created by the spray cone interaction to the nearest suction point or siphon. Both of these design features can be seen in Fig. 3.4.

The siphons have an inner diameter of 2.3 mm and outer diameter of 3.1 mm. The siphon size was chosen out of convenience of its design, a larger siphon diameter in theory would be able to pull more fluid away from the surface and thus improve drainage at the cooled surface.

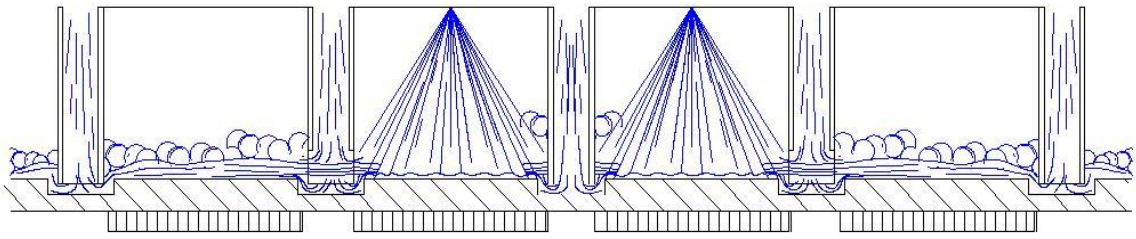

Figure 3.4: Fluid Flow Observed from the Side of the Spray Cooler with the Un-Modified Siphons

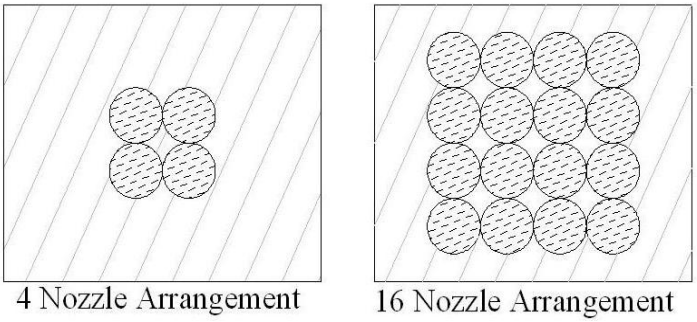

Figure 3.5: Spray Nozzle Configurations

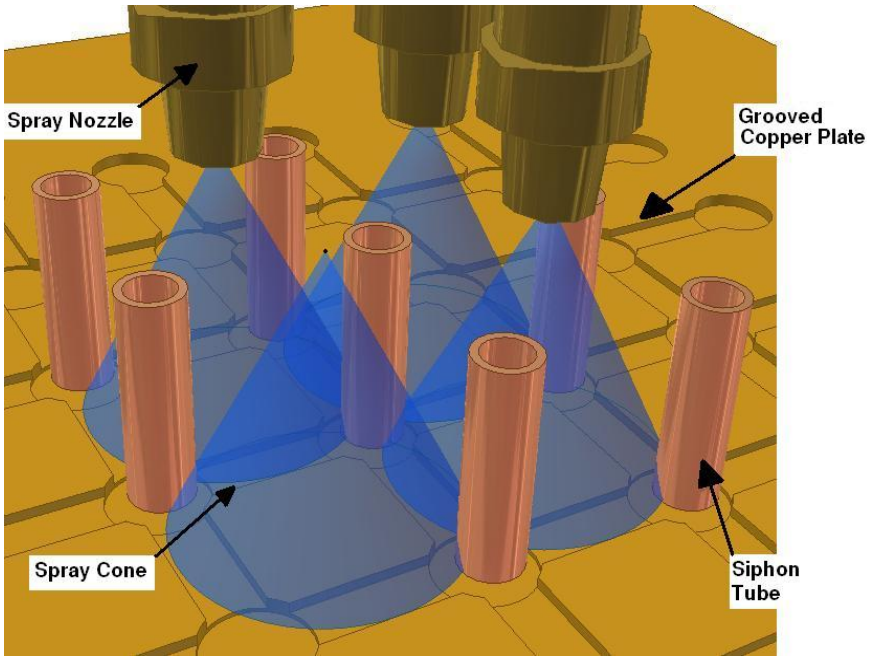

Figure 3.6: Overall Siphon Placement

The groves in the copper plate were 0.5 mm deep and 2.8mm wide. The siphon tubes and the groves can be clearly seen in Fig. 3.6 along with the spray cones. The array of 25 & 37 siphons are in close contact with the cooled surface in design 1 (Fig. 3.7) & Design 2, respectively. The full size of the spray cooler array is 4 by 4 for a total of 16 nozzles and can be seen in figure 3.5. The sixteen spray nozzles were distributed evenly

so that their spray cones covered a square area of 16.8 cm^2, this roughly give a cooled area of 1cm^2 for a single nozzle. The selected spray nozzles were 1/8GG-FullJet 1 from Spray Systems co. and were selected based on their even spray distribution and higher droplet velocities [46] [47]. The spray cooler array was tested in two configurations being a 4 nozzle and 16 nozzle arrangements Fig. 3.5. The 4-nozzle arrangement was mainly used to visualize the fluid dynamics occurring at the cooled surface.

The fluid management system and the spray coolers nozzles were designed to be compact and scalable to any surface area. The spray-cooling unit (Fig. 3.7) consists of two manifolds, one being the high-pressure water manifold, which feeds the spray nozzles, and the second manifold is the suction manifold, which pulls suction from all the siphons. The spray nozzles are isolated from the suction manifold via an array of 16 copper tubes, which pass through the suction manifold.

The siphons in both designs are 1 mm above the grooved plate. This was done so that the thin film thickness may be controlled via the use of varying the suction through the siphons. The spray nozzles are positioned 13mm above the cooled surface, which was determined as the optimum distance. The suction manifold is evacuated via eight holes around the side of the suction manifold. Detailed design drawings for all parts in this assembly are given in Appendix B.

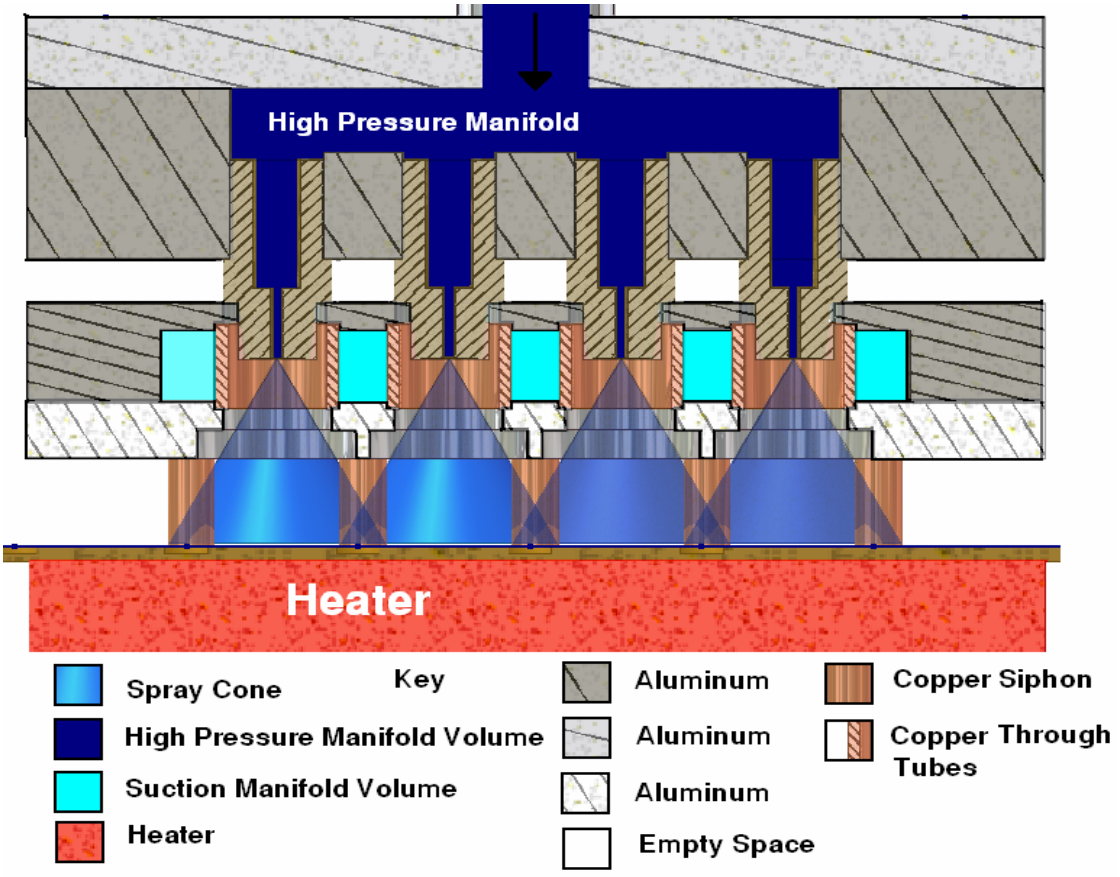

Figure 3.7: Overall Spray Cooler Design

3.4 Experimental Setup

The spray cooler and the fluid management system were tested in an open loop setup with the spray cooler in the horizontal position as shown in Fig. 3.8. The loop starts at the main water reservoir then a gear pump capable of pumping 116 gallons/min at 90 psi was used in conjunction with a bypass valve to provide water to the spray cooler at a range of 20 to 40 psi. The flow rates of the pump depend upon spray nozzle configuration shown in Fig. 3.5.

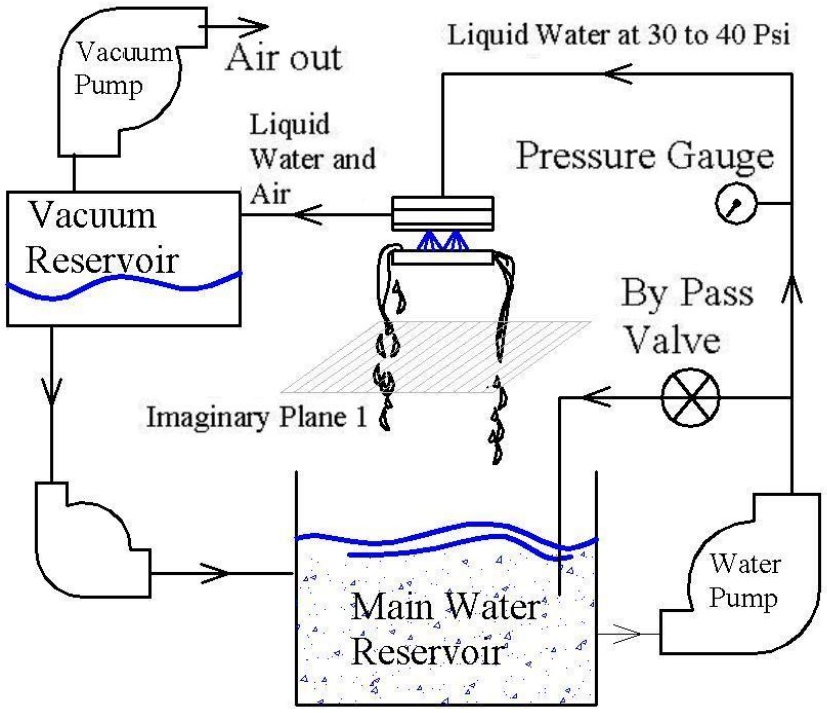

Figure 3.8: Experimental Setup

The water is then passed through the spray cooler nozzle and atomized into a spray via the head pressure. Excess liquid that was not removed by the siphons was allowed to drain over the edge of the cooled plate back into the water reservoir. The vacuum reservoir was evacuated to 2 in-Hg via a single air drive vacuum (Level 1 Suction) and to 4 in-Hg via two vacuums (Level 2 Suction). The liquid that accumulated in the vacuum reservoir was then pumped back into the main water reservoir with a diaphragm pump. Flow rates for all experiments were measured by capturing the excess liquid in a graduated cylinder for 30 seconds at the imaginary plane shown in Fig 3.8. This gave an error in the flow rates of +/- 0.2 liter/min.

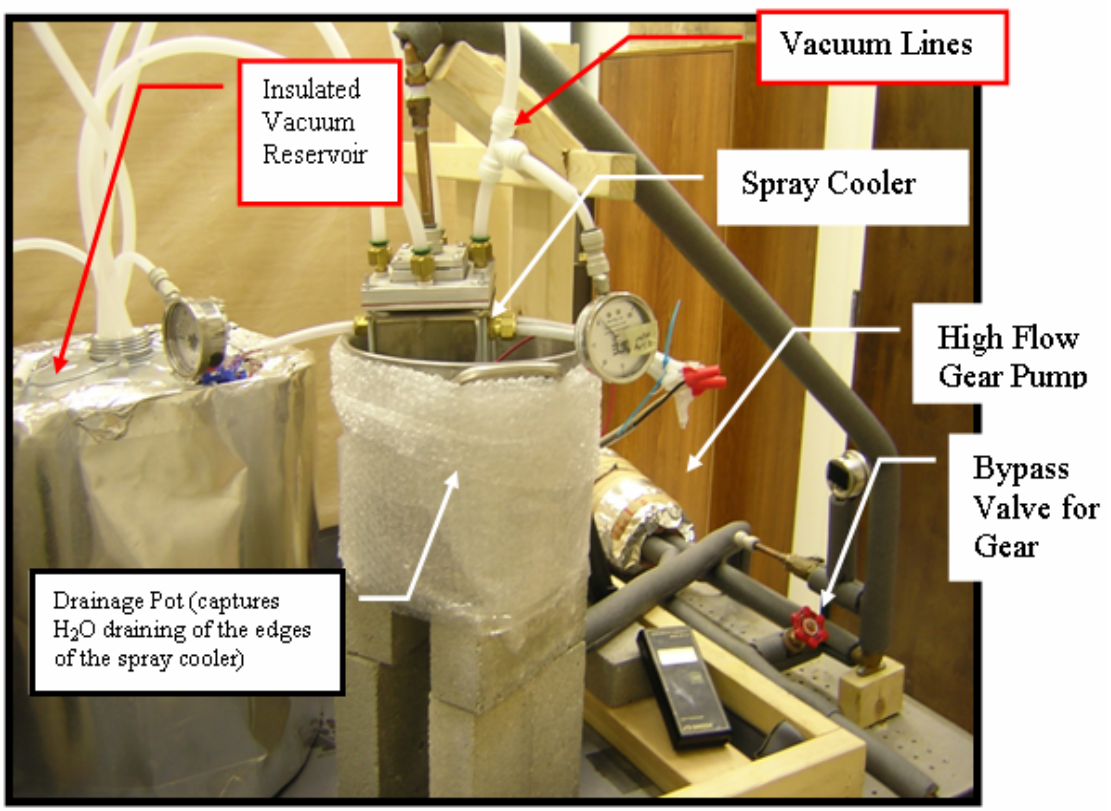

Figure 3.9: Experimental Setup for Multiple Nozzle Spray Cooler

The setup as seen in figure 3.9 is very large because of the increase in flow rates. The water heater is not shown in this picture but it is located directly underneath the table. The water heater is a 6 gallon standard water heat, the thermostat was bypass and the heater coil was connected directly to the wall so that a water temp of 90°C could be achieved. The pump and drainage lines were made of 5/8 in and ½ in copper tubing respectively. There are 4 vacuum lines that are 3/8 in vinyl tubing. All reservoirs were insulated and so to was the water heater. The vacuum reservoir has 6 in of home insulation around it and the drainage pot had bubble rap insulation around it. All of the copper tubing was cover by water heater insulation (1 inch thick). All of this insulation kept the heat loss to a minimum which helped maintain the working fluid's temperature.

The experimental test setup was an open loop so the vapor created at the heated surface could escapes freely to the atmosphere.

Figure 3.10: Vacuums Used in Series

The vacuum chosen to proved suction for this experiment are simply two 2.5 hp RIDIGED brand shop vacs. These vacuums were attached in series proved two levels of suction for the experiment. The associated vacuum levels were 2in-hg and 4in-hg respectively. During the experiment it was noticed that the vacuums performance was diminishing. This was due to the filter inside becoming saturated with water vapor. Removing the filter inside of each vacuum solved this problem. The vacuums input line was connected to the vacuum reservoir chamber as shown in figures 3.8 & 3.9. These vacuums were selected because they were easily obtainable, that way testing could start as soon as possible.

Finally, a custom LabView© interface was created for these tests. The National Instruments© PCI-4351 hooked up to a TBX-68 board and came with a custom LabView Data Logger that was modified to fit our needs. The original LabView application that

came with this DAQ card was the Data Logger, Graph, & Thermocouple Temperature readout.

Figure 3.11 shows the many items that were then placed in the custom LabView panel such as: Two Heat Flux Calculate so heat flux could be calculated from the input voltage and the thermocouple readings, and an overheat alarm which gave an audible warning if the heater was approaching its upper limits.

The data from the experiments was then logged to excel and then placed into a template file, which displayed graphs of Temp vs. Time and Heat Flux vs. Time.

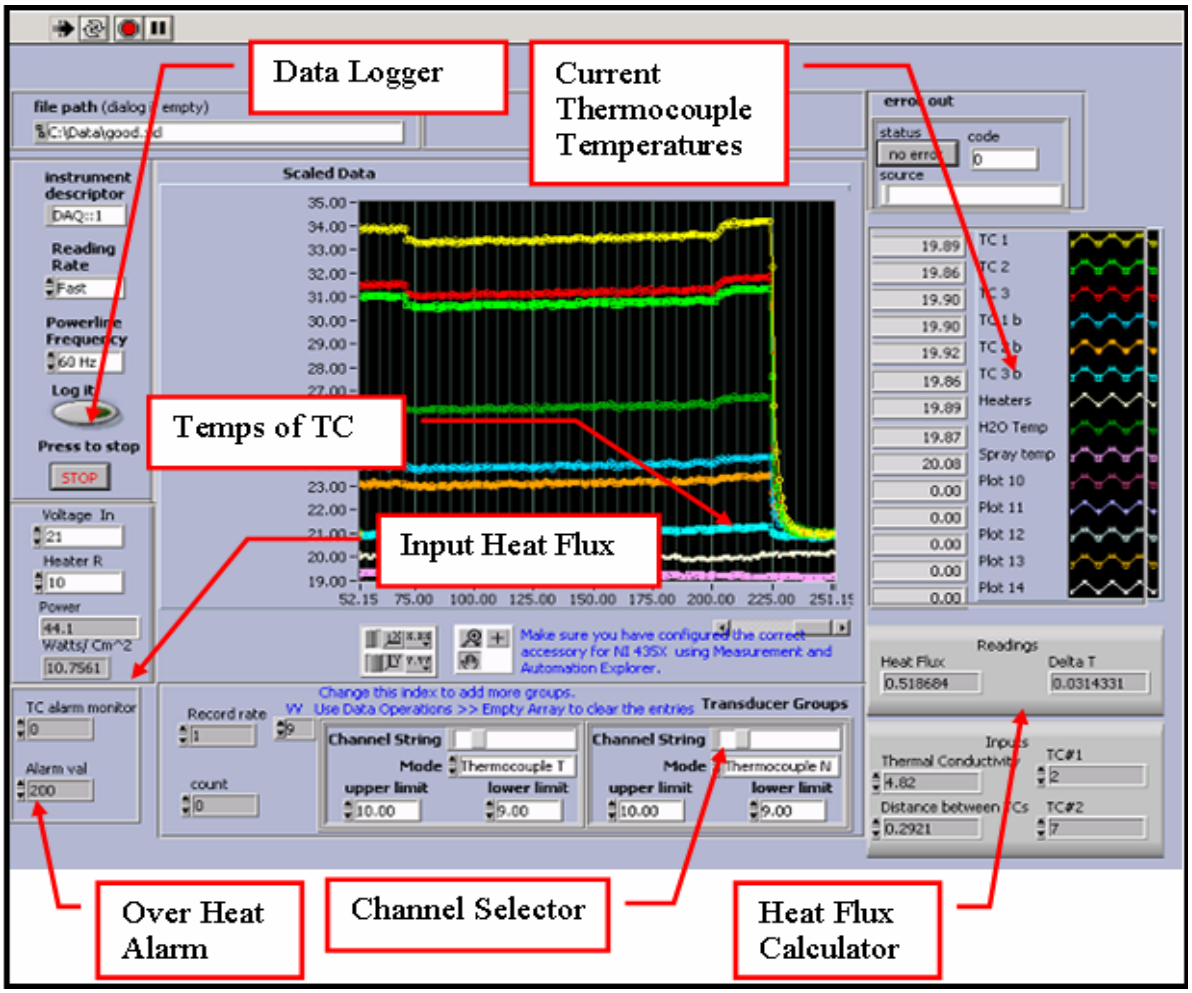

Figure 3.11: Custom Labview© Layout

Interfaces such as LabView or DasyLab© allow easy viewing of the data collected in real time. The thermocouple board used again was a TBX-68T from national instruments; this board utilized a built in cold junction and a differential reading mode. The differential reading mode allowed for higher thermocouple accuracy, this setup used T-type thermocouple and had a reading accuracy of 0.07°C; however, the thermocouple has an accuracy of 0.3°C. It is important that the thermocouple wires were kept away from any high power lines such as AC-power lines, because this increases the noise that the DAQ must filter out and thus reduces the accuracy. The sampling rate was adjusted in LabView from 60Hz to 1 Hz so that the data recorded to Excel could be more manageable.

3.5 Fluid Dynamic Analysis and Setup

A fluid dynamic analysis was conducted so that the removal of the excess liquid from the cooled surface may be maximized. All of the experiments concerning visualizing of the fluids were done in horizontal position and in the absence of heating. Suction effectiveness is defined by Eq. 3.1.

$$Eff_{Suc} = \frac{\dot{V}olume_{in} - \dot{V}olume_{edges}}{\dot{V}olume_{in}} * 100\% \qquad \text{(Eq. 3.1)}$$

The spray cooler has one input and two exits, one being over the edges and the other being the siphons. The input volume flow rate was measured with the suction

system off. The volume flow rate over the side ($Volume_{edge}$) was then measured when the suction system was turned on.

The main steps taken to improve the suction effectiveness were done by modifying the suction tube or siphons in the spray cooler. For visualization purposes a clear piece of grooved Plexiglas was used to replace the grooved copper plate (Fig. 3.6). All of the observed flows were transferred to AutoCAD drawings for easy visualization.

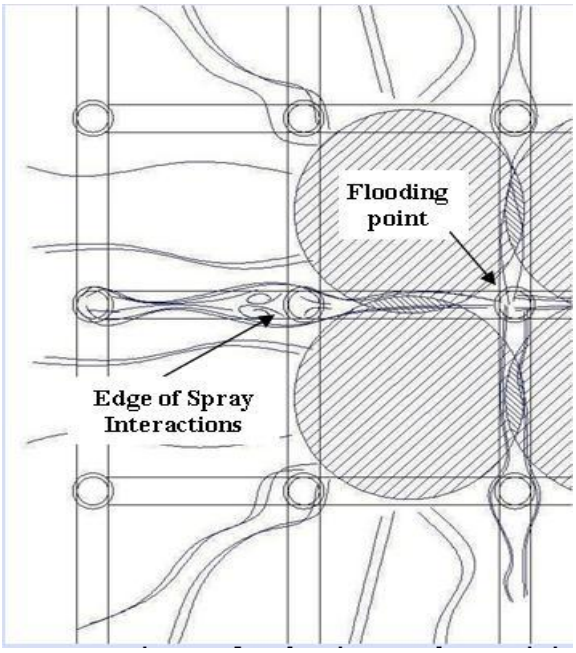

Figure 3.12: Observer Flow from Bottom of Grooved Plate: Un-Modified Siphons

Figure 3.4 shows the fluid flow observed from the side of the spray cooler in the 4 nozzle spray nozzle arrangement. The full 16 nozzle fluid flow could not be observed from the side of the spray cooler due to a lack of visibility created from excess misting. Figure 3.4 shows clearly that the fluid has to pass underneath the siphons to be removed

from the cooled surface. Figure 3.4 also shows a small amount of flooding in between the four nozzles.

Figure 3.12 is a bottom view of the grooved plate in the horizontal configuration, only the left portion of the plate is shown here since the flow pattern is symmetric. It should be noted that the fluid mainly exits via spray cone interaction lines as in Fig. 3.3. Additionally, it was noticed that the grooves in the Plexiglas helped channel the fluid away from the spray cones.

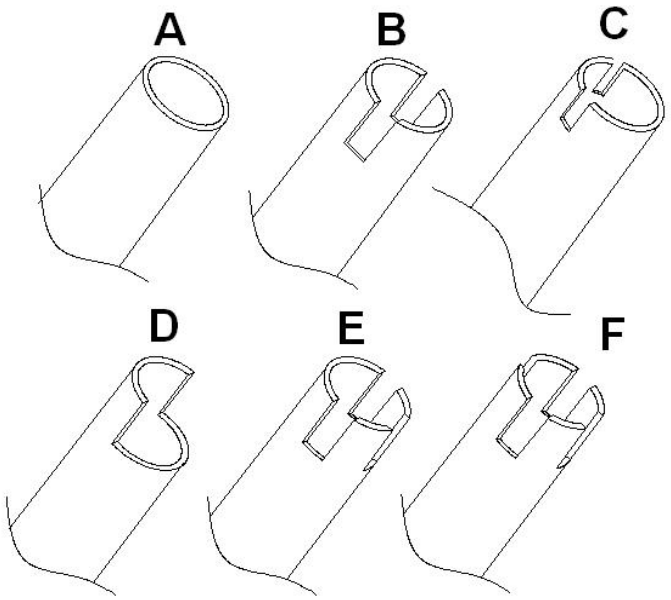

Figure 3.13: Modified Siphon Designs

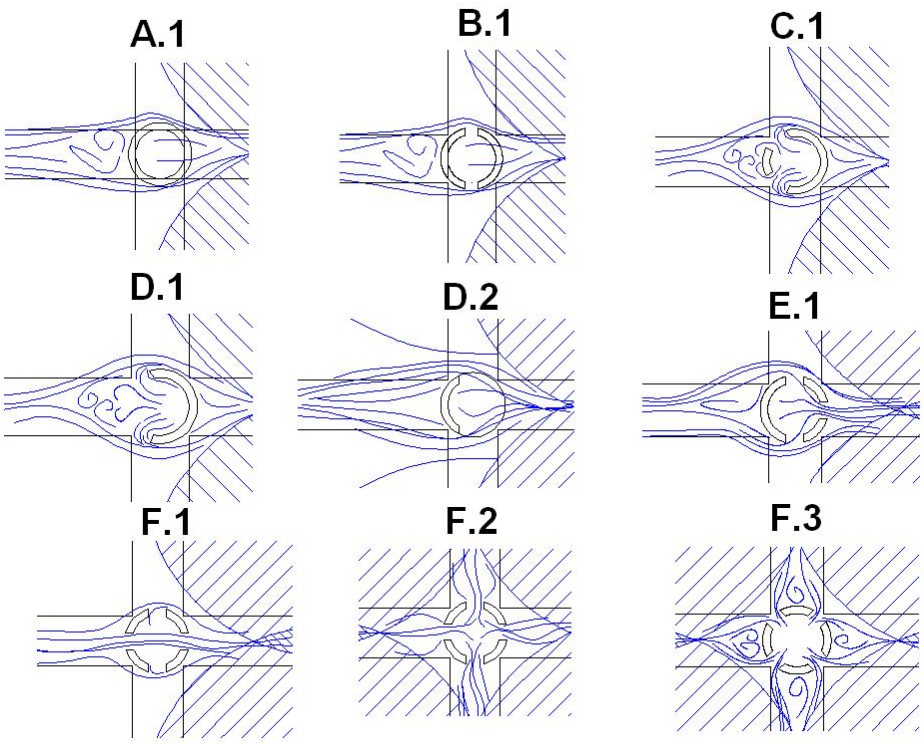

Figure 3.14: Fluid Dynamics Visualization around the Base of the Siphons

The siphons were placed at the intersection of the grooves on copper plate to catch the excess liquid, but due to the high fluid momentum a lot of the excess liquid flowed around the siphons then off the edge of the cooled plate (Fig. 3.12). The poor efficiency results (Eff_{suc}< 50% for 4 nozzle array at 30 Psi head pressure) obtained from this initial siphon design led to the design and testing of five different siphon nozzles as seen in Fig. 3.13.

The siphon designs are as follows: siphon B has two slits opposite to each other, siphon C has two slits at 60° to each other, siphon D is a 160° cut of the tube, and siphon E had three cuts each at 90° from each other, and siphon F has 4 equally spaced cuts. These siphons were then tested in several areas in the spray cooler and the flow around

them was noted with the suction on and off. The results of these tests can be seen in Fig. 3.14. The bulk of the liquid leaving the plate flowed down the grooves shown in figure 3.14 from the right to the left and then around the modified siphons. The flow around the unmodified siphons (siphons A) can be compared to the flow of air over an infinitely long circular cylinder [48].

Again, the effectiveness of siphon at removing excess liquid was determined by observing the flow through the clear grooved Plexiglas plate. Due to the space constraints the fluid velocity on the grooved plate could not be measured around or in front of the siphons. All of the siphon designs were tested at the edges of the spray interactions (Fig. 3.12). Only Design F was tested between the spray cones at the fluid build up points shown in figures 3.12, 3.13. The results of these tests are shown in Fig 3.14.

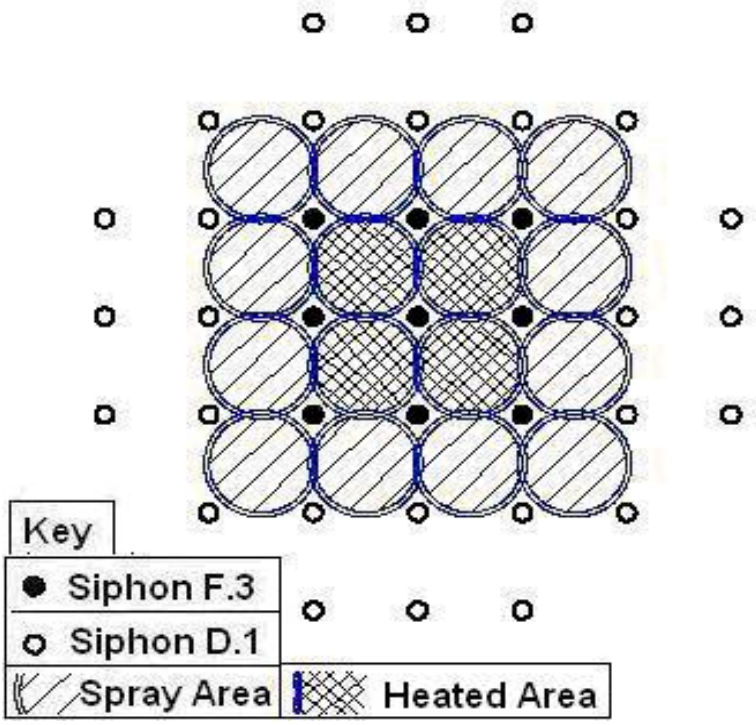

Figure 3.15: Siphons Placement and Siphon Type, *ref to Fig 10 for Siphon Type*

Siphon A.1 in Fig. 3.14 was the least effective in removing liquid from the cooled surface. This is due to the liquid flowing around the siphon with a very small amount fluid being removed by flowing under it. Siphon B.1 also showed a low effectiveness in removing the liquid. This can be accounted to the liquid flowing faster around the sides due to circular shape of the siphon. Siphon C.1 was based on the idea that behind the siphon a steady wake region was formed [48]. This region would have a reduced pressure so it should be a logical place to extract the excess liquid. Testing this design confirmed that it was better at liquid removal. This was taken one step further in siphon D.1 which when tested was an improvement over siphon C.1. Siphon D was tested in different orientation the most notable being siphon D.2 which was not as effective as siphon D.1. Siphon D.1 & E.1 was tested in the hope that the stagnation point in front of the siphon would force the liquid into it. But upon testing E.1 showed the same effectiveness as siphon D.2. Siphon F.1, surprisingly, allowed liquid to flow through the siphon. Only siphons F.2 & F.3 were tested between the spray cones at the fluid build up points, because they had the most even slit distributions. Testing proved that siphon F.3 was superior to siphon F.2. These series of siphon tests lead to the final spray cooler design which is slightly different than the one shown in figure 3.7 for it had additional siphons on the outside of the spray area, this new layout labeled design 2 can easily be seen in Fig. 3.15.

3.6 Suction Effectiveness Testing

The suction system was tested at two levels of suction, the first being only one suction pump that producing 2 in-Hg at the suction reservoir and 1 in-Hg in the suction manifold. For the second level of suction two suction pumps were used in series to

produce 4 in-Hg at the suction reservoir and 2 In-Hg at the suction manifold. The method of determining suction effectiveness is described at the beginning of the fluid dynamic analysis section.

The suction system underwent one evolution from *Design 1* to *Design 2* before the actual thermal testing; details on design 2 can be seen in Appendix B. Design 1 was the initial suction system design where *only 25* siphon tubes were employed to regulate flooding on the cooled surfaces; whereas, design 2 *utilized 37 siphon tubes* to drain the cooled surface. All suction efficiency data is the average of four trials.

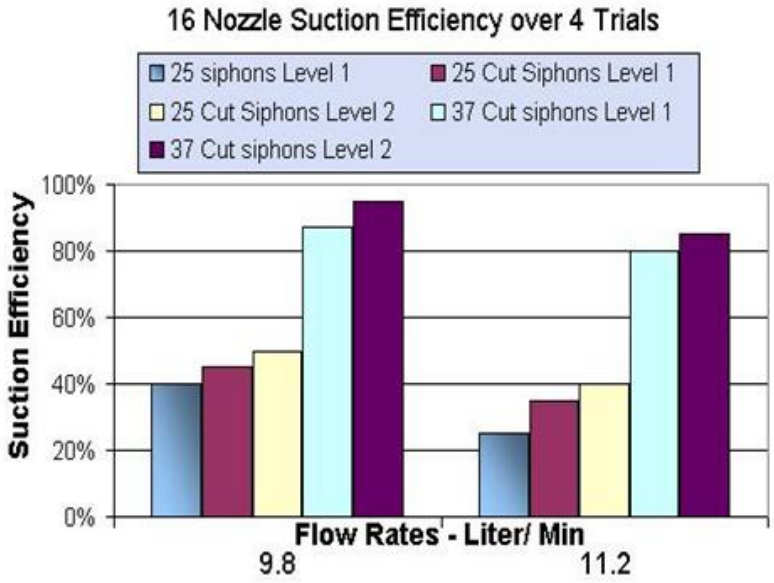

Figure 3.16: Suction Effectiveness for a 16 Nozzle Array-Without Heating

Figure 3.16 shows that the suction effectiveness was greatly improved by the addition of the 12 extra siphons outside the spray-cooled area. This led us to conclude that the bulk of the fluid is removed at the edges of the spray-cooled area not in the center as has hoped for. Without the suction it was observed that the edges of the spray cooler

(design 2) were completely flooded with liquid that flowed freely over the sides. With the suction on, regardless of the suction level, it was observed that the spray cones would become visible and liquid flowing over the sides would reduce to a trickle the results of the suction effectiveness testing can be seen in figure. 3.16. It should be noted that the suction effectiveness testing used the amount of fluid flowing over the edges of the spray cooler as an indication of how well the suction system was working. This testing could not determine how much liquid was being removed at the center of the array where flooding is the largest problem.

3.7 Thermal Design and FEM Analysis

It was decided to heat only the areas of the 4 inner spray cones; the heated area can be seen in Fig 3.15. This was done for several reasons: the design of the heater was much more simple and compact; the heat flux would be more uniform over a smaller area ($4.41 cm^2$), and the electrical input power would be lower and more manageable.

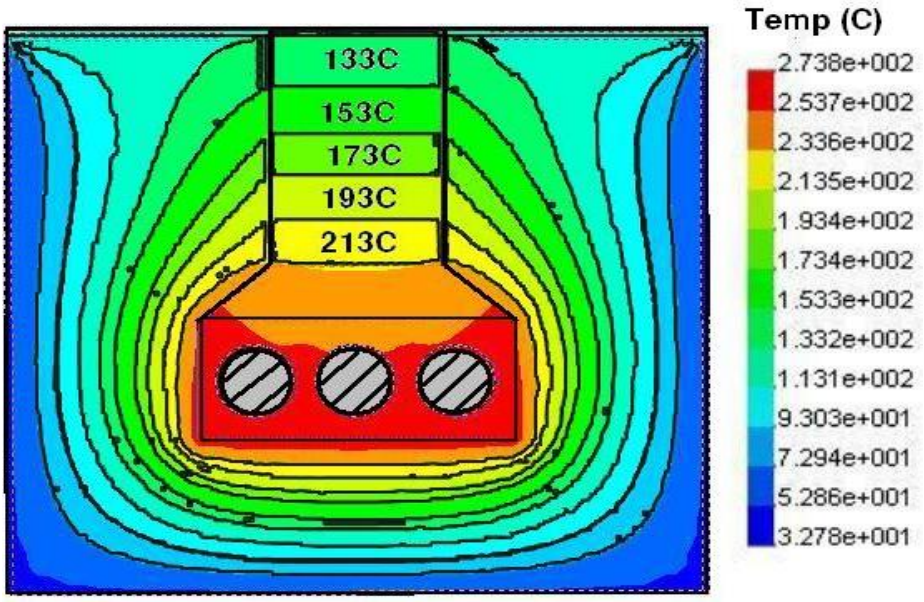

Figure 3.17: Sectional Temperature Profile of Heater

A pedestal heater was chosen for the heating, mainly due its accuracy in measuring heat flux via differential temperatures. Figure 3.17, 3.18 shows the detailed design of the pedestal heater where all the units are in mm. The pedestal was machined out of a solid piece of pure copper. Three 3/8 in diameter by 2 in length, 400 Watt cartridge heaters were inserted in the three holes at the base of the pedestal block and hooked up in parallel (total resistance of 13Ω) to provide even heating. The pedestal heater was insulated all around with DuraBlanket© insulation which has a thermal conductivity of k = 0.013 W/m-K [46]. The pedestal heater was soldered to the 1mm grooved copper plate with aluminum solder which has a melting point of 250°C. Assuming a perfectly insulated pedestal the theoretical maximum heat flux of

$$\frac{E_{in}}{A_{top}} = \frac{3*400W}{2.1cm*2.1cm} = 272\frac{W}{cm^2} \qquad \text{(Eq. 3.2)}$$

Six thermocouple holes were drilled around the neck of the heater; their spacing from the top of the heater is 5.08mm, 15.24mm and 22.86mm for thermocouples (T.C.) T_1, T_2, & T_3. Thermocouple T_{1b} through $T_{3\ b}$ are a mirror image of T.C. T_1 – T_3. Additionally the distance T_1 is from the cooled surface 5.08 mm plus the thickness of the grooved copper plate, which is 1mm. Now, the symbol $X_{1\text{-}w}$ will represent the distance T.C. 1 is from the cooled surface, which is 6.08mm. The distances between the T.C.s is needed to calculate the experimental heat fluxes and are as follows. The distance between

TC_1 and TC_2 will be denoted by the symbol $X_{1\text{-}2}$ that is 10.16mm. Following this notation $X_{2\text{-}3}$, and $X_{1\text{-}3}$ are 7.62mm & 17.78mm respectively.

A Finite Element analysis was conducted on the heater block with the use of Cosmos Design Star 3.0. The FEM analysis was conducted to find out the effects of heat spreading at the cooled surface and to see if 4.8mm depth of the T.C is enough to accurately measure the heat fluxes.

The results of the FEM analysis were displayed in Fig. 3.17. Here the three heaters were supplied with 205W each for a total of 615 W, which translates to a theoretical heat flux of 140 W/cm^2 over the top area of the pedestal, which is 4.41 cm^2. In the FEM analysis the top of the pedestal was maintained at a temperature of 127°C and the outer surfaces of the DuraBlanket insulation was cooled at 5 W/cm^2 and at a sink temperature of 50°C, to simulate water flowing over the sides of the heater as it occurred during experimentation. The thermal conductivity of the copper was taken as 393 W/m-K.

The temperature distribution along the pedestal heater is a uniform gradient, thus implying that the flux inside of the pedestal is uniform too. The FEM model shows a heat flux of 135 +/- 2 W/cm^2, inside the neck, whereas, the heat fluxes through the Durablanket insulation is less than 0.5 W/cm^2 around the neck. From this one can conclude that the FEM models is predicting a loss of,

$$E_{in} = E_{out} = E_{cooled} + E_{loss} \qquad \text{(Eq. 3.3)}$$

$$615W = 135\frac{W}{cm^2} * 4.41cm^2 + E_{loss} \qquad \text{(Eq. 3.4)}$$

$$\frac{E_{loss}}{A_{out}} = \frac{61.5W}{302cm^2} = 0.2\frac{W}{cm^2} \qquad \text{(Eq. 3.5)}$$

Solving for E_{loss}, the heat loss through the insulation is found to be 61.5 W at the outer heater shell is. Taken the outer surface area of the heater shell is to be 302cm^2, gives a heat loss of 0.2 W/cm^2 on the outer shell of the heater. The FEM model results were proven valid after comparing the predicted heat loss of the FEM analysis to the actual experimental heat loss.

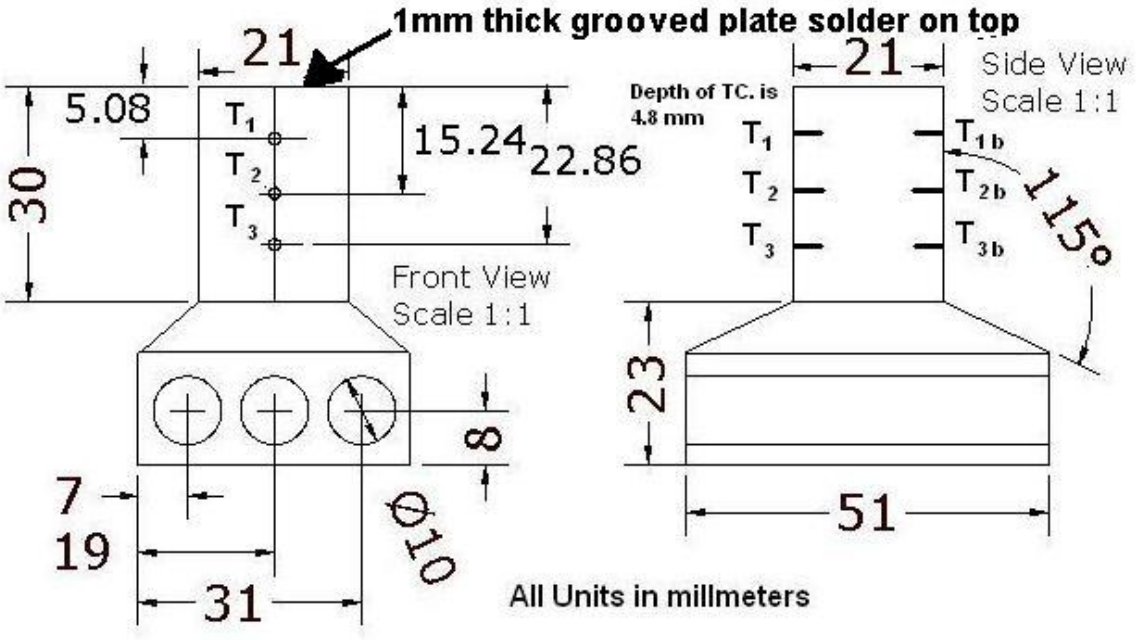

Figure 3.18: Heater Design with Thermocouple Locations

3.8 Thermal Testing Procedures

All thermal tests were conducted in the same manner. First the water in main water reservoir (Fig 3.8*)* was heated to 70°C, and then the spray coolers were turned on. Next the spray cooler were set to a flow rate of 9.8L/min, this setting was based upon the

head pressure of the spray coolers. The errors in the flow rates were estimated to be +/- 0.2 L/min that is based on the previous suction effectiveness testing data. Next the heaters were set to the desired heat flux, via an AC variac which range from 0 to 120 volts. The input voltage was read from a voltmeter with an accuracy of +/-0.05 volts. Thus the theoretical input heat flux was calculated by

$$E_{in,\max} = \frac{Volt^2}{R * A_h} \qquad \text{(Eq. 3.6)}$$

Equation 3.7 represents the maximum heat flux attainable, Note this agrees with Eq. 3.6.

$$E_{in,\max} = \frac{Volt^2}{R * A_h} = \frac{120V^2}{13\Omega * 4.1cm^2} = 270\frac{W}{cm^2} \qquad \text{(Eq. 3.7)}$$

Once the flux levels were set and a steady state temperature was achieved, the DAQ (National Instruments PCI-4351 hooked up to a TBX-68 board) would log all the channels at a rep rate of once a second. Secondly the DAQ measured temperatures in a differential or floating mode and combined this with a cold junction ground temp. error is +/- 0.35°C. The T.C data was collected for 1 min with the suction off, 1 min. with the suction at level 1, and 30 sec. with the suction at level 2. This was repeated for all successive heat fluxes up to a maximum input of 169 W/cm^2. Once one round of testing was completed the flow rate was readjusted to 11.2 L/min and the experiment was repeated. Additionally, the heaters were tested only up to 150W/cm^2 which is about 60% of their total power. This was done because the author could not afford to damage the heater.

3.9 Thermal Calculations and Results

A set of experimental data graphs are provided in Appendix E

The T.C.s temperatures were used to calculate the experimental heat flux via Eq. 3.8

$$q''_{n-m} = \frac{k_{inter} * (T_n - T_m)}{X_{n-m}} \qquad \text{(Eq. 3.8)}$$

Note: At 200°C, *k* for copper is 393 W/m-K and at 27°C; k is 401W/m-K.

The cooled surface temperature T_w was calculated via T_1 and the averaged heat flux.

$$T_w = T_1 - \frac{q''_{ave} X_{1-w}}{k_{inter}} \qquad \text{(Eq. 3.9)}$$

3.10 Thermal Results and Uncertainties

This section presents the experimental heat transfer data from the spray cooler design 2 with 37 siphons in the form of two plots. Both plots show average heat flux vs. T_w- T_{sat} and are for water sprayed at 70 +/- 1°C, only their input volume flow rates per nozzle differ from between the two plots labeled Fig. 3.19 to Fig. 3.20.

Figure 3.19 shows the impact suction has on the heat flux at a input flow rate of 9.8 Liter/min. The flooded surface situation presented in Fig 3.19 by the trend line labeled "NO Suction". From the "1 Vac" line (One Vacuum) one can see an average improvement from the pervious of 20W/cm^2 at similar T_w-T_{sat} temperatures above 10°C. Secondly; the "2 Vacs" trend line shows even greater improvement over the flooded

situation. In Fig. 3.19 the "2 Vacs" trend line shows an average of 30W/cm^2 for similar temperatures above 5°C for T_w-T_{sat}.

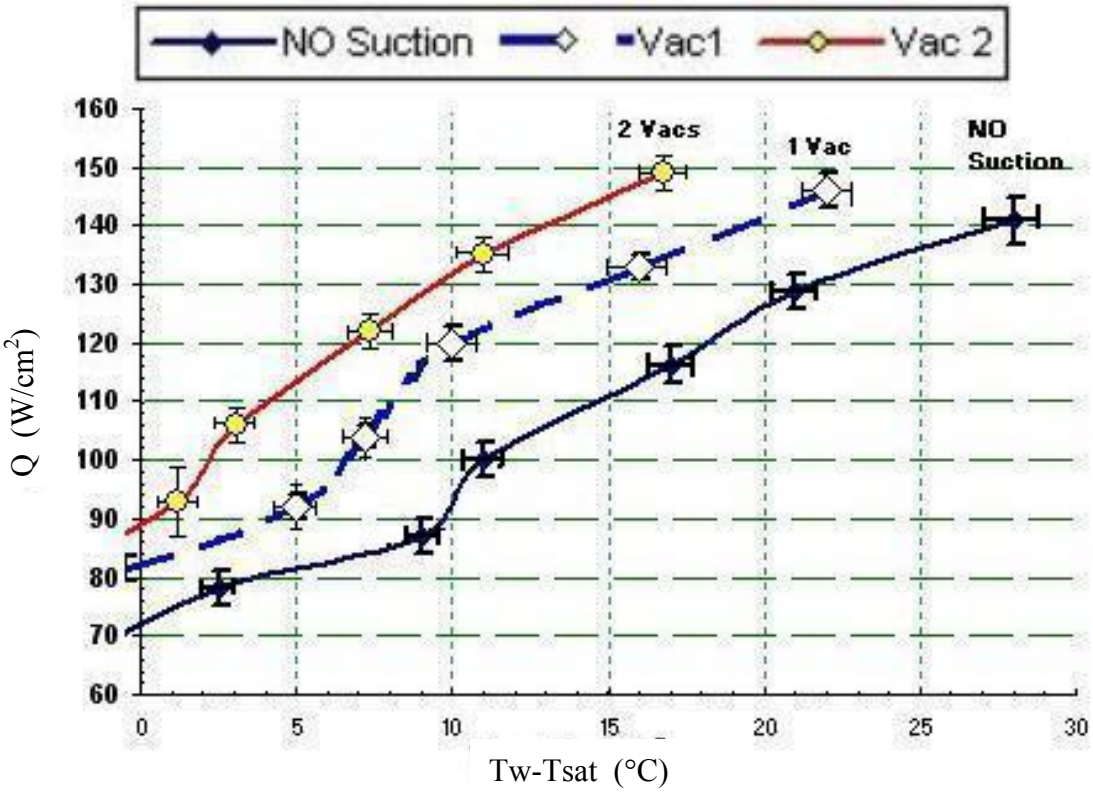

Figure 3.19: Q vs. T_w-T_{sat} for 20 Psi Head Pressure

at Flow Rate of 0.6125 L/min per nozzle

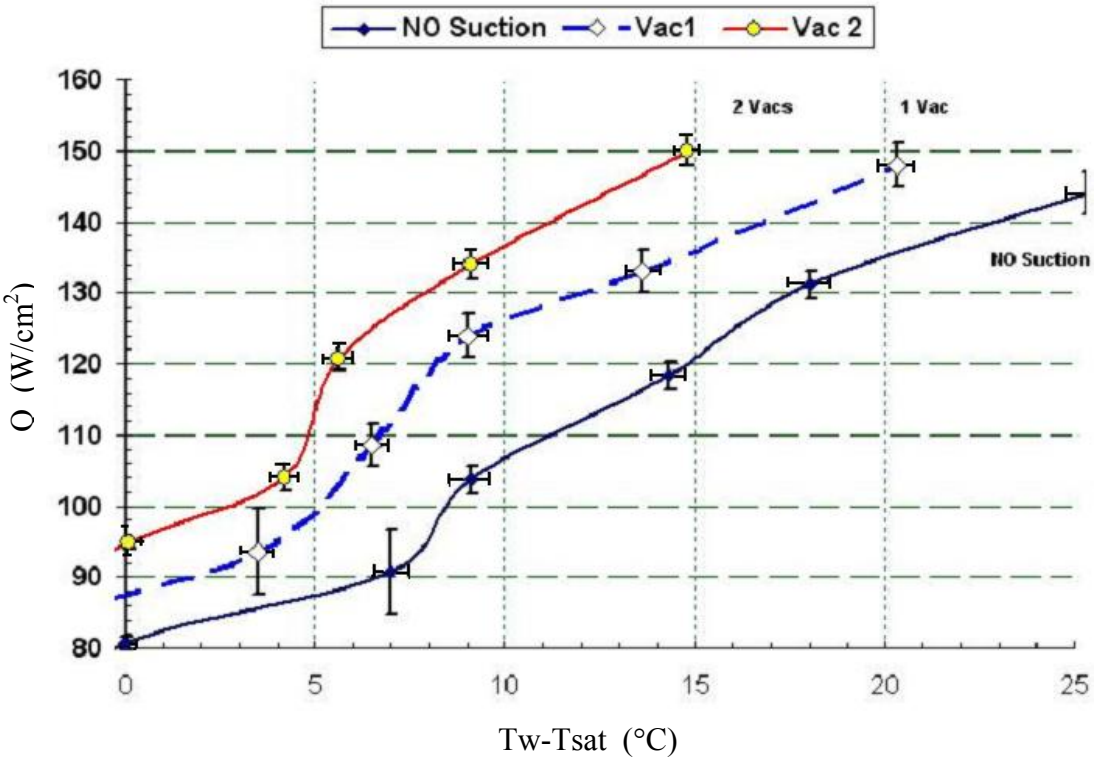

Figure 3.20: Q vs. T_w-T_{sat} for 30 Psi Head Pressures

at Flow Rate of 0.7 L/min per nozzle

Figure 3.20 shows the heat flux vs. T_w-T_{sat} results for a higher input volume flow rate of 11.2L/min. The higher spray nozzle volume flow rate along with the increase in droplet velocity [49] due to higher head pressures helped the heat flux on the average 10W/cm^2 over the results shown in Fig. 3.19. Figure 3.20 also shows that the suction improves the heat flux at a similar T_w-T_{sat} temperature.

From both plots one can see that the higher the suction the greater the heat flux achieved. Greater heat fluxes could have been achieved if the smooth grooved copper plate top surface was roughened by sand blasting. But this was not done because it was outside of the scope of this experiment.

Experimental results from the thermal testing show at an input power of 615W the heat loss was 96W, this translates to average heat loss of 0.3 W/cm^2 through the shell of the heater. The similarity between the FEM heat loss result, which was 0.2W/cm^2, and the experimental heat loss helps validate the FEM analysis.

Uncertainties in this experiment were calculated in detail and can be seen in Appendix D. The thermocouples on both sides of the heater were systematically 0.4°C different from each other. This causes a slight difference in the heat fluxes calculated from T.C. 2b, it was also found that T.C. 2b was not in direct contact with the copper block as the other T.C.s were. This created a slight discrepancy in the data, and thus the heat fluxes calculated using T.C.2b were not used. The plotted averages of heat fluxes had an error of 2 to 3 W/cm^2 at higher heat fluxes. The error in the calculated surface temperature is heat flux dependent and is mainly due to the error in the thermocouples (+/-0.35°C). At high heat fluxes the error in the surface temperatures were +/- 1.5°C. Also the calculated surface temperature could have a systematic error due to the solder contact between the copper heater and the copper grooved plate, this error was estimated to be +/- 1°C.

3.11 Discussion

Comparing the data collected from this experiment to that of a single nozzle's data shows the effectiveness of the suction system at improving heat transfer. Tilton's dissertation provides spray cooling data for a single nozzle spray cooler using water at a 25°C subcooled, which is very similar to the subcooled temperature of 30°C in this experiment [50]. The nozzles used by Tilton were T.G.3 of Spray Systems and had a flow rate of 0.26 liters per nozzle. Tilton found that increasing the flowrates increase heat

transfer in his single nozzle setup, the highest heat fluxes were recorded at the highest flowrates which was at 0.438 liters/min. Figure 3.21 compares heat flux vs. superheat between the single nozzle and multiple nozzle arrays.

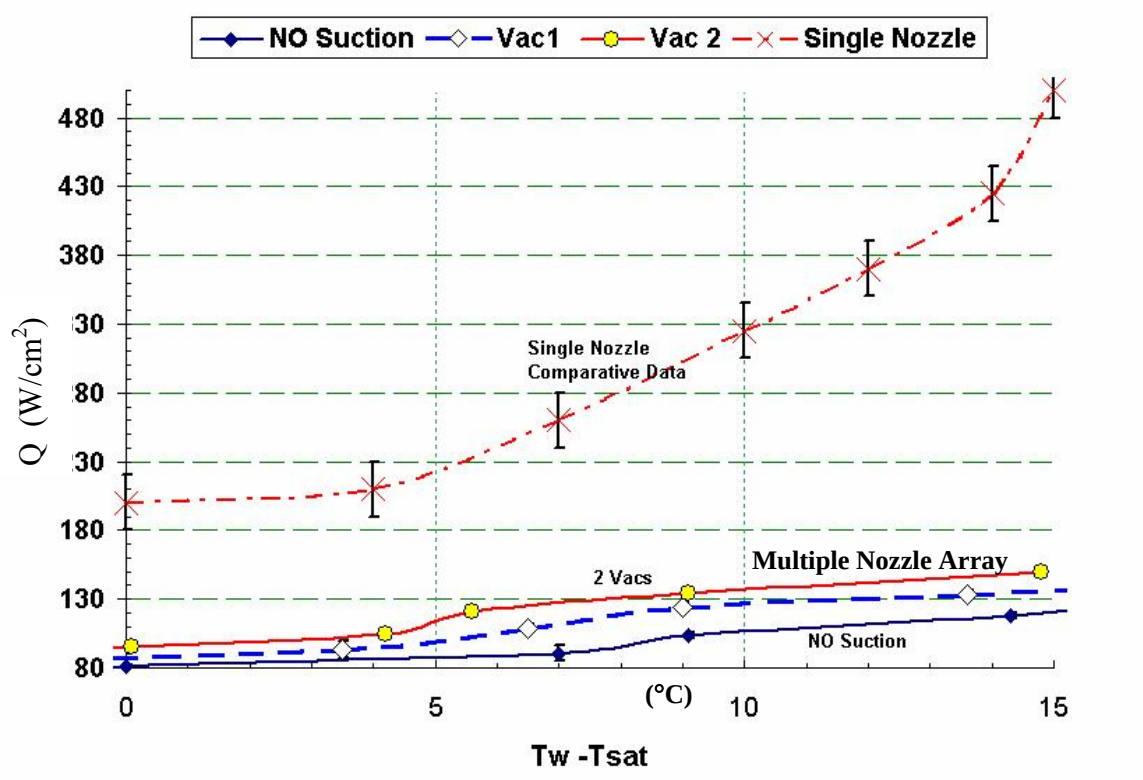

Figure 3.21: Comparison of Heat flux vs. Superheat for

Single Nozzle to Multiple Nozzle

The results of the multiple nozzle array are most unsatisfying when compared to that of the single nozzle spray cooler at a similar level of sub-cooling. Between superheats of 0-5°C the multiple nozzle arrays has 50%of the heat transfer of a single nozzle. At super heat above 5°C the single nozzle quickly departs from the multiple nozzle arrays' trend line. At superheats of 10°C the heat transfer is 40% and at 15°C the heat transfer drops to 30% of a single nozzle (without suction). This effect was

mentioned by Lin [45]. The fluid management system did increase heat transfer but not to a great degree when compared with that of the single nozzle's data. The fluid management system increased heat transfer from 40% to 50% for 10°C superheat and from 30% to 40% for 15°C. Ideally one would want the heat flux vs. superheat curve of a multiple nozzle system to be similar to that of a single nozzle system. This did not happen in this experiment.

Although Tilton's data indicated better heat transfer performance at higher flowrates his tests were done with a single nozzle in which excess fluid would run off and not lead to flooding. Unfortunately, the suction effectiveness testing could not determine how much liquid was being removed at the center of the array where flooding was unfavorable. Moreover, suction effectiveness testing did not give a measurement of the liquid film thickness in the inner four spray cones, where it was critical. The extremely poor heat transfer curves associated with the multiple nozzle array spray cooler did not correlate with any data from spray cooling with water [4]. The heat transfer curve for the multiple nozzle spray cooler in figures 3.19-3.21 more closely resembles that of forced convective boiling than spray cooling [1]. Assuming the droplet velocities of the single nozzle by Tilton and multiple nozzles GG-FullJet were the same, and that surface roughness only played a minor role in heat transfer the only explanation for the poor heat transfer of this array would be attributed to flooding still taking place, in which the excess fluid caused a thick film of liquid to form not a thin one as desired. The thick film caused the heat transfer mechanism to be mainly forced convective boiling not the desired spray cooling.

It was also observed that increasing the flow rates to the multiple nozzle spray cooler increased heat transfer. In single nozzle spray cooling increasing the flow rates increases heat transfer [4]. However, since it was concluded that the heat transfer mechanism was mainly forced convective boiling and not spray cooling, an increase in flow rate would increase the spray velocities. This would result in increased heat transfer for the multiple nozzles array due to the additional convection associated with the increase flow rate and additional agitation of the heat surface due to increase spray momentums.

Now, why did heat transfer increase with suction? If one assumes that the heat transfer mechanism was forced convective boiling across a thick film, one can deduce that suction increases heat transfer by reducing the film thickness slightly and directly removing excess heat. If the suction reduced the thick film thickness slightly, the vapor created at the heated surface would have an easier time of being released to the atmosphere. Additionally, a reduced film thickness would allow the impinging spray to create more convection. This would be due to the reduced film thickness lessen the resistance to the momentum of the impinging spray, resulting in increased agitation at the heated surface. The other reason is that the suction system removed heat directly. The siphons would remove some of the heated liquid at the hot surface. Removing some of the heated liquid through the siphons would have created another exit path for the heated liquid to escape. The exact amount of liquid removed by the inner siphons was unknown so this explanation can not be taken any further. Unfortunately, the exact reason why the heat transfer increased with the aid suction systems is unknown.

3.12 Conclusion to Chapter

The fluid management system or suction system which regulated flooding on this 16 nozzle spray array improved heat transfer on the average of 30W/cm^2 for similar values of superheat above 5°C. The heat transfer curves associated with the multiple nozzle spray cooler, even with the aid of the suction system, are well below any heat transfer data from a single nozzle spray cooler. Thus, it is concluded that the heat transfer mechanism taking place was mainly forced convective boiling and not spray cooling. This would be due again to the initial design problem being flooding of the sprayed surface due to excess fluid from the spray nozzles not being removed effectively. The excess fluid leads to a film to thick for effective spray cooling. This pushed the heat transfer mechanism from a spray cooling regime into a less effective forced convective boiling regime.

The suction system was optimized by a series of suction effectiveness tests. Modification such as adding extra siphons to the outside of the spray area and adding small slits to the sides of the siphons also increased the suction effectiveness. However, it is now realized that the suction effectiveness testing could not determine the amount of flooding in the inner four spray cones where it was critical. Thus, it is unknown if the modification to the suction system actually help drainage in the inner four spray nozzles. Heat transfer did increase by 30W/cm^2 with the aid of the suction system. It was concluded that in a forced convective boiling regime the increase in heat transfer associated with the suction systems was due to the following. The suction systems could have slightly reduced the film thickness allowing for more convection to take place from

the impinging spray and the suction systems could have provided another exit path for the heated liquid to escape.

It is recommended that lower flow rate nozzles (0.07 to 0.2 Liters/min) with comparable droplet velocities to that of the FullJet (+30 m/s) & GG-3 nozzles should be used for a retest of this design. It is believed that reducing the flowrates will alleviate the flooding problem. Furthermore, the diameter of the siphons should be increased so that they may remove more fluid. Thus, this design shows promise but has not shown conclusively to solve the problem of surface flooding in a multiple pressure atomized spray nozzle array.

4. HIGH HEAT FLUX HEATER DESIGN

4.1. Introduction to Chapter

Through out the author's studies, he has found a lack of *detailed* information on high heat flux heater designs. Eventually, the author collected enough information from various publications and other people's theses to be well informed on the aspects of designing a high heat flux heater. Azar's *Thermal Measurements in Electronics Cooling* in particular gives a good overview of heat flux measurement devices [7]. This research prepared the author for designing two of his own heaters, which were proven to be solid designs through repeated testing.

This chapter outlines the process of designing and manufacturing a heater for high heat flux measurement. This will included in detail the following: type of heat source to select, methods of measuring heat flux, common problem associated with the high heaters and gives a step by step guide to designing a heater.

4.2. Heat Source Selection

Choosing the correct heat source is extremely important in a high heat flux heater design. Many heater options exist and the correct heater should be chosen based on the applications needs. The following questions should be answered to identify the needs of the application.

- What is the area or dimension of the area being heated?
- What is the desired maximum heat flux?
- What is the heat flux range in which the heater surface will be operating?

  Remark: For Spray cooling the bottom limit of this range is 40W/cm^2 and the upper can be 1000W/cm^2, so it is pointless to designing a heater to measure average heat flux around 20 W/cm^2.
- Will the heater be enclosed in a small space, or open to the atmosphere?
- What is the maximum temperature of the heated surface & the chances this temperature could go higher than you expect?
- How much space is allowed for the heater?

Answering these questions will help select the most appropriate heat source from the following list of possible heat sources: cartridge heaters, thick film resistors, ITO heaters, Quarts lamps, and thin wires.

4.2.1 Cartridge Heaters

Cartridge heaters are the author's most preferable form of heating; this is mainly due to their reliability, how simple they can be integrated into the design, and the heat density which they can provide. Heater cartridges are usually, cylindrical and range in nominal diameters of 1/8", 1/4", 3/8", 1/2", 3/4", 1" & bigger. The smaller diameters like the 3/8" and the 1/2" have the highest heat densities. The larger diameter heaters present thermal resistance problems, the heat generated in the middle of the heater has to travel a larger distance and thus has a chance of burning out at a lower surface temperature. The author recommends staying with cartridge heaters with diameters between, 1/4" to 1/2". Furthermore, cartridge heaters range in length from 3/4 " to a foot or more. When

choosing the length of the heater remember a hole corresponding to the cartridge heaters length must be made in the conduction material, usually copper. The longer the hole (2" or more) the more chance that it will not be able to be machined or the machinist will drill it incorrectly and a poor heater fit will occur. ***Note:*** A poor heater fit means that conduction between some points on the heater and the conduction medium may be low and cause a premature burnout of the heater at those points.

The number of cartridge heaters can range from 1 to 5 or more; it is mainly depended upon the heat flux requirements. So if you are heating an area of $1cm^2$ and want to provide a maximum of $1500W/cm^2$ then one can select four 400 Watt 3/8" diameter 2" long cartridge heaters to provide the needed heating. Remember heat loss at the higher heat fluxes may be as large as a 100W and mainly depends upon the design and placement of the insulation.

The cartridge heaters as far as the author knows do not have a maximum heat flux only a maximum inner temperature of 1000°F to 1600°F. This slightly limits the design and placement of the heater which will be discussed in the next section. Cartridge heaters can be purchase from companies such as www.mcmaster.com or www.omega.com. Omega provides much more literature with their heaters; however on McMaster it is easier to quickly select a heater. A sample spec sheet on cartridge heaters is included in Appendix A.

Cartridge heater heat densities are defined by equation 4.1. For example a high power 3/8" diameter cartridge heater has a maximum heat density of 100-110 W/cm^3, regardless of the length; whereas, a 1/2" diameter heater has a density of 60-70 W/cm^3,

regardless of the length. The cartridge heaters are listed according to their total wattage and their watts per surface area (W/cm^2).

$$\text{Heat Density } (W/cm^3) = \frac{4 * wattage}{L * \pi * D^2} \qquad \text{(Eq. 4.1)}$$

However, in high heat flux heater design only heat densities and heat per unit length actually are important. The higher the heat densities mean one can optimize the heat transfer of the heater by minimizing the heaters size and thermal resistance to the flow of heat. So, heat per unit length can be found by

$$\text{Heat per length } (W/cm) = \frac{wattage}{L} \qquad \text{(Eq. 4.2)}$$

Average heat per lengths for a 3/8" diameter cartridge heat are around 58-78 W/cm. It is important to look at this specification when selecting a cartridge heater, because this varies from model to model & length to length.

Controlling a cartridge heater is relatively easy; most if not all cartridge heater can be operated on DC or AC current. This is because there design is that of a coiled wire placed inside a quarts impregnated shell with a thermally conductive compound. Current passed through the internal wires causes it to heat up. The cartridge heaters range in resistance and maximum voltage. They come in two types 120 Volt or 220 Volt; both provide the same amount of heat, and the author recommends 120 Volts. The author's 2"

long heaters had an electrical resistance of 30Ω, and a max power rating of 400W. So using the following formula, one can find the power to be

$$P_{in,\max} = \frac{Volt^2}{R} = \frac{(120V)^2}{30\Omega} = 480W \qquad \text{(Eq. 4.3)}$$

One can see that the putting in the maximum wall outlet voltage will burn out the heater even with proper cooling. So this means if one is powering this single cartridge heater they must limit the voltage to 109V. When more then one cartridge is used they must be placed in parallel not series, if they are placed in series the first couple heaters will be heated more than the last. In parallel the heater resistance add together as,

$$\frac{1}{\sum 1/(\Omega Heaters)} = \text{Heater Resistance} \qquad \text{(Eq. 4.4)}$$

So three 35Ω heaters in parallel give 11.6Ω , and using Eq. 4.3 one finds that 400 Watts per heater (1200W total) and again the voltage is limited to 118 V. Now the amps needed to power this can be found by V/R=I, to be 10.2 amps. So the heaters would be attached in parallel to the variac but the variac has to be able to supply 10 amps or the maximum voltage will not be achieved. For this example say the variac could only provide 5 amps using V = I (5amps)*R (11.6Ω) gives 58 volts and using Eq 4.3 this only give 96 Watts per heater which is far below its capability of 400 Watts per heater. Thus one can see that it is extremely important that the variac has enough amperes to supply the cartridge heaters with the full voltage.

4.2.2 Quarts Lamp

The next type of heater is a Quarts lamp heater; however the author has not had much direct experience with this heater type. It operates based on the conducting medium absorbing irradiated energy of the photons given off by the quarts lamp. The quarts lamp is quarts bulb usually filled with halogen or xenon and powered by a platinum or pure tungsten filament. Controlling or powering this lamp is extremely complicated because the output of the lamp degrades over time. That means a PID controller is needed to operate the lamp and control its output. The quarts lamp creates heat densities comparable to that of cartridge heaters. The only design of a high heat flux quarts lamp heater the author know of is by M.S. Sehmbey & L.C Chow at University of Kentucky [4]. This heater utilized two cylindrical quarts radiation lamps capable of providing 1000W each. Sehmbey mentioned that the wires exiting the ends of the lamps would over heat and thus had to be cooled via force air convection. Another problem with the lamps is they can not be handled with bare hands because the oils from ones hands would fracture the lamp during operation. In the author's opinion this type of heat source is difficult to work with because: of the method of controlling, the reliability due to degradation and the problems with the wire end connections and thus should be avoided.

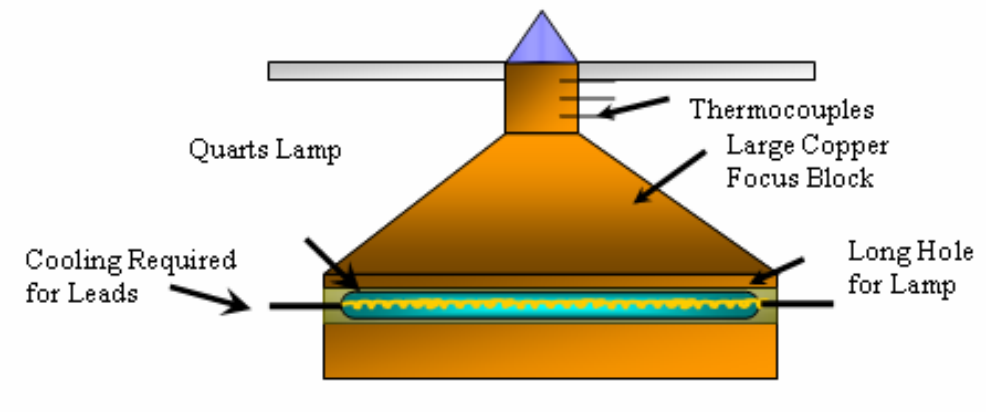

Figure 4.1: Quarts Lamp Heater Design

4.2.3 Thick Film Resistors

Thick Film resistors (TFR) are extremely cheap when compared to cartridge heaters and quarts lamps. A 1cm^2 thick film resistor can cost as low as $10 each. Thick film resistors vary in area from 1cm^2 to 3 by 3 cm square and have various other shapes. So far there is no maximum heat flux associated with the resistors only a maximum operational temperature. The temperature distribution across the thick film resistor should be isothermal. The thick film resistors are extremely brittle and any large temperature gradients would cause a fracture of the main substrate.

Thick film resistors come in a couple of types; but mainly display the same design. That is of a resistor film usually green, on top of a substrate sometime alumina (which is a ceramic) or glass; a sample spec sheet is attached in Appendix A and an example of a thick film resistor can be seen below.

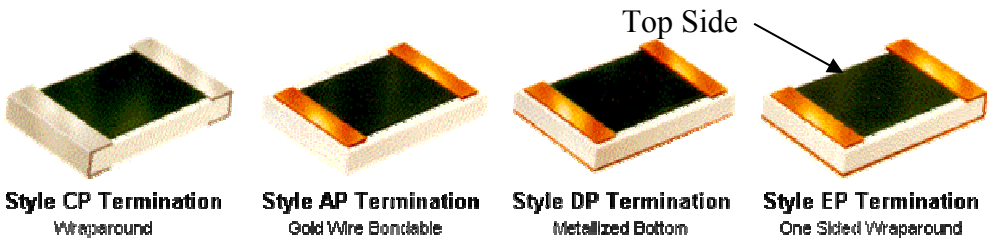

Figure 4.2: Thick Film Resistors

The heat generation surface of the thick film resistor is displayed as green in figure 4.2. In heater application the backside of the TFR are usually faced toward the cooling. The most common type of TFR has a metallic bottom seen in Fig. 4.2 because the back side of the heater can be soldered onto the cooling substrate. Figure 4.3 show the thick film resistor solder face down on to the cooling substrate, the solder insures that the heat flux through the contact will be even. The red arrow represents the direction of heat loss due to cooling and is represented by the symbol $\dot{Q}_{cooling}$. The heat lost due to the air on the TFR is denoted by the small lined red arrows and is represented by the symbol $\dot{Q}_{loss}$.

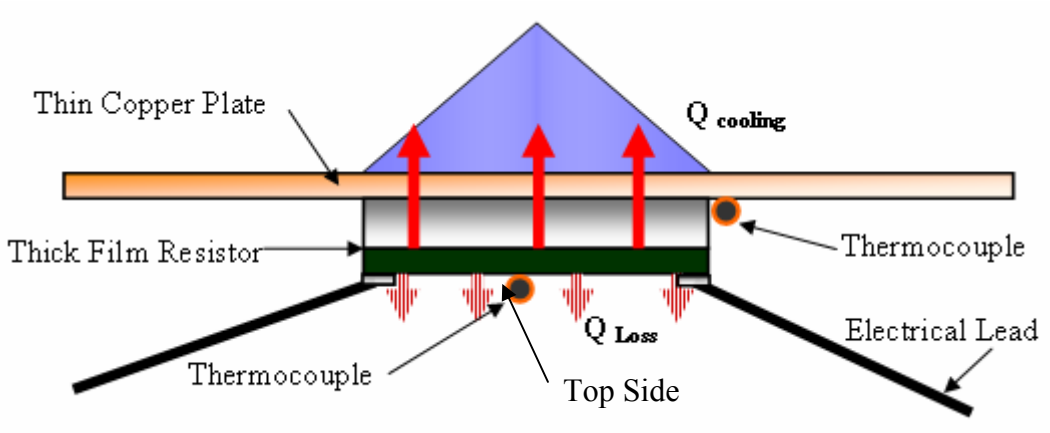

Figure 4.3: Thick Film Heater Using Estimated Heat Loss

The bulk of the heat passed via $\dot{Q}_{cooling}$ through the thin copper plate to the sink or in this case the spray cooler. A very small fraction of the heat is lost through the bottom to the air ($\dot{Q}_{Loss}$); this even though it is small must be quantified.

$$E_{in\ electrical} = \dot{Q}_{cooling} + \dot{Q}_{loss} \qquad \text{(Eq. 4.5)}$$

Assuming $\dot{Q}_{loss} << \dot{Q}_{cooling}$ the heat flux can be calculated as,

$$\dot{Q}_{cooling}(W/cm^2) = {}^{E_{in\ electrical}}\!/_{Area} \qquad \text{(Eq. 4.6)}$$

The convection coefficient has a high degree of uncertainty, and thus so does the estimated heat loss. The author's experience with this design, taught him several important things. Firstly, soldering the electrical leads onto the thick film resistor is hard because the TFR contact pads are fragile, and soldering an array of TFR is extremely difficult. Secondly, the thermocouple can not touch the green resistor film or they will become energized and burn out. Thirdly, the TFR's have a small operational window, that is they can't go above 150°C or 160°C or they will fracture. In other words, the thermal resistance of the copper plate and the TFR's substrate increase the backside temperature by 20°C to 30°C, so they easily can reach the operational maximum if one is not careful. Fourthly, they work well with coolants that have boiling points below 60°C and poorly for ones that have boiling points above 100°C like water. This is because the maximum operational temperatures are reached at low heat fluxes. Example, water

sprayed at 100°C and atmosphere pressure will only allow TFR to reach a maximum heat flux of 400W/cm^2 before the maximum backside temperature of 160°C is reached. Where as, ammonia sprayed with a boiling point of 40°C at 1atm will allow the T.F.R. to reach 600+W/cm^2. Overall, the first TFR design shown in figure 4.3 is not very robust and is not recommend for repeated testing.

The author's solutions to the TFR overheating problem, is to spray the TFR directly, on its backside, this can be seen in figure 4.4. This reduced the thermal resistance of the TFR and increases the maximum achievable heat flux. In this design the sides of the TFR are seal with a machined Teflon block and the gaps filled in with high temperature epoxy.

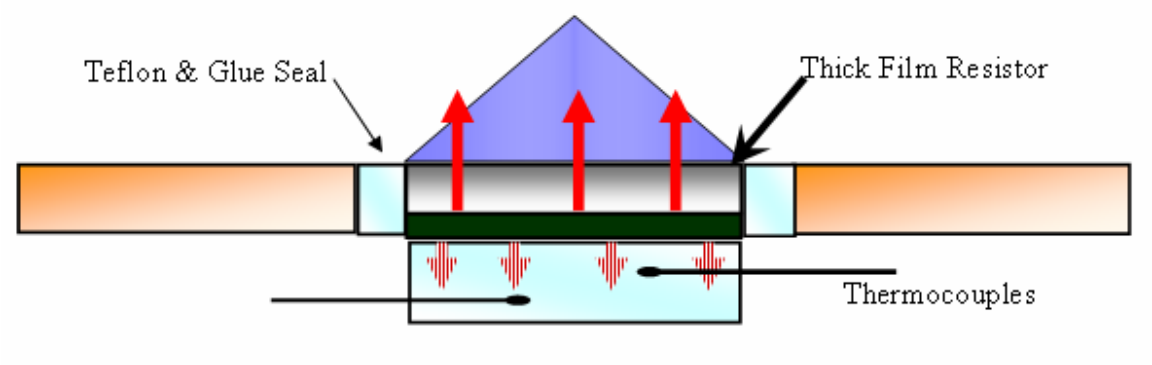

Figure 4.4: Thick Film Heater Utilizing a 1D Conduction Block

The $\dot{Q}_{Loss}$ can be measured in three ways, the first being thermocouples on the surface, which are used to estimate the convection coefficient and find the lost heat flux, again the author considers this some what inaccurate. The second way is to utilize a heat flux measurement block, to measure the loss heat flux seen in figure 4.4. However, in this design the distance between thermocouples must be very large to measure the small heat fluxes.

Figure 4.5: Heat Flux Sensor

So, this may be as inaccurate or worst than a single thermocouple. The final way which just presented itself involves a heat flux sensor which was invented by Omega Corp. in 2001. The sensor shown in figure 4.5 utilizes an array of thermocouples which has three layer of T.C and utilizes the temperature differences between the T.C.s to calculate heat flux. Some of the downsides to this sensor are that the thermocouples average the temperatures between themselves so an uneven heat flux will not be shown. The sensor is large at a size of 3.5cm by 2.8cm so only can be applicable to large TFR applications. And finally, the sensor has a max operational temperature of 150°C.

The concept of a heat flux sensor by omega can be extended to a customized one created for a specific application. A custom heat flux sensor could be manufacture utilizing thermocouples floating in air a fixed distance apart from each other. As long as the distance between the T.C.s is known accurately, and the spacing between them small, the sensor will measure heat flux accurately. The other alterative to having air between the T.C.s is placing at thermal barrier between of known thermal resistance. This will allow the heat flux sensor to measure larger heat fluxes.

The author's conclusions on thick film resistors are that they are well suited to high heat flux heater design where the surface temperatures do not exceeded 80°C. In addition, their low maximum temperatures of 150°C limit the working fluids that can be spray on to them. Finally, the heat flux measurements depend upon knowing the heat loss from the bottom of the TFR. Even though the heat loss may be small this does introduce error into the final heat flux measurement. This makes thick film resistors ideal for heater applications where surface temperatures are low and highly accurate heat flux measurements are not required.

4.2.4 ITO Heaters and Thin Wires

ITO heaters are short for Indium Tin Oxide and are interesting because they are transparent. In the case of spray cooling they would allow someone to visualize the bubble generation while spray cooling is taking place. They theoretically have infinite heat fluxes but have a limit on there operational temperature which is specified by the substrate which they are deposited on. The most common substrate used with ITO heaters is Quarts. The author does not see why this will not allow the heater to operate up to temperatures of 150°C or more. ITO heaters are relatively expensive and the author has

heard of quoted prices of \$1000 for $3cm^2$, but ITO is relatively easily created by any chip manufacturing lab and can be deposit on many substrates. Many ITO heaters have been made many times here at the University of Central Florida for a minimal cost.

The newest ITO heaters on the market are even being deposited on thin bendable plastic; however these substrates will never be applicable in high heat flux heaters due to their low thermal conductivity and low melting points. One utilizes an ITO heater exactly like the way a thick film resistor is used, except the heat is generated at the top surface and can be spray directly onto. This would allow the ITO heater to reach extremely high heat fluxes. Since the heat is generated at the top surface and cooled immediately the heat loss would be very small, and could be found by placing a thermocouple on the backside of the substrate. In other words one would assume 98% of the electrical energy is going into $Q_{cooling}$ and calculate the heat flux via Eq. 4.6. The measurement of the surface temperature is much more difficult since one can not place a thermocouple on top of the ITO surface. This is because direct electrical contact between the ITO film and the T.C. will energies the T.C and burn them out. If one would spray on the backside of the heater instead of directly on the ITO film one would then increase the thermal resistance greatly. However, spraying on the backside would allow one to measure the surface temperature with a thermocouple on the sprayed surface.

Another design which was manufactured at Wright Paterson Airforce base what that of an ITO heater deposited on top of a polycarbonate pedestal [12]. They used simple 1D heat conduction formula to calculate heat loss and surface temperature.

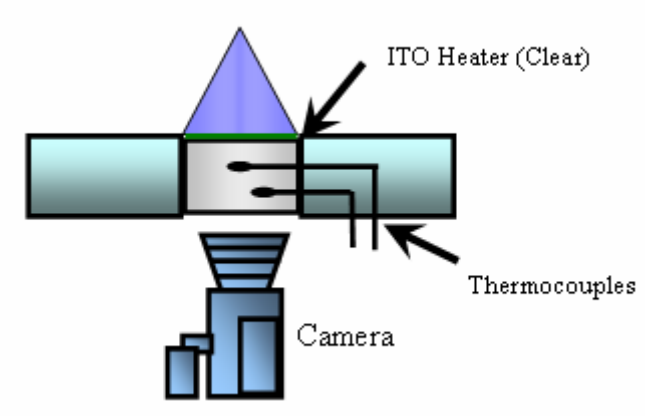

Figure 4.6: Ideal ITO Heater Setup

Thin wires are also a possible heat sources. Platinum & Tungsten thin wires utilize electrical current to generate thermal resistances which can provide heat fluxes in excess of 1500W/cm^2 at temperature of 1500K [51]. The problems with these wires are repeatability and the errors associated with heat flux and surface temperature measurements. The surface temperature of the wire is calculated based on the electrical resistance of the wire, thus a calibration curve is required to determine the surface temperature at a respective electrical resistances. The heat flux is only calculated by the amount of current going through the wire and the small diameters of the wires do not allow for redundant heat flux measurements. Unfortunately thermal cycling (going from low to very high temperatures) changes the electrical resistance of the wire slightly, this would change the calibration curve associated with the surface temperatures of the wire. Thus, a recalibration is needed after each high temperature test. Additionally, the heat flux of the wires can be uneven over the length of the wire and over the surface of the wire. All of these downsides make wire heat sources only suitable for extremely high heat flux measurements with extremely high surface temperatures.

4.2.5 Future Heat Sources

Heat sources such as cartridge heaters, thick film resistors, & ITO heaters are limited by their size, and operational limits. Future heat sources for high heat flux heaters should be able to attain extremely high temperatures and heat fluxes and offer distinct advantages over the current types of heat sources. Lasers, and microwave heat sources are presenting themselves as possible candidates. However, things like the uneven heating of laser and microwave beams present problems. Lasers as heat sources will not become possible until the high cost of high powered lasers come down to a reasonable level. But it is still possible to rent laser equipment for testing at a reasonable price. Microwaves as a heat source are becoming more probable because of the small size of their antennas. However, to utilize microwaves as a heat source one would have to deal with many problems like, how to provide even heating, how to trap all the microwaves with out burning out the antenna and how to power the antenna. Clearly future heat sources have a long way to progress before being utilized in high heat flux heaters. Luckily current heat sources like cartridge heaters and ITO heaters can provide high heat fluxes in very small packages which in the end might make them the most ideal technology for high heat flux heaters.

4.3 Heater Design

This section will concentrate on the design aspects associated with cartridge heaters as a heat source. This will include the orientation of the cartridge heater, the insulation used, and the methods of sealing around the heated surface.

Cartridge heaters used in high heat flux heater designs are always placed in some type of heat focusing block. The focusing block utilizes a high thermal conductivity metal

(almost always pure copper) to transfer heat from the cartridges to the heated surface. The shape and mass of this block governs the maximum operation heat flux, temperature and response time of the heater. Additionally, the cartridge heater may have operational temperatures up to 1600°F, & copper has a melting point of 1900°F but it becomes extremely ductile around 1100°F, so for safety the bottom temperature of the focus block should not exceed 1292°F (700°C). Thus, a careful design of the heater is required to meet ones designs goals & to not exceed the heater block's maximum temperature.

4.3.1 Cartridge Heater Orientation and Placement

Cartridge heaters can be placed in two orientations either vertically or horizontally, each orientation has the benefit of smaller size in the aligned direction. However the horizontal orientation has a slightly lower operational temperature.

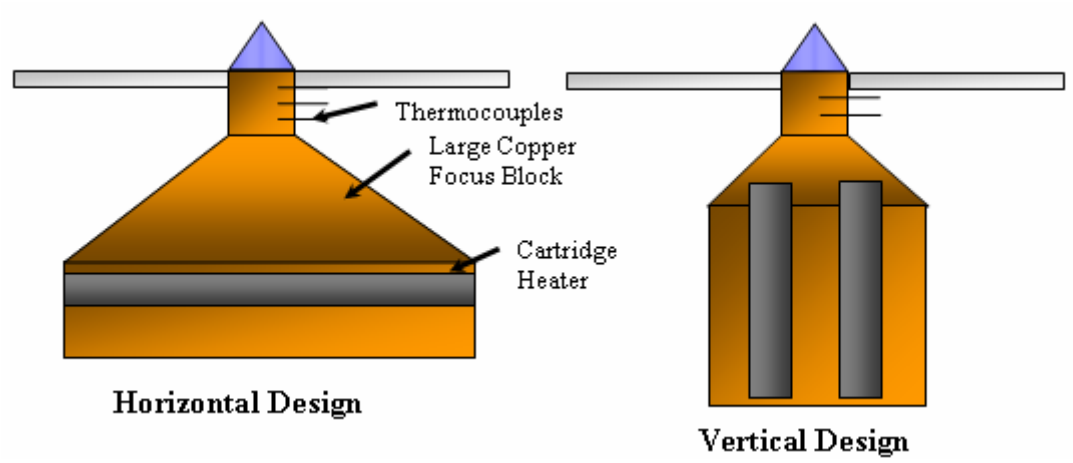

Figure 4.7: Cartridge Heater Orientations

The horizontal design heater in figure 4.7 shows the heater cartridge running horizontally inside of the focus block. In this case, the top of the cylindrical cartridge heater has a lower associated temperature than the bottom at corresponding heat fluxes.

This is because the heat generated at the bottom of the cartridge heater has to travel around the cartridge heater and then to the cooled surface. This increases the length of the conduction path for the bottom of the cartridge heater and consequently its associated temperatures.

In the vertical cartridge heater arrangement the bottoms of the heater cartridges have a much higher associated temperature than the top. Now, if the heater being designed requires extremely high heat fluxes, 1000W/cm^2, then cartridge heaters must be a minimum length of 2 inches. That translates too a conduction path between the top of the heater cartridge and the bottom being 2 inches. That will increase the bottom of the focus block's temperature considerably! So the temperature at the bottom of the vertical cartridge heater design might reach the operational temperature of copper at a lower heat flux than one has designed for. Consequently, vertical heaters are very well suited for heat fluxes below 800W/cm^2.

Regardless of the heater chosen a preliminary *Finite Element Analysis must be done* to guarantee that the copper in the focus block will not reach its critical temperature in this case chosen to be 700°C.

The length and placement of the holes is some what important in a horizontal design. The bottom of the heater block must have at least 0.8 cm of copper so that the heat can flow around the cartridge heaters. A thermocouple can be placed in a small hole drilled in the bottom of the heat block to insure the heater does not exceed the chosen safety temperature. Figure 4.8 shows two different placements of the cartridge heaters. In one placement the cartridge heaters are in line, thus the middle heater has a slightly lower temperature than the outer heaters. Whereas in the other placement, the heaters are

aligned along a central radius, which would insure they all have the same operating temperatures.

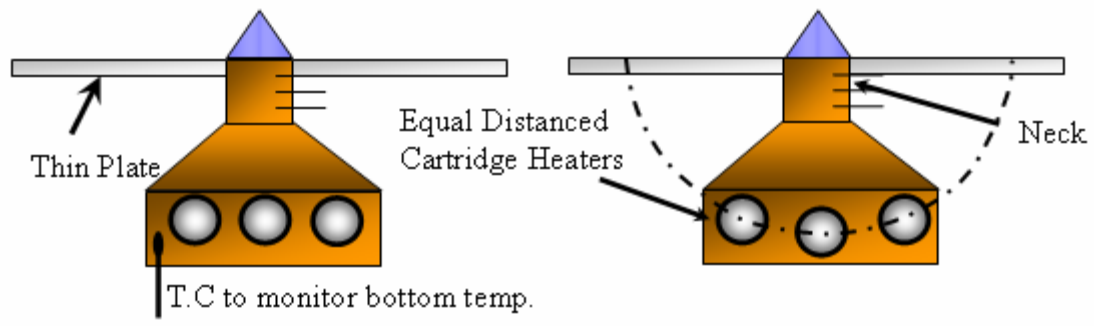

Figure 4.8: Cartridge Heater Placement

4.3.2 Insulation

Insulating the focusing block is done very easily, with high temperature air filled insulation such as DuraBlanket © insulation which has a thermal conductivity of k = 0.013 W/m-K. DuraBlanket basically has the thermal conductivity of air, but it stops convection currents from setting up. When using any insulation it is important to give some room, 3cm or more, between the heater block and the shell of the heater so the insulation can reduce the heat lost. A simple one dimensional thermal conductivity calculation would tell one what the heat loss is. DuraBlanket insulation has a max temperature of 2,200°F so the copper block will melt way before the insulation does. It is important when installing the insulation that one does not compresses or squeezes the insulation. Doing so would reduce the amount of trapped air inside of the insulation and increase the thermal conductivity of the insulation.

4.3.3 Neck Sealing

In many of the figures like figure 4.7, 4.8 one can see the neck of the copper focus block passing through a thin plate. The liquid in this case has the possibility of leaking through the cracks between the neck and the thin plate. The solution presented by Tilton was to minimize the gap size to 1mm and seal it with high temperature silicon sealant (red color sealant) [50]. The other solution for sealing comes into play for larger area heaters. The solution is to solder the neck of the heater on to a thin copper plate, as shown in figure 4.9. The surface temperature can be calculated based on the thermal resistance of the solder, and the gap size. To minimize the thermal resistance variation over the soldered surface, one should machine polish both surfaces to a mirror finish. This will insure a constant thin film over the contact area. One can then measure the solder thickness with a micrometer by placing the block and thin copper plate assembly on a machinist's marble measuring table before and after the soldering. Knowing the typical solder thermal conductivity of 160 W/m-K, one can then estimate the temperature drop across the solder.

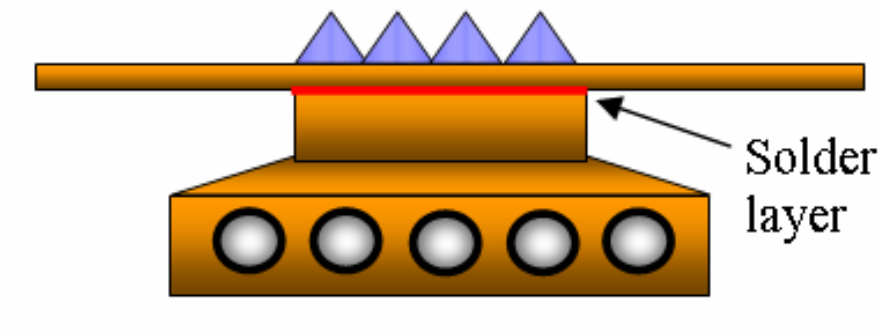

Figure 4.9: Seal-less Heater

$$\Delta T = \frac{\dot{Q} * X}{160 W/m - K} \qquad \text{(Eq 4.7)}$$

The only downside to using a solder neck heater is that the solder gap introduces error in surface temperature calculation. In the author's experiments the error estimated due to soldering was found to be around 1 °C.

4.4. Methodology for Design

The methods of measuring heat flux differ based on the heat source chosen. The following section will concentrate on designing a heat flux measurement neck mainly for uses with cartridge heaters, although other heat sources can be used. The typical heat flux measurement design is that of a neck of a constant cross sectional area with thermocouples inserted into it. The thermocouples measure the temperature at different vertical locations along the neck. Utilizing the 1D conduction formulas one can then calculate the heat flux based on the temperature of the different thermocouples. Small variations in this design have been done such as integrating the thermocouples into the neck, or rapping them around the outside of the neck. Regardless of the design, this part of the heater should be given special attention so that uncertainties associated with the heat flux measurement can be minimized. The most important aspect of this design is the material selected for the neck and the placement of the thermocouples. The following section will go over step by step how to design a high heat flux heater using cartridge heaters as a heat source.

4.4.1 Step One: Surface Temperature, Material and Maximum Heat Flux

The first step is to identify the maximum heat flux and surface temperature one expects from the heater. So if one expects 150°C to be the max surface temperature one should add on a safety margin of 10°C or 20°C and let the max surface temperature be around 160°C. The maximum heat flux is going to be the main limiting factor in the designing of the neck, which directly affects the accuracy of a heat flux measurement. A longer neck has more accuracy in the heat flux measurement, and a shorter neck has less accuracy. A heater with a maximum heat flux of 300W/cm^2 will be able to have a longer neck and thus more measurement accuracy than a heater with a max heat flux of 1000W/cm^2. So, there is a small trade off between higher heat fluxes and measurement accuracies.

Once the maximum heat flux and surface temperatures have been chosen one can pick a preliminary neck length for their design. This requires one to know the material that the heater is made out of. The material chosen mainly has to do with the maximum heat flux chosen; table 4 was generated to display this point. Table 4 used equation 4.8 to generate all of the temperature rises [1].

$$\Delta T = \frac{\dot{Q} * X}{k} \qquad \text{(Eq. 4.8)}$$

From table 4, one can see that if the heat flux is above 500W/cm^2 only copper should be selected as the material for the conduction block and the neck. The ability to pick other materials only comes into play below 300W/cm^2. The benefits to picking a

material other than copper is that one would have a lower thermal conductivity and thus one can get a larger temperature gradient on the neck.

Table 4: Temperature Rise of Different Materials at Various Heat Fluxes

Heat Flux (W/cm^2)	Metal	Melting Point (K)	Melting Point (°C)	Conductivity (W/m-K)	Distance (cm)	Temp Increase °C	Over Heated
100	Copper (Pure)	1358	1085	401	1	25	
100	Aluminum (Pure)	933	660	237	1	42	
100	Aluminum 1100	913	640	220	1	45	
100	Red Brass	990	717	160	1	63	
100	Plain Carbon Steel	1000-1500	700-1200	60	1	167	
100	*Stainless Steel*	*1670*	*1397*	*15*	*1*	*667*	Yes
300	Copper (Pure)	1358	1085	401	1	75	
300	Aluminum (Pure)	933	660	237	1	127	
300	Aluminum 1100	913	640	220	1	136	
300	Red Brass	990	717	160	1	188	
300	*Plain Carbon Steel*	*1000-1500*	*700-1200*	*60*	*1*	*500*	Yes
300	*Stainless Steel*	*1670*	*1397*	*15*	*1*	*2000*	Yes
500	Copper (Pure)	1358	1085	401	1	125	
500	**Aluminum (Pure)**	**933**	**660**	**237**	**1**	**211**	
500	***Aluminum 1100***	***913***	***640***	***220***	***1***	***227***	Yes
500	*Red Brass*	*990*	*717*	*160*	*1*	*313*	Yes
500	*Plain Carbon Steel*	*1000-1500*	*700-1200*	*60*	*1*	*833*	Yes
500	*Stainless Steel*	*1670*	*1397*	*15*	*1*	*3333*	Yes
1000	**Copper (Pure)**	**1358**	**1085**	**401**	**1**	**249**	
1000	*Aluminum (Pure)*	*933*	*660*	*237*	*1*	*422*	Yes
1000	*Aluminum 1100*	*913*	*640*	*220*	*1*	*455*	Yes
1000	*Red Brass*	*990*	*717*	*160*	*1*	*625*	Yes
1000	*Plain Carbon Steel*	*1000-1500*	*700-1200*	*60*	*1*	*1667*	Yes
1000	*Stainless Steel*	*1670*	*1397*	*15*	*1*	*6667*	Yes

A larger temperature gradient means that one would have greater accuracy in the heat flux measurements. Say for example, one's maximum heat flux was $200W/cm^2$ with a max surface temperature of 100°C. The ideal material would be red brass because the neck could be 3 cm long and have a temperature increase of 375°C across it. This is a reasonable temperature rise and will be discussed more in the following paragraph. Again

for heaters with *heat fluxes above 300W/cm^2* only *copper can be used* as the neck and focus block material!

4.4.2 Step Two: Neck Length and Reduction of Uncertainties

Now that the material has been selected, the second step is to pick a preliminary neck length based on the maximum heat flux. Maximizing the length of the neck is important in the uncertainty calculation. The errors that contribute to uncertainty in the heat flux calculation are as follows: errors associated with the thermocouple placement, error in the thermal conductivity constant, & the errors in temperature measurement. When holes are drilled in the neck there is a given tolerance in which they can drift from the desired position. This tolerance is the error in the T.C.s' placement, and if the neck is small the uncertainty in the heat flux is extremely large. The author has seen a heater with a neck length of 1cm with three T.C.s drilled in it with tolerances of 0.01 inches or 0.0254cm. Just this factor alone would give an uncertainty in heat flux as large as 15-20 W/cm^2. This clearly is unacceptable as demonstrated by Eq. 4.9 below.

$$\partial\dot{Q} = \dot{Q} * \left(\frac{\partial X}{X}\right) = 600\frac{W}{Cm^2}\left(\frac{\sqrt{(0.0254cm)^2 + (0.0254cm)^2}}{1cm}\right) = +/-21\frac{W}{Cm^2} \qquad \text{(Eq. 4.9)}$$

The error in hole placement is the sum of the squares, so in this case, two holes drilled with an accuracy of 0.01" gives a 0.014" error (0.03556 cm error) in the hole's placement. Just by changing the length to 3cm between the thermocouple the uncertainty is reduced by a factor of 3, as seen below in Eq. 4.10.

$$600\frac{W}{Cm^2}\left(\frac{\sqrt{(0.0254cm)^2+(0.0254cm)^2}}{3cm}\right)=600\frac{W}{Cm^2}\left(\frac{0.0359cm}{3cm}\right)+/-7.1\frac{W}{Cm^2} \quad \text{(Eq. 4.10)}$$

Now if one changes the machining tolerance from 0.01" to 0.005" and the neck length then the uncertainty is reduced by a factor of 5 which is demonstrated by Eq. 4.11.

$$600\frac{W}{Cm^2}\left(\frac{\sqrt{(0.0127cm)^2+(0.0127cm)^2}}{3cm}\right)=600\frac{W}{Cm^2}\left(\frac{0.0179cm}{3cm}\right)+/-3.5\frac{W}{Cm^2} \quad \text{(Eq. 4.11)}$$

One can see, from these example calculations that the length of the neck and the holes' tolerances will have the most impact on the uncertainty associated with the heat flux calculation. Hence, for a low heat flux heater design one should maximize the neck's length by choosing a metal other than copper with a lower thermal conductivity, that way the error associated with the temperature measurement is minimized too.

The longest neck length should be chosen so that the maximum operational temperature of the bottom of the heater is achieved. A simple formula can be used to estimate the bottom temperature based on the neck length chosen.

$$\frac{\dot{Q}_{\max} * X_n}{k} + (Surface \quad T) + (Focus \quad block \quad T) = (T \quad Bottom) \quad \text{(Eq. 4.12)}$$

The temperature increase due to the focus block is found on table 5. Again T Bottom is the temperature of the bottom of the heater and for safety reasons should be set 3/4th of the melting point of the metal used, so for copper, 700°C is the limit.

Table 5: Increase in Temperature Across Focus Block at Various Heat Fluxes

Heat Flux (W/cm^2)	Horizontal Heater Focus Block Temperature Increase (°C)	Vertical Heater Focus Block Temperature Increase (°C)
500 W/cm^2	60-75	80-95
800 W/cm^2	120-130	130-150
1000 W/cm^2	110-120	160-190

So, a horizontal heater configuration with a 1.75 cm neck made out of copper and a surface temperature of 120°C operating at a heat flux of 1000W/cm^2 would have a bottom heater temperature of 698°C using Eq. 4.12. Most importantly, the neck length can also be solved for by setting the maximum bottom temperature then using Eq. 4.12.

4.4.3 Step Three: FEM Analysis and Design Refinements

Now that the material is chosen and the neck length is found one can move on to step three. Step three is the finite element analysis of the heater design. The heater would be designed in the CAD program then exported in a *.step or *.sat file format, which would then be opened in the FEM analysis software. The author designed his solid model in Inventor 7.0 by AutoDesk, and then exported it to Cosmos Design Star 4.0 for analysis. Remember the focus block should have sloped sides so the heat can have a simple conduction path to the top. This can be seen in figures 4.7 through 4.10. In Cosmos, the boundary conditions were set, which are the top surface was cooled at a infinite cooling rate but kept at a bulk temperature in the author's case it was 100°C. The next condition was the heating rate; the surface area which the heater cartridge touches

had an applied heat load placed on it. The heat load could be chosen by wattage by which the program automatically applied the correct heat fluxes to the chosen surfaces.

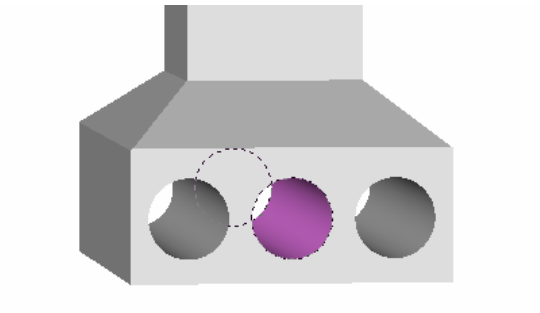

Figure 4.10: Applying Heat Loads

So, for example say one was utilizing three heater cartridges to heat a $1cm^2$ surface area with $1000W/cm^2$ of heat flux. One would then select the surface area which one of the heater touch as shown in figure 4.10 and apply a heat load of 333.3 W. This then would be repeated for the other two cylindrical surfaces. *Note:* When conducting a cartridge heater analysis one assumes the heat exits only through the sides of the cartridge heater not through the ends.

In Cosmos, the cooling is provided by applying a film coefficient to the cooled surface, for a spray cooling this can range from $30W/cm^2$-K to $50W/cm^2$-K. Additionally the bulk temperature must be defined. In the author's cases, he assumed saturated water at atmosphere pressure which has a bulk temperature of 100°C; remember one might have different working fluids with different bulk temperatures. Now that the heat loads, cooling loads and mesh are provided one can run then run the steady state thermal analysis. The first set of results obtained should be checked for two things, the bottom operational temperature, to see if it is within limits, and the heat flux through the neck. If

the neck is sufficiently long the heat flux should be evenly distributed, however if the neck is extremely short (1cm or less) the heat flux may be uneven. If the heat flux is uneven the meshing must first be changed and analysis reconducted. If the problem still persisted despite many changes to the analysis one must seriously consider redesigning the heater to even out the heat flux. Again the heat flux will be evenly distributed for flat top heaters with necks longer than 0.5cm; the author would not recommend designing a heater with necks smaller than 1cm due to the uncertainties associated with the heat flux measurements. So, if the bottom temperature of the neck is too high then the neck's length should be shortened slightly. Using Eq. 4.8 one can determine how much to shorten the neck by, after that one should re-run the analysis's to verify that the bottom temperature is achieved.

One can also predict the temperature of the bottom at any heat flux by doing the following. Run two FEM analysis one at a low heat flux say for instance 300W/cm^2 and one at a higher heat flux say 500 W/cm^2. Now for each analysis record the maximum bottom temperature. Using these two analyses one can interpolate between the temperatures to see what the maximum heat flux would be as shown in table 6. This can be easily done in excel with the Forecast Formula.

Table 6: Interpolating of Bottom Temperature

Heat Flux (W/cm^2)	Bottom Temp (°C)
300	326
500	548
750	**682 (found)**

4.4.4 Step Four: Thermocouple Placement

Now that the heater has been thoroughly designed the exact locations of the thermocouples can be determined. The previous section, explained why longer necks reduced the uncertainty associated with the heat flux measurement (Eq. 4.9). The uncertainty can possibly be further reduced by using three or more thermocouples.

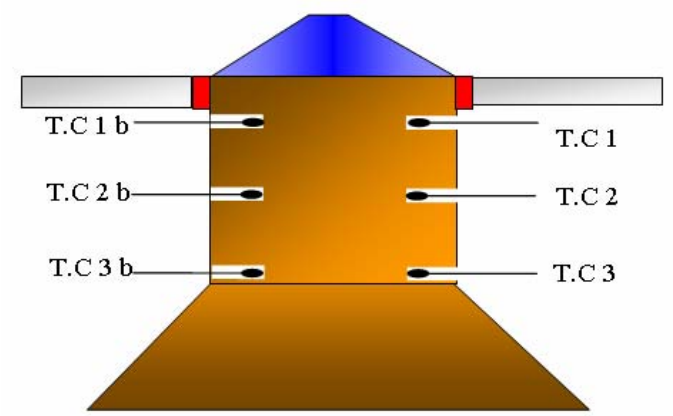

Figure 4.11: Thermocouple Placement

Figure 4.11 shows a zoomed in view of the neck of a focus block (remember the neck and the focus block should be made out of the same piece of metal, i.e. no soldering). The figure shows three T.C.s on each side, this can give 3 possible heat flux measurements (between T.C.s 1 & 2, 2 & 3, 1&3). At low heat fluxes the best measurement possible will be (between T.C 1&3) and at high heat fluxes comparison between all three heat fluxes measurements are useful. The three heat flux measurements can also be average, doing this will reduce the effects of thermocouple placement inside of the drilled holes; however uncertainty analysis must be conducted to see if this will reduce the overall uncertainty associated with the heat flux (see Appendix D).

Finally redundant pairs of thermocouples added together will reduce uncertainly. So taking the average of the heat fluxes measured by T.C.s 1&3 & 1b&3b would reduce the uncertainty. Also having a redundant or mirror pair of T.C.s provides a back up in case one of the primary T.C. fails.

The holes drilled in the neck can disrupt the heat flow; as a result larger holes would possibly make the heat fluxes uneven in the neck. Smaller holes are ideal; the author recommends holes no bigger than 0.06 inches. The holes must be drill perpendicular to the direction of the heat flux, or they will possibly disrupt heat flow. The holes should be deep enough that they contact a plane of the neck with a constant temperature; this can be seen in figure 3.17 in chapter 3. The author recommends a depth of 0.1 inches or more. Thermocouples come in multiple wire sizes and some even come with pre-made heads, the smaller holes require smaller T.C. The author recommends choosing a T.C with a wire gauge which with one is comfortable handling; in the author's case he prefers using a 30 gauge wire (Omega TT-T-30), that way one can prepare the thermocouple ends themselves.

When drilling the T.C. holes the accuracy of the placement is important. The example associated with Eq. 4.9 shows that the uncertainty in the heat flux measurements is greatly linked to the accuracy or tolerance of the drill thermocouple holes. Reducing this tolerance greatly helps reduce the uncertainty that is why drilling the holes with a precision mill or even better a C&N machine is necessary. The depth and position of the T.C holes should have tolerances of 0.05 in or better! Now the first T.C holes (T.C 1) should be drill so that the T.C.s are just below the top plate as shown in figure 4.11. The bottom T.C holes (T.C 3) should be drill as close as possible (0.1 inches) to the base of

the focus block. It has been determined that the sectional neck temperature is mostly even at 0.2 inches above the focus block. *Note:* The number of T.C used will be limited by how many holes can be drill without disrupting the heat flow and the number of T.C available for the data acquisition system. A sample set of heat flux uncertainty calculations is located in Appendix D.

4.4.5 Step Five: Housing Design

Finally the housing must be design for the heater block and top plate. Care must be taken to insure that the housing is water tight so that liquid does not enter. If liquid, such as water, enters the heater housing it will vaporize taking valuable heat along with it. This will totally throws off all the heat flux calculations. Additionally conductive liquids such as water can short out the cartridges heaters. Symptoms for this occurring are large differences between the calculated heat flux from the voltage, and the measured heat flux from the thermocouples.

In designing the housing leave at least 2" of space between the focus block and the nearest housing wall. That will allow the insulation mention previously, to reduce the heat flux to a very low level. Rubber seals can be used inside of the housing as long as they are located a sufficient distance from the heating block. Securing the block in position is also needed. This can be done with a threaded rod, or ceramic block position underneath or to the sides of the heater focus block. Care must be taken in designing these components because they could potentially transferred valuable heat away from the focus block. High temperature machineable ceramics are available for these components. If the heater block is solder to a top plate as in figures 3.17 & 4.9 a bottom support such as a steel spring can be use to insure that the stress on the solder is minimized. Remember

when designing the housing to leave sufficient room for the cartridge heater cables and thermocouple wires to exit the housing without passing to close to the heater block.

4.4.6 Short Summary of Steps

1. Pick the maximum heat flux one wants to achieve, be realistic.
2. Pick the maximum temperature that the cooled surface will experience and add a safety margin.
3. Determine the orientation of and how many heater cartridges are required.
4. Pick a conduction material, copper is only recommended for fluxes above $300 W/cm^2$.
5. Pick a preliminary neck size using conduction Eq. 4.12.
6. Design a heater & conduct a FEM analysis without thermocouple holes.
7. Lengthen or shorten neck accordingly using Eq. 4.8.
8. Conduct the FEM analysis again.
9. Pick the locations for the thermocouples.
10. Design the housing and the mechanism for securing the heater block in place.

4.5 Common Problems

The following paragraph describes some common problems and tips that should be considered when manufacturing the heater block. Insure there are no burs in the cartridge heater holes and that the holes are drilled extremely straight. Use a conductive paste to help lubricate and insert the heater cartridges. Be sure that the T.C.s are in direct electrical contact with the focus block that way they read the most accurate temperatures. When securing the T.C.s in their holes use a heat resistance epoxy or high temperature

silicon sealant. Insure that the T.C.s' wires are well way from the bottom of the focus block, that way the wires don't melt. The focus block must be electrically grounded! This is imperative when using heater cartridges running off of AC current or even in some cases DC. Solder or anchor a grounded wire to the focus block. This is done to insure minimal noise in the T.C.s readings. Do not over compress the insulation; it requires air pockets to work properly. Again, double check that the T.C.s are in electrical contact with the focus block and they are grounded. Use only heat resistant materials with low thermal conductivities to support the heater block (Alumina Silicate Ceramics work well).

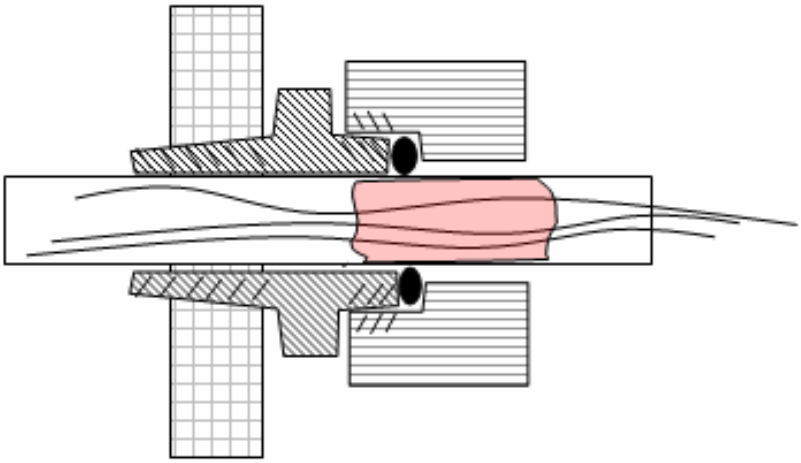

Figure 4.12 Wire Feed Through Design

If the heater is enclosed one must proved an air and water tight seal around contact points including around the T.C wires and power wires. The T.C and power wires can be sealed using wire feed throughs sold by Omega or Conax out of Buffalo NY. Or one could use the setup which the author developed, which utilizes a low cost pipe flange adapter (Fig.12). A through hole is drill in a pipe fitting, then a tube is pass through with

the T.C wire and sealed with a silicon sealant or preferably an epoxy. The author found this to works up to pressure of 150 Psi and more; the only downside is that the wires are permanently secured inside the tube.

4.6 Conclusion to Chapter

This chapter was written as a guide for the design and construction of a high heat flux heater for experimental uses where the measurement of surface temperatures and of heat fluxes are extremely important. Firstly, this chapter outlines the heat sources available for high heat flux heaters, and the pros and cons of each. Secondly, the chapter outlines all components and design aspects of a high heat flux heater utilizing cartridge heaters. Thirdly, this chapter gives a step by step method for designing high heat flux heater utilizing cartridge heaters. Finally, a short summary of the design steps and common problems are given to conclude the chapter.

The authors review of high heat flux heater options, led him to prefer heater utilizing cartridge heaters due to there high reliability, large operational range, and extremely high heat generation densities. The author then reviewed methods of determining heat fluxes and surface temperatures, and determined that utilizing a conduction neck with several embedded thermocouples gave the smallest uncertainties associated with heat flux and surface temperature measurements. Additionally the author determine that the combination of cartridge heaters and a conduction neck would give the most reliable and robust design for his spray cooling applications.

APPENDIX A: CARTARTRIDGE HEATERS AND TFR SPECIFICATIONS

Cartridge Heaters

Cartridge Heaters

Economical heaters have elements that are insulated with magnesium oxide and protected by a Type 304 stainless steel sheath. Leads are 10" long. Temperature limit for the element is 1000° F; 482° F for leads. UL recognized and CSA certified. Heaters should be used with a temperature control switch (see 3626K and 7079K on page 494; and 7981K on page 496). To determine amperage, divide watts by volts.

120 VAC

Cartridge Lg.	Watts		Each
3/16" (0.185") Dia.			
1 1/2"	20	3618K511	$13.69
2"	30	3618K122	14.71
3"	45	3618K514	16.82
4"	65	3618K123	18.89
5"	80	3618K518	21.11
1/4" (0.248") Dia.			
2"	32	3618K412	12.93
2 1/2"	30	3618K413	12.95
4"	100	3618K416	15.34
6"	150	3618K419	19.34
3/8" (0.373") Dia.			
1 1/2"	40	3618K311	11.61
2"	50	3618K312	12.21
2 1/2"	75	3618K313	12.95
3"	100	3618K34	13.70
3 1/2"	120	3618K35	14.88
4"	130	3618K314	15.02

120 VAC (Cont.)

Cartridge Lg.	Watts		Each
3/8" (0.373") Dia. (Cont.)			
4 1/2"	150	3618K37	$16.79
5"	200	3618K315	16.90
5 1/2"	200	3618K38	17.87
6"	225	3618K39	18.53
1/2" (0.496") Dia.			
1 1/2"	60	3618K21	11.89
2"	75	3618K22	12.49
2 1/2"	125	3618K211	13.70
3"	150	3618K24	14.72
3 1/2"	150	3618K25	15.78
4"	180	3618K26	16.96
4 1/2"	200	3618K27	18.01
5"	200	3618K212	17.99
5 1/2"	300	3618K28	18.02
6"	300	3618K29	18.82
5/8" (0.622") Dia.			
2"	100	3618K12	14.14

120 VAC (Cont.)

Cartridge Lg.	Watts		Each
5/8" (0.622") Dia. (Cont.)			
2 1/2"	150	3618K111	$14.56
3"	175	3618K112	15.45
4"	200	3618K114	17.40
4 1/2"	240	3618K115	17.41
5"	250	3618K116	17.42
5 1/2"	285	3618K117	17.88
6"	300	3618K118	18.75

240 VAC

Cartridge Lg.	Watts		Each
7/16" (0.437") Dia.			
5 1/2"	300	3618K913	$17.27
1/2" (0.496") Dia.			
3"	150	3618K908	14.72
4"	180	3618K911	16.96
6"	300	3618K914	18.00
5/8" (0.622") Dia.			
6"	300	3618K924	26.79

High-Temperature Cartridge Heaters

Tightly wound heating elements are insulated by magnesium oxide and condensed to produce a more durable heater with higher heat output and better resistance to impact and vibration than the cartridge heaters above. Heaters are protected by an Incoloy sheath. Leads are 12" long. Temperature limit for heater element is 1600° F; 842° F for leads. UL recognized and CSA certified. Heaters should be used with a temperature control switch (see 3626K and 7079K on page 494; and 7981K on page 496). To determine amperage, divide watts by volts.

Prices below are for heaters with mica-insulated leads. Heaters are also available with wire leads that have an additional braided stainless steel covering for added protection against wear and tear. Prices are 20% to 30% higher. **To Order:** Please specify with or without braided stainless steel lead covering, 120 or 240 volts, and wattage (where applicable) from the choices listed below.

Cartridge Lg.	*1/4" (0.248") Dia.* Available Watts		Each	*5/16" (0.310") Dia.* Available Watts		Each	*3/8" (0.371") Dia.* Available Watts		Each
1"	80, 100	3618K181	$17.77	80	3618K199	$15.91	100, 150	3618K235	$16.33
1 1/2"	100, 150, 200	3618K182	18.15	100	3618K221	16.26	100, 150, 200, 250	3618K236	16.85
2"	125, 150, 200, 250	3618K183	18.27	150	3618K222	16.81	100, 200, 300, 400	3618K237	16.89
2 1/2"	200, 250	3618K184	18.62	150, 200	3618K223	17.41	200, 250, 400, 500	3618K238	16.91
3"	100, 200, 250, 300	3618K186	20.50	225	3618K224	18.65	200, 250, 375, 400	3618K239	17.01
3 1/2"	300	3618K187	20.69	250	3618K225	19.27	250, 300, 350, 500	3618K241	17.09
4"	200, 265, 300	3618K188	23.39	275	3618K226	20.36	250, 300, 400, 500	3618K242	17.23
4 1/2"	325	3618K189	23.37	300	3618K227	21.11	300, 450, 500	3618K243	17.38
5"	350, 400	3618K191	23.56	350	3618K228	22.36	150, 300, 400, 500	3618K244	17.62
5 1/2"	350	3618K192	23.72	250	3618K229	23.57	550, 600, 1000	3618K245	18.34
6"	300, 400, 450	3618K193	25.35	450	3618K231	24.72	250, 400, 500, 600	3618K246	18.84
7"	525, 600	3618K194	28.49	550	3618K232	25.72	350, 400, 600, 1000	3618K247	27.29
7 1/2"	525	3618K195	28.66				600, 725, 1000	3618K333	28.10
8"	600	3618K196	29.44	650	3618K234	27.53	300, 500, 600, 900	3618K334	28.99
9 1/2"	525	3618K197	30.34	—	—	—	200, 600, 1000	3618K335	32.53
10"	750	3618K198	31.17	—	—	—	600, 1000	3618K336	33.84
	1/2" (0.496") Diameter			*5/8" (0.621") Diameter*			*3/4" (0.746") Diameter*		
1"	50, 150	3618K337	$11.42	—	—	—	—	—	—
1 1/2"	150, 200	3618K249	14.89	250	3618K266	$15.37	—	—	—
2"	200, 250, 300, 400	3618K251	15.17	200, 250	3618K267	15.59	—	—	—
2 1/2"	250, 300, 400, 500	3618K252	15.55	275, 400	3618K268	16.01	—	—	—
3"	250, 300, 400, 500	3618K253	15.75	250, 500, 750	3618K269	16.23	500, 600	3618K283	$21.43
3 1/2"	250, 500	3618K254	16.11	525	3618K271	16.49	—	—	—
4"	300, 400, 500, 750	3618K255	16.27	250, 500, 750	3618K272	16.85	500, 1000	3618K284	21.88
4 1/2"	500, 650, 750	3618K256	23.30	750	3618K273	17.13	875	3618K285	23.23
5"	200, 400, 500, 750	3618K257	24.03	500, 750, 1000	3618K274	17.37	500, 1000	3618K286	24.65
5 1/2"	500, 750	3618K258	25.22	800	3618K275	17.75	—	—	—
6"	500, 750, 850, 1000	3618K259	25.88	500, 750, 1000, 1500	3618K276	18.10	1000, 1200, 2000	3618K287	26.28
7"	500, 600, 1000	3618K261	29.78	1000, 1500	3618K277	31.10	1000, 1500	3618K288	38.53
7 1/2"	500, 1000	3618K262	30.56	750, 1000	3618K278	31.80	—	—	—
8"	500, 750, 1000	3618K263	31.60	1000, 1200, 1500	3618K279	33.17	1000, 2000	3618K289	42.34
9 1/2"	800, 1000	3618K264	34.62	1700	3618K281	34.54	—	—	—
10"	500, 1000, 1500	3618K265	35.41	800, 1000, 1500	3618K282	37.76	1000, 2000	3618K322	48.59

High-Temperature Cartridge Heaters with Nonstick Coating

The bonded graphite coating greatly eases insertion and removal, and improves heat transfer. Heaters have an Incoloy sheath and 12" long leads. Temperature limit for the element is 1600° F; 842° F for leads. UL recognized and CSA certified. Heaters should be used with a temperature control switch (see 3626K and 7079K on page 494; and 7981K on page 496). To determine amperage, divide watts by volts.

To Order: Please specify voltage from those available (where applicable).

Cartridge Lg.	Watts	Available VAC		Each
1/4" (0.247") Dia.				
1"	80	120	3614K34	$23.02
1 1/2"	100	120	3614K35	23.22
2"	200	120	3614K36	23.26
3/8" (0.370") Dia.				
1"	100	120	3614K51	21.63
1 1/2"	150	120	3614K52	21.52
2"	200	120	3614K531	21.87
2 1/2"	250	120, 240	3614K54	22.83

Cartridge Lg.	Watts	Available VAC		Each
3/8" (0.370") Dia. (Cont.)				
3"	375	120	3614K551	$24.09
4"	250	120, 240	3614K57	26.67
4 1/2"	450	120	3614K58	27.93
6"	600	120, 240	3614K62	32.00
9 1/2"	600	240	3614K65	40.61
1/2" (0.495") Dia.				
2"	300	120, 240	3614K69	23.22
3 1/2"	500	120, 240	3614K73	27.20

Cartridge Lg.	Watts	Available VAC		Each
1/2" (0.495") Dia. (Cont.)				
6"	850	120, 240	3614K78	$34.43
10"	1000	240	3614K83	44.37
5/8" (0.620") Dia.				
2 1/2"	275	120	3614K851	25.57
3"	500	120	3614K861	27.61
4"	500	120, 240	3614K88	29.80
6"	1000	120, 240	3614K93	36.72

Thin-Film Heat Flux Sensors

Shown with OMEGA's DP41-E Digital Process Indicator, $545. see page M-27.

Shown actual size

HFS Series

$130

Basic Unit

- **Effective for Convection, Conduction and Radiation Heat Transfer**
- **Conveniently Interfaces with Voltmeters and Recorders**
- **Easily Attaches to Curved and Flat Surfaces**
- **Temperature Range from -200 to 150°C (-330 to 300°F)**

Applications

- **Determining Thermal Properties of Materials**
- **Monitoring Structural Heat Transfer**
- **Process Control in Heat Treating, Rolling Mills, and Glass Production**
- **Determining Heat Loss and Insulation Efficiency in Housing**
- **Analyzing Aerodynamic Wind Tunnels**

Each HFS series Heat Flux Sensor functions as a self-generating thermopile transducer. It requires no special wiring, reference junctions or signal conditioning. A readout is accomplished by connecting a sensor to any direct reading dc microvoltmeter or recorder.

The HFS series sensor is designed for precise measurement of heat loss or gain on any surface. It can be mounted on flat or curved surfaces, and employs butt-bonded junctions with a very low thermal profile for efficient reading. The sensor is available with an integral thermocouple for discrete temperature measurement needed to describe the heat flux, and is available in two different sensitivity ranges. All models utilize a multi-junction thermopile construction. The carrier is a polyimide film which is bonded using a Teflon® lamination process.

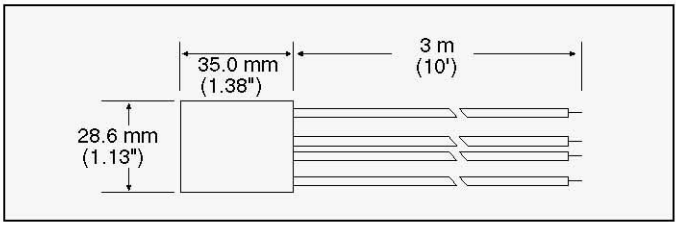

ALL MODELS AVAILABLE FOR FAST DELIVERY!

Model No.	Nominal† Sensitivity (μ V/Btu/ Ft²-Hr)	*Max Rec'd Heat Flux (Btu/ Ft²Hr)	Built-in T/C Type K	Resp. Time (sec)	Thermal Capacitance (Btu per Ft² °F)	Thermal Resistance (°F per Btu/ Ft² Hr)	Nominal Thickness mm (inches)
HFS-3	3.0	30,000	YES	0.60	0.02	0.01	0.18 (0.007)
HFS-4	6.5	20,000	YES	0.60	0.02	0.02	0.18 (0.007)

**Exceeding the maximum recommended heat flux can result in a large enough temperature rise to cause delamination of the Kapton bonding material. The given maximum values assume a 38°C (100°F) ambient*

†Nominal sensitvity is ±10%. Sensitivity is supplied with unit

Heat Flux Sensors
Ideal for Precise Heat Transfer Measurement

HEAT FLOW MEASUREMENT INSTALLATION AND HOW IT WORKS

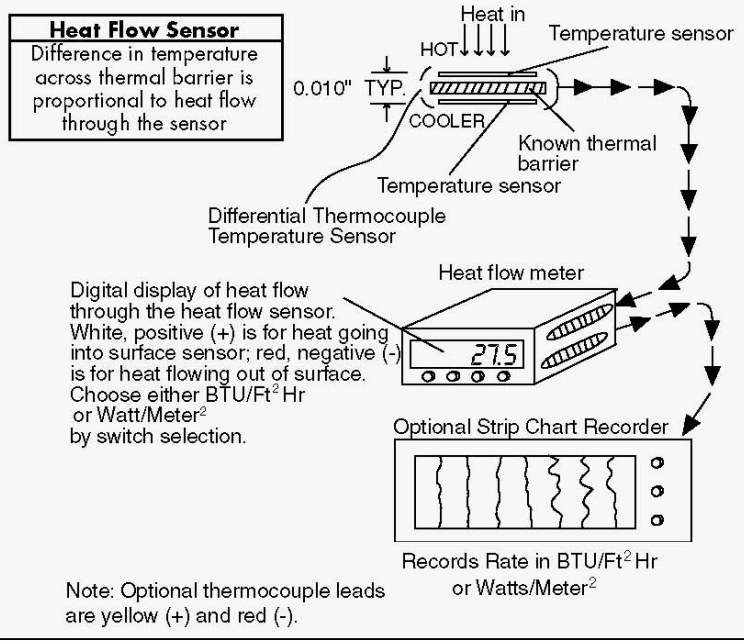

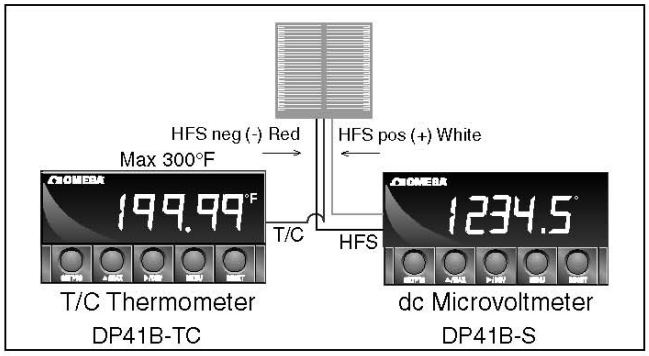

Specifications

Upper Temperature Limit: 150°C (300°F)

Number of Junctions:
- **HFS-3:** 54
- **HFS-4:** 112

Carrier: Polyimide Film (DuPont Kapton)

Nominal Sensor Resistance:
- **HFS-3:** 140 ohms
- **HFS-4:** 175 ohms

Lead Wires: #30 AWG Solid Copper, Teflon Insulated color coded, 3.1 m (10' long)

Weight: Models HFS-3 and HFS-4, 1.0 oz

For Epoxies and cements compatible with HFS Series, see OMEGABOND® epoxies on page F-23.

ALL MODELS AVAILABLE FOR FAST DELIVERY!

To Order *(Specify Model Number)*		
Model Number**	**Price**	**Description**
HFS-3	**$130**	3.0 µV/BTU/Ft²Hr sensor w/ type K t/c
HFS-4	**136**	6.5 µV/BTU/Ft²Hr sensor w/ type K t/c

Comes with complete operator's manual and sensitivity calibration.
***Other sizes and styles available, consult Applications Engineering.*
Ordering Example: HFS-4**, thin-film heat flux sensor, **$136

CIR SERIES HIGH WATT DENSITY CARTRIDGE HEATERS - WITH INCOLOY SHEATH 3/8" DIAMETER

- Premium Quality
- Rugged Construction
- 120V & 240V Models Available
- Lengths from 1¼" (3cm) to 24" (61cm)

OMEGALUX® CIR series high watt density cartridge heaters are especially well suited for use in applications involving molds, dies, platens, hot plates, and sealing operations. They are available in lengths from 1" to 24".

SPECIFICATIONS

Sheath: Material, Incoloy; black oxide finish for efficient heat transfer; max. temp. 1500°F; welded, sealed tip.
Leads: Type "F"; stranded, flexible manganese nickel wire insulated with fiberglass, max. temp. 450°C (842°F), 10" standard length. Longer leads available.
Heater Wire: Premium grade nickel-chromium resistance wire for longer life, and consistent performance.
Insulation: Specially formulated refractory insulation, rigidly controlled, densely compacted to improve thermal conductivity and dielectric strength.
Internal Connections: Patented connector for high reliability and longer life. Vibration and shock resistant construction.
Voltage: 120V or 240V ac -must be specified at time of order.

D

.000"

To Order 3/8" Nominal Diameter CIR Series (Actual Dia. & Tolerance: 0.373" ± .005")

Shth. Lgth. (cm)	Watt	W/in²	Model No.	Price	Wt. lbs. (kg)	Shth. Lgth. (cm)	Watt	W/in²	Model No.	Price	Wt. lbs. (kg)	Shth. Lgth. (cm)	Watt	W/in²	Model No.	Price	Wt. lbs. (kg)
1¼(3)	100	114	CIR-2013/120	$29	.05(.2)	2½(6)	250	107	CIR-20251/*	$32	.10(.05)	5 (13)	750	142	CIR-2054/240	$42	.20(.09)
1¼(3)	125	143	CIR-20131/120	29	.05(.2)	2½(6)	300	129	CIR-2029/*	32	.10(.05)	5 (13)	1000	190	CIR-2056/240	42	.20(.09)
1¼(3)	150	171	CIR-2012/*	29	.05(.2)	2½(6)	400	171	CIR-2026/*	32	.10(.05)	5¼(13)	200	44	CIR-2057/240	42	.21(.1)
1¼(3)	200	228	CIR-2014/*	29	.05(.2)	2½(6)	500	214	CIR-20252/*	32	.10(.05)	5½(14)	600	102	CIR-2058/240	43	.22(.1)
1½(4)	50	43	CIR-2018/120	30	.06(.3)	2⅞(7)	250	91	CIR-20253/120	33	.11(.05)	5½(14)	1000	171	CIR-2059/240	43	.24(.1)
1½(4)	85	73	CIR-2016/120	30	.06(.3)	2⅞(7)	300	109	CIR-20254/240	33	.11(.05)	6 (15)	200	31	CIR-2064/120	45	.24(.1)
1½(4)	100	85	CIR-20151/*	30	.06(.3)	3 (8)	100	34	CIR-2032/*	34	.12(.05)	6 (15)	250	39	CIR-2061/*	45	.24(.1)
1½(4)	130	111	CIR-20152/240	30	.06(.3)	3 (8)	150	51	CIR-2033/*	34	.12(.05)	6 (15)	400	62	CIR-2065/*	45	.24(.1)
1½(4)	150	129	CIR-2019/*	30	.06(.3)	3 (8)	200	68	CIR-2031/*	34	.12(.05)	6 (15)	500	78	CIR-2060/*	45	.24(.1)
1½(4)	200	171	CIR-2015/*	30	.06(.3)	3 (8)	250	85	CIR-2034/*	34	.12(.05)	6 (15)	600	93	CIR-2066/*	45	.24(.1)
1½(4)	250	214	CIR-20191/*	30	.06(.3)	3 (8)	300	103	CIR-20301/*	34	.12(.05)	6 (15)	750	117	CIR-2062/240	45	.24(.1)
1¾(4)	125	85	CIR-2017/120	30	.06(.3)	3 (8)	400	137	CIR-20302/*	34	.12(.05)	6 (15)	1000	155	CIR-2063/240	45	.24(.1)
1¾(4)	175	120	CIR-2017/120	30	.06(.3)	3 (8)	500	171	CIR-2030/*	34	.12(.05)	6½(17)	600	85	CIR-2067/240	47	.26(.1)
1¾(4)	250	170	CIR-20172/*	30	.06(.3)	3 (8)	600	205	CIR-2036/240	34	.12(.05)	6½(17)	1000	143	CIR-2068/240	47	.26(.1)
1⅞(5)	200	128	CIR-20173/120	30	.06(.3)	3½ (9)	250	71	CIR-2037/*	36	.14(.06)	7 (18)	250	33	CIR-2070/*	49	.28(.1)
2 (5)	50	29	CIR-20201/120	30	.07(.3)	3½ (9)	300	86	CIR-2038/*	36	.14(.06)	7 (18)	600	79	CIR-2076/*	49	.28(.1)
2 (5)	75	42	CIR-20209/120	30	.07(.3)	3½ (9)	500	142	CIR-2035/*	36	.14(.06)	7 (18)	1000	131	CIR-2079/240	49	.28(.1)
2 (5)	100	57	CIR-20202/*	30	.07(.3)	3⅞ (10)	150	37	CIR-2039/120	37	.15(.07)	7½(19)	600	73	CIR-2075/240	51	.30(.1)
2 (5)	150	85	CIR-2021/*	30	.07(.3)	3⅞(10)	500	128	CIR-20303/240	37	.15(.07)	7½(19)	1000	122	CIR-2077/240	51	.30(.1)
2 (5)	200	114	CIR-20203/*	30	.07(.3)	4 (10)	125	30	CIR-2045/*	38	.16(.07)	8 (20)	300	34	CIR-2081/*	53	.32(.1)
2 (5)	250	142	CIR-2020/*	30	.07(.3)	4 (10)	150	37	CIR-2041/*	38	.16(.07)	8 (20)	400	45	CIR-2082/120	53	.32(.1)
2 (5)	300	171	CIR-20204/*	30	.07(.3)	4 (10)	175	44	CIR-2046/120	38	.16(.07)	8 (20)	500	57	CIR-2085/*	53	.32(.1)
2 (5)	350	199	CIR-20205/*	30	.07(.3)	4 (10)	200	51	CIR-2044/240	38	.16(.07)	8 (20)	600	68	CIR-2086/*	53	.32(.1)
2 (5)	400	228	CIR-20206/*	30	.07(.3)	4 (10)	250	61	CIR-2042/*	38	.16(.07)	8 (20)	700	80	CIR-2080/*	53	.32(.1)
2 (5)	500	262	CIR-20207/*	30	.07(.3)	4 (10)	300	73	CIR-2040/*	38	.16(.07)	8 (20)	1000	115	CIR-2089/240	53	.32(.1)
2¼(6)	75	37	CIR-20225/120	31	.08(.4)	4 (10)	400	102	CIR-2047/*	38	.16(.07)	9½(24)	600	57	CIR-2090/240	64	.38(.2)
2¼(6)	100	49	CIR-20221/*	31	.08(.4)	4 (10)	450	110	CIR-2048/240	38	.16(.07)	9½(24)	1000	97	CIR-2091/240	64	.38(.2)
2¼(6)	125	61	CIR-2023/*	31	.08(.4)	4 (10)	500	122	CIR-2043/*	38	.16(.07)	10 (25)	400	36	CIR-2102/120	67	.40(.2)
2¼(6)	150	73	CIR-20222/*	31	.08(.4)	4 (10)	550	133	CIR-2049/120	38	.16(.07)	10 (25)	600	54	CIR-2100/*	67	.40(.2)
2¼(6)	175	86	CIR-20226/120	31	.08(.4)	4½ (11)	300	64	CIR-20401/*	40	.18(.08)	10 (25)	1000	90	CIR-2101/240	67	.40(.2)
2¼(6)	200	98	CIR-20223/*	31	.08(.4)	4½(11)	500	106	CIR-20402/*	40	.18(.08)	12 (30)	400	30	CIR-2122/120	69	.48(.2)
2¼(6)	250	122	CIR-2022/*	31	.08(.4)	4⅞(12)	300	58	CIR-20403/240	41	.19(.09)	12 (30)	600	45	CIR-2123/*	69	.48(.2)
2¼(6)	300	147	CIR-20224/*	31	.08(.4)	4⅞(12)	500	97	CIR-20404/240	41	.19(.09)	12 (30)	900	67	CIR-2120/*	69	.48(.2)
2¼(6)	350	172	CIR-20227/*	31	.08(.4)	5 (13)	150	29	CIR-2055/*	42	.20(.09)	12 (30)	1000	74	CIR-2121/240	69	.48(.2)
2⅝(6)	75	34	CIR-2025/120	32	.09(.4)	5 (13)	200	38	CIR-2051/*	42	.20(.09)	15 (38)	1100	65	CIR-2150/240	80	.80(.4)
2⅝(6)	165	75	CIR-2024/*	32	.09(.4)	5 (13)	300	57	CIR-2052/*	42	.20(.09)	20 (51)	1300	57	CIR-2200/240	90	.80(.4)
2½(6)	100	43	CIR-2027/240	32	.10(.05)	5 (13)	400	76	CIR-2050/*	42	.20(.09)	24(61)	1500	55	CIR-2240/240	115	.90(.4)
2½(6)	200	86	CIR-2028/*	32	.10(.05)	5 (13)	500	95	CIR-2053/*	42	.20(.09)						

Designate voltage, insert 120 for 120VAC or 240. for 240VAC. Those catalog numbers containing 120 or 240 are only available in that voltage. † †Consult Sales. Note: ¼" (1cm) diameter CIR series cartridge heaters use 17 AWG stranded lead wire.

Ordering Example:** Model CIR-2054/240. ¼", high watt density cartridge heater, **$ 42.

State of the Art, Inc.
0402 Thick Film Chip Resistor
Standard Grade, Surface Mount, Solderable

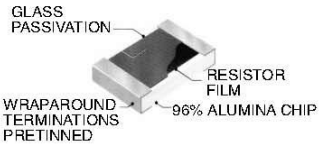

FEATURES

- Tolerances to ± 0.5%
- Operating temperature range : -55° C to +150° C
- Pretinned (Sn60) nickel barrier terminations
- TCR's to ± 100 ppm
- Made with the same materials and process as our MIL-PRF-55342 "S" level qualified chips
- Suitable for solder reflow, vapor phase, or wave solder attachment

PERFORMANCE CHARACTERISTICS

Resistance Range (1)	IΩ–40MΩ
Tolerances (2)	1%, 2%, 5%, 10%
Maximum Power	50 mW
Maximum Voltage	30 Volts

ENVIRONMENTAL PERFORMANCE (3)

TCR (-55 to +125 °C in ppm/°C)	< 100 ppm
Thermal Shock	±0.03%
Low Temperature Operation	±0.03%
Short-time Overload	±0.03%
Resistance to Bonding Exposure	±0.03%
Moisture Resistance	±0.05%
High Temperature Exposure	±0.05%
Life	See Chart

(1) SOTA offers milliohm and high megohm resistors with excellent performance.
(2) ±0.5% in limited availability
(3) Typical resistance change, the maximum is the same as MIL-PRF-55342. Test methods are per MIL-PRF-55342.

CURRENT NOISE

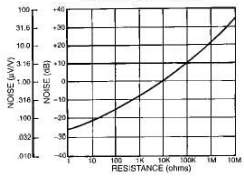

POWER DISSIPATION

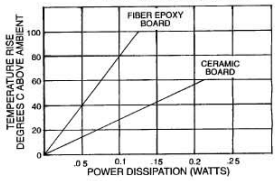

TYPICAL LIFE TEST PERFORMANCE

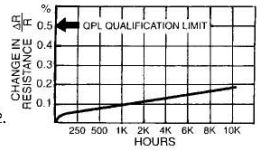

POWER DERATING

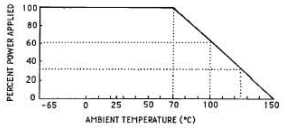

PART NUMBERING

S0402CPX 150 J 20

TCR
10: ±100 ppm 20: ±200 ppm 30: ±300 ppm

TOLERANCES
D: 0.5% F: 1% G: 2% J: 5% K: 10% M: 20%

RESISTANCE VALUE
Three or four digits are used with all leading digits significant. Four digits are used for 1% tolerance or lower, otherwise three digits are used. The last digit specifies the number of zeros to add. The letter "R" is used to represent the decimal for fractional ohmic values. Example: 5R6 is 5.6 ohms.

MECHANICAL

	INCHES	MM
Length	.040 (+.005/-.002)	1.02 (+.13/-.05)
Width	.020 (±.003)	.51 (±.08)
Thickness	.008 - .020	.20 - .51
Top Term.	.005 - .015	.13 - .38
Bottom Term.	.008 - .015	.20 - .38

Approx. Weight .00108 grams

Solderability: Solder coating compatible with Sn60, 62 or 63 solders, provides good wetting with all types of solder attachment. All product is tested IAW Mil-Std-202, method 208, including 8 hour steam aging.

PACKAGING

Three packaging options are available:

- Bulk Packaging - (5000 per Bag Max.)
- Waffle Pack - (400 per Tray Max.)

OPTIONS

SOTA offers a full line of component parts in the 0402 size including High-Reliability (customer specified testing). Available options are epoxy bondable and wire bondable terminations, custom part marking, and untrimmed resistors.

STATE OF THE ART, INC. 2470 Fox Hill Road, State College, PA 16803-1797
Phone (814) 355-8004 Fax (814) 355-2714 **Toll Free 1-800-458-3401**

10/01/97

Where Quality Isn't a Goal...It's Our Tradition

RIEDON

Type CRS
Miniature Thick Film Chip Resistors

- **Thick Film Resistance Element**
- **Resistance from 0.1Ω to 500 MΩ**
- **Tolerances from ± 0.5% to ± 20%**
- **TCR's from ± 50 ppm/°C to ± 250 ppm/°C**
- **Available Trimmed and Untrimmed**
- **Sizes; 0302, 0402, 0504, 0603, 0805, 1206**

Riedon's new precision chip resistors use thick film resistance layers, glass passivation, and tinned contact areas for soldering. This ensures a highly stable and reliable resistor. General properties are to CECC 40401 standards.

SPECIFICATIONS

CRS Size	0302	0402	0504	0603	0805	1206
Power Rating (mW) [1]	35	50	100	100	125	250
Working Voltage(V) *Trimmed* (*Untrimmed*)	15 (50)	30 (90)	50 (150)	75 (220)	100 (300)	200 (600)
Resistance	Tolerances Available (%) TCR's Available (± ppm/°C)					
0.1 - <1	-	-	-	10 to 20% 100, 250	5 to 20% 100, 250	5 to 20% 100, 250
1 - <10	10 to 20% 250	10 to 20% 250	5 to 20% 100, 250	5 to 20% 100, 250	5 to 20% 100, 250	5 to 20% 100, 250
10 - <100	5 to 10% 100	5 to 10% 100	2 to 10% 100	1 to 10% 100	1 to 10% 50, 100	1 to 10% 50, 100
100 - 1M	5 to 10% 50, 100	5 to 10% 50, 100	1 to 10% 50, 100	1 to 10% 50, 100	0.5 to 10% 50, 100	0.5 to 10% 50, 100
>1M to 10M	5 to 20% 100, 250	5 to 20% 100, 250	1 to 10% 50, 100	1 to 10% 50, 100	0.5 to 10% 50, 100	0.5 to 10% 50, 100
>10M to 100M	-	5 to 20% 100, 250	2 to 20% 100, 250	1 to 20% 50, 100	0.5 to 20% 50, 100	0.5 to 20% 50, 100
>100M to 500M	-	-	-	5 to 20% 100, 250	2 to 20% 100, 250	2 to 20% 100, 250

[1] mW @ 70°C, 0mW @ 155°C

Temperature Range - -55°C to +155°C
Climatic Category - 55/125/56
Solderability - 235°C, 2 Seconds
Max. Soldering Temperature - 260°C, 10 Seconds

Riedon Inc. 300 Cypress Avenue Alhambra CA 91801 (626) 284-9901 Fax: (626) 284-1704
www.riedon.com
REV 10.03

RIEDON

Type CRS
Miniature Thick Film Chip Resistors

Long Term Stability	10Ω-10MΩ	<10Ω, >10MΩ
Storage 125°C/1000h	<0.5%	<1%
Storage 155°C/1000h	<1%	<2%
Load P_{70}/70°C/1000h	<0.5%	<1%
Short Term Overload	<0.25%	<0.5%
Damp Heat (56d/40°C/96%)	<0.5%	<1%

DIMENSIONS

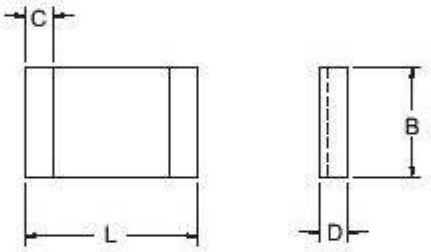

Size	L	B	D	C
CRS0302	0.79 ±0.05	0.5 ±0.05	0.3 ±0.05	0.1 $^{+0.1}_{-0.05}$
CRS0402	1.05 ±0.05	0.5 ±0.05	0.3 ±0.05	0.1 $^{+0.1}_{-0.05}$
CRS0504	1.25 $^{+0.15}_{-0.05}$	1.0 $^{+0.15}_{-0.05}$	0.3 $^{+0.15}_{-0.05}$	0.2 $^{+0.2}_{-0.1}$
CRS0603	1.5 $^{+0.15}_{-0.05}$	0.8 $^{+0.15}_{-0.05}$	0.4 $^{+0.15}_{-0.05}$	0.2 $^{+0.2}_{-0.1}$
CRS0805	2.0 $^{+0.15}_{-0.05}$	1.2 $^{+0.20}_{-0.05}$	0.4 $^{+0.15}_{-0.05}$	0.3 $^{+0.2}_{-0.1}$
CRS1206	3.2 $^{+0.15}_{-0.05}$	1.5 $^{+0.20}_{-0.05}$	0.4 $^{+0.15}_{-0.05}$	0.3 $^{+0.2}_{-0.1}$

Units: mm per CECC40401

Packaging:

Bulk or Tape & Reel per IEC 286-3 / EIA 481-1-A

Tape width 8mm, Reel diameter 180 or 330mm
Minimum quantity Bulk, 100 pieces per value
Minimum quantity Tape & Reel, 1000 pieces per value

Ordering information:

Type/Size - Resistance - Tolerance - TCR - Packaging (if not Bulk)

Example: **CRS1206 - 1M - 5 - 50 - Tape**
(Note: if no TCR is specified, the highest value will be supplied)

Riedon Inc. 300 Cypress Avenue Alhambra CA 91801 (626) 284-9901 Fax: (626) 284-1704
www.riedon.com

REV 10.03

APPENDIX B: MANUFACTURING DRAWINGS FOR MULTIPLE NOZZLE SPRAY COOLER AND HEATER

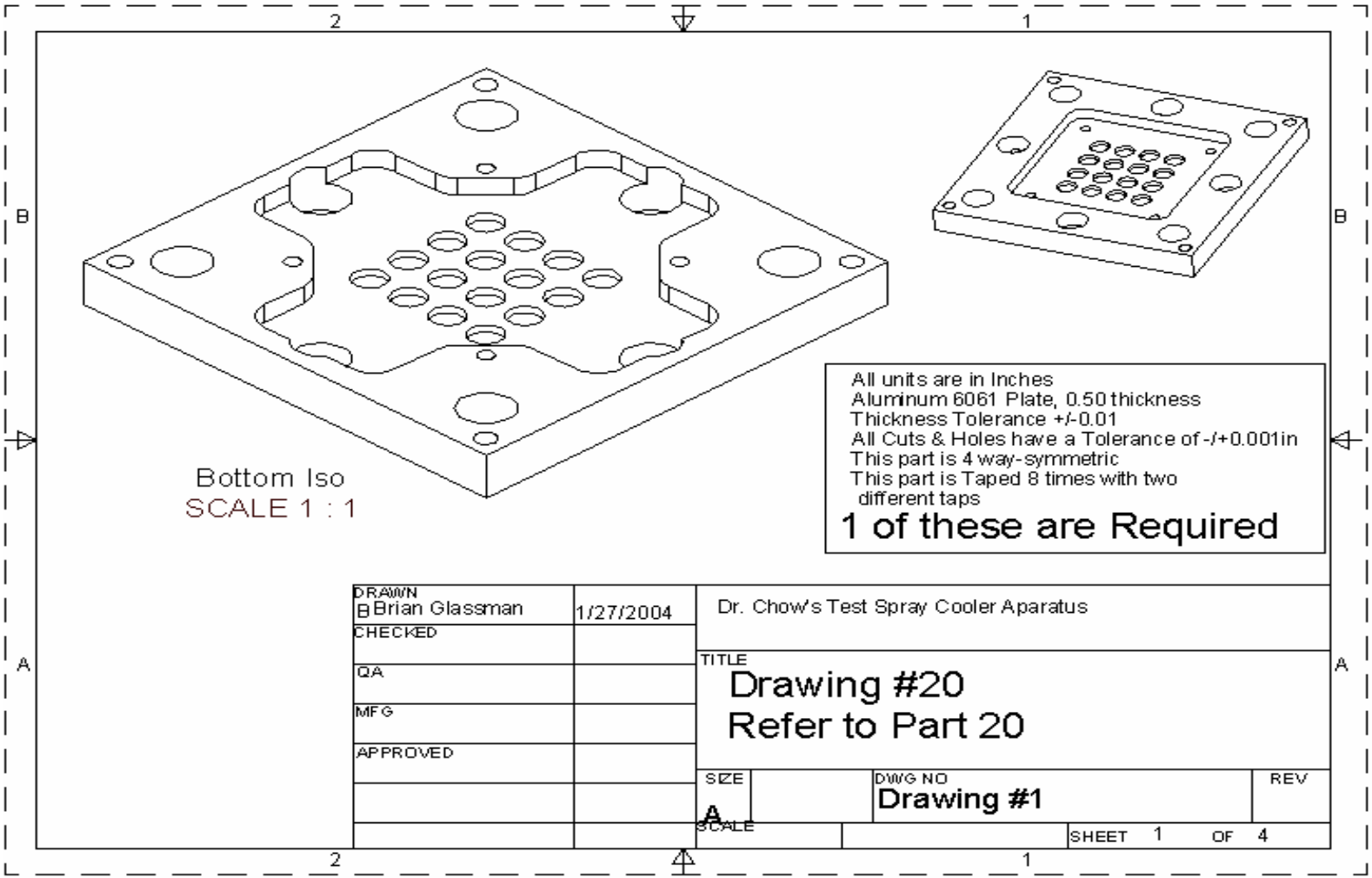
2
1
B
A
Bottom Iso
SCALE 1 : 1
All units are in Inches
Aluminum 6061 Plate, 0.50 thickness
Thickness Tolerance +/-0.01
All Cuts & Holes have a Tolerance of -/+0.001in
This part is 4 way-symmetric
This part is Taped 8 times with two
different taps
1 of these are Required
DRAWN
Brian Glassman
1/27/2004
CHECKED
QA
MFG
APPROVED
Dr. Chow's Test Spray Cooler Aparatus
TITLE
Drawing #20
Refer to Part 20
SIZE
A
DWG NO
Drawing #1
REV
SCALE
SHEET 1 OF 4

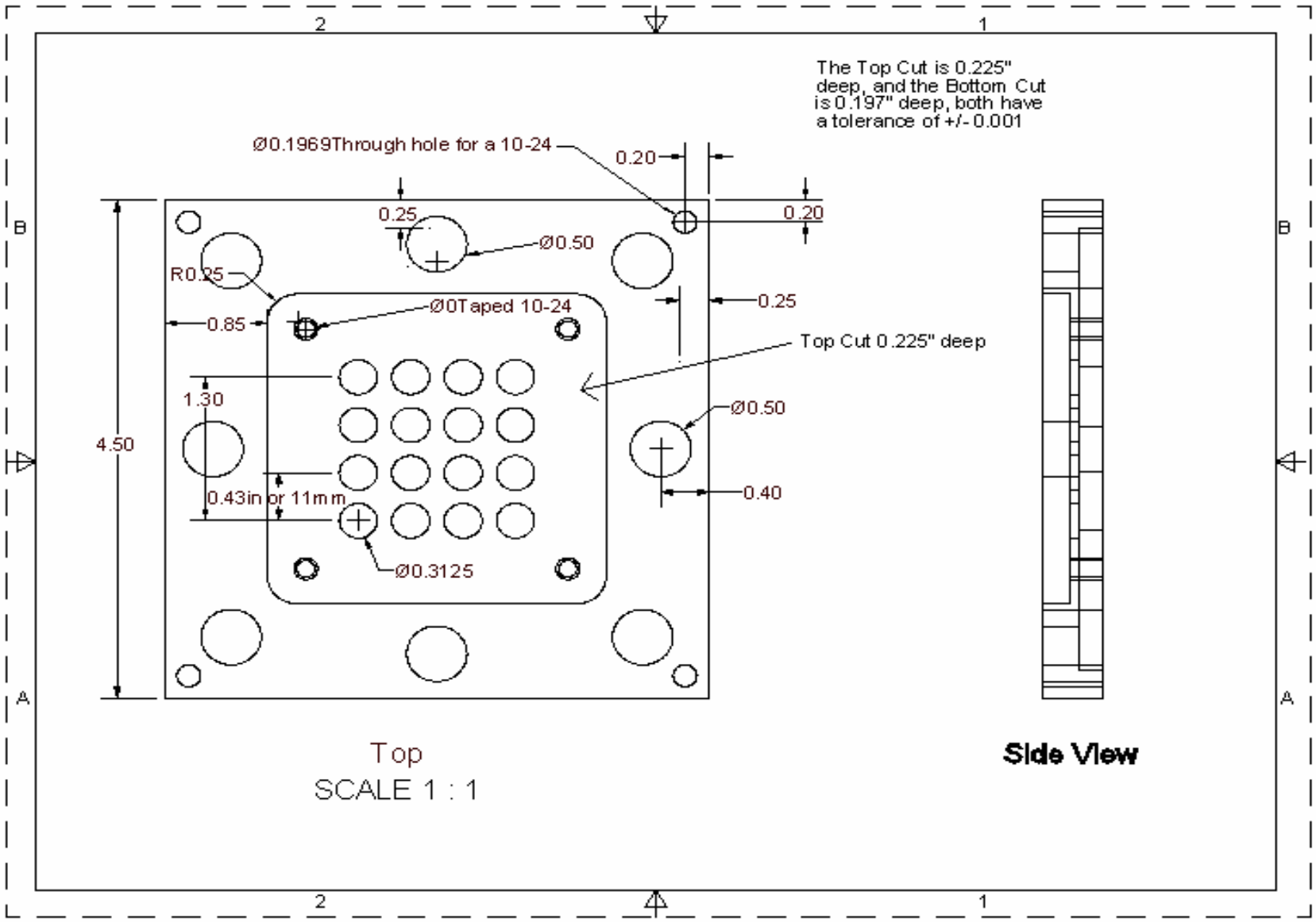
2
1
The Top Cut is 0.225" deep, and the Bottom Cut is 0.197" deep, both have a tolerance of +/- 0.001
Ø0.1969Through hole for a 10-24
0.20
0.25
0.20
Ø0.50
R0.25
0.25
Ø0Taped 10-24
0.85
Top Cut 0.225" deep
1.30
Ø0.50
4.50
0.40
0.43in or 11mm
Ø0.3125
B
A
Top
SCALE 1 : 1
Side View

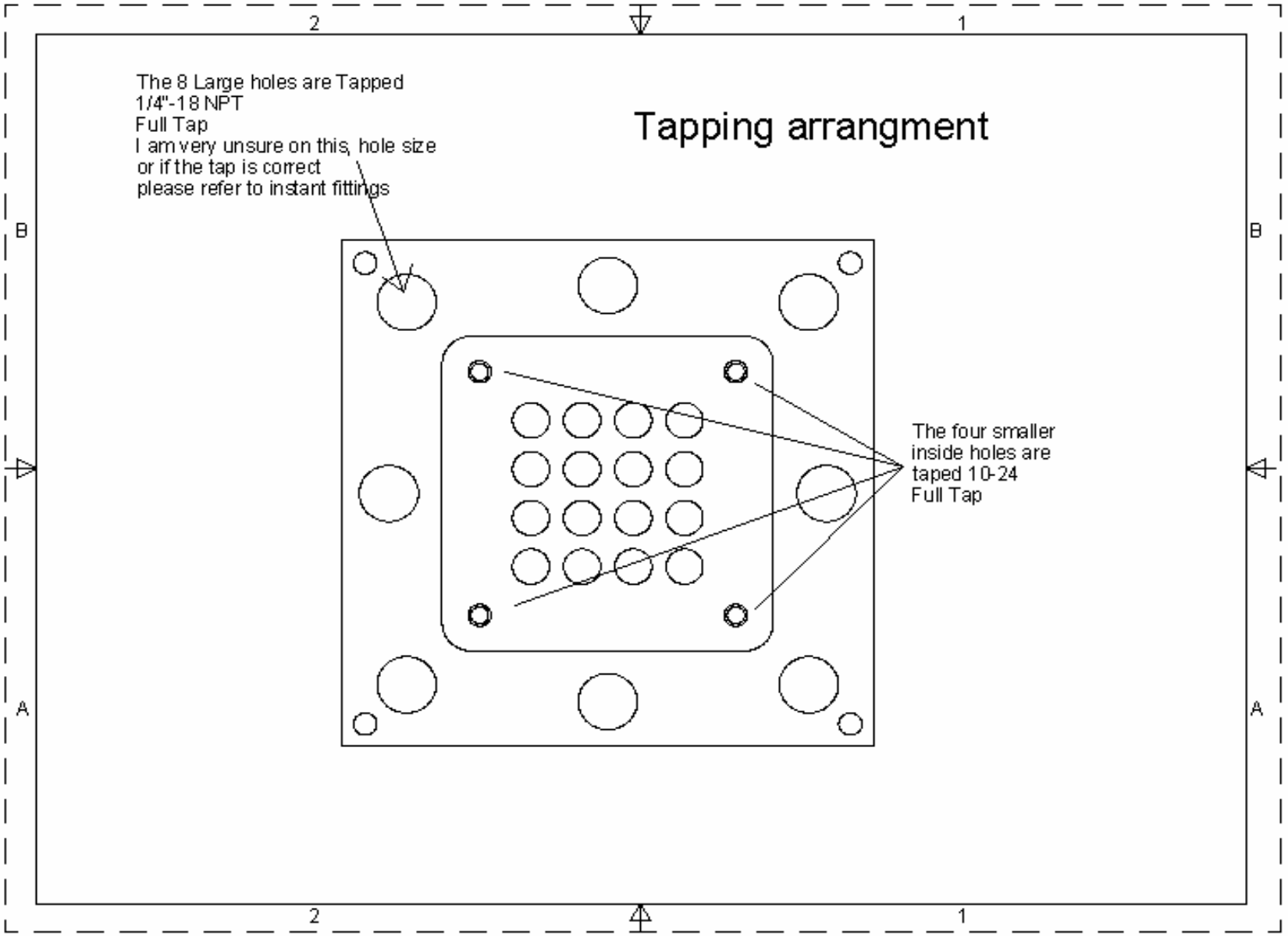
2
1
The 8 Large holes are Tapped
1/4"-18 NPT
Full Tap
I am very unsure on this, hole size
or if the tap is correct
please refer to instant fittings
Tapping arrangment
B
A
The four smaller
inside holes are
taped 10-24
Full Tap

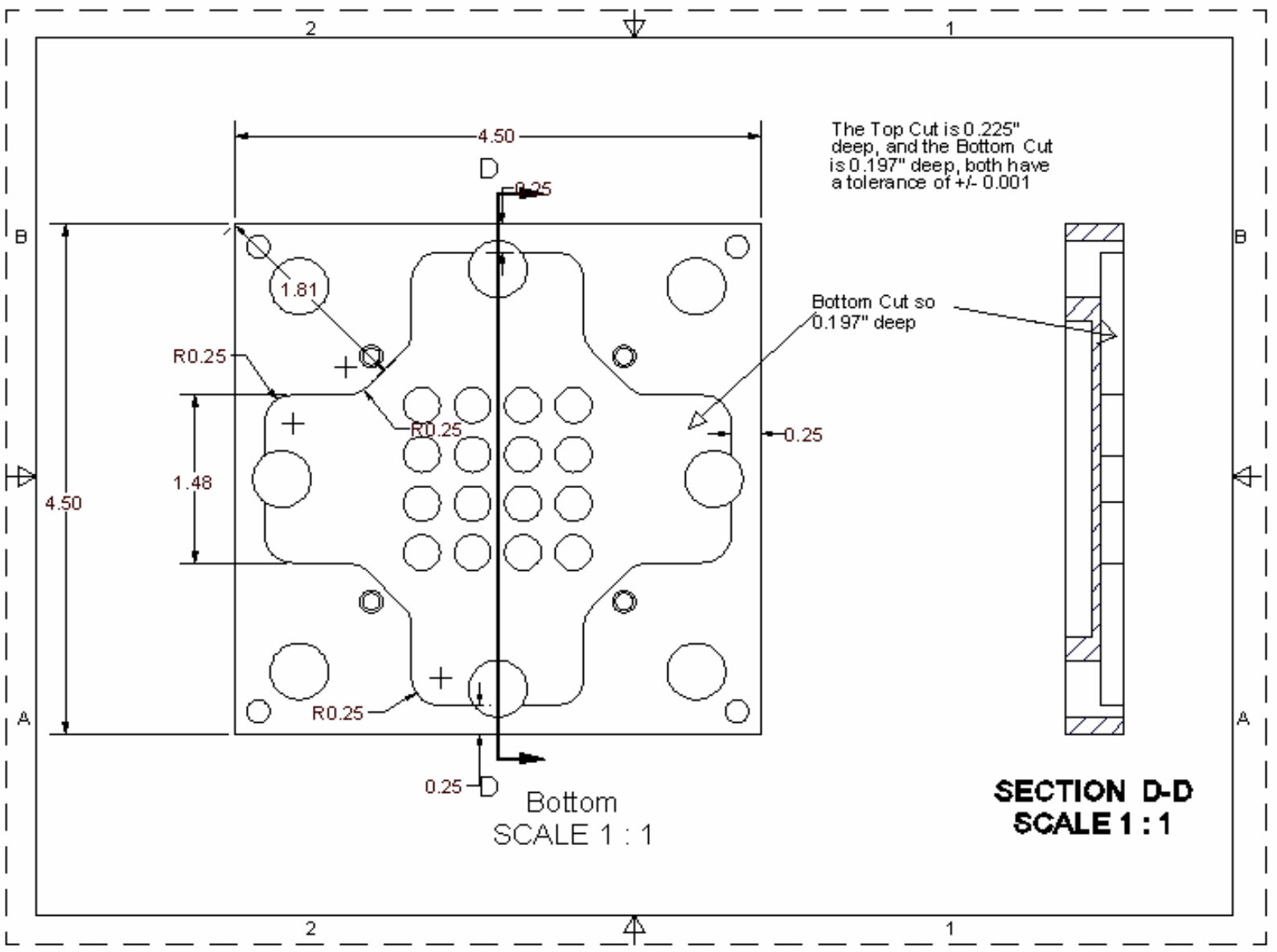
2
1
B
A
4.50
D
0.25
1.81
R0.25
R0.25
1.48
4.50
R0.25
0.25
0.25
D
Bottom
SCALE 1 : 1
The Top Cut is 0.225" deep, and the Bottom Cut is 0.197" deep, both have a tolerance of +/- 0.001
Bottom Cut so 0.197" deep
SECTION D-D
SCALE 1 : 1

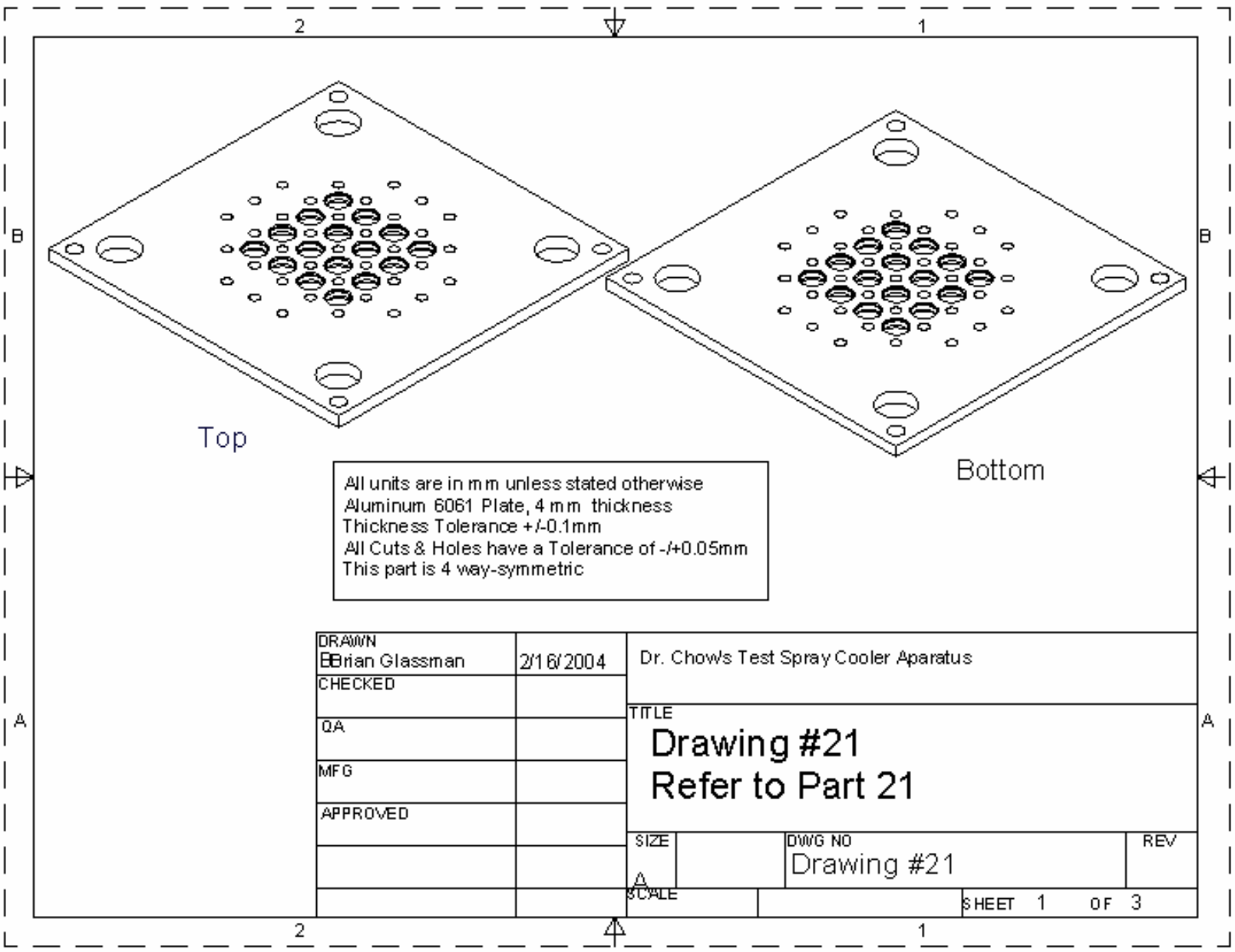
2
1
B
A
Top
Bottom
All units are in mm unless stated otherwise
Aluminum 6061 Plate, 4 mm thickness
Thickness Tolerance +/-0.1mm
All Cuts & Holes have a Tolerance of -/+0.05mm
This part is 4 way-symmetric
DRAWN
BBrian Glassman
2/16/2004
CHECKED
QA
MFG
APPROVED
Dr. Chow's Test Spray Cooler Aparatus
TITLE
Drawing #21
Refer to Part 21
SIZE
A
DWG NO
Drawing #21
REV
SCALE
SHEET 1 OF 3

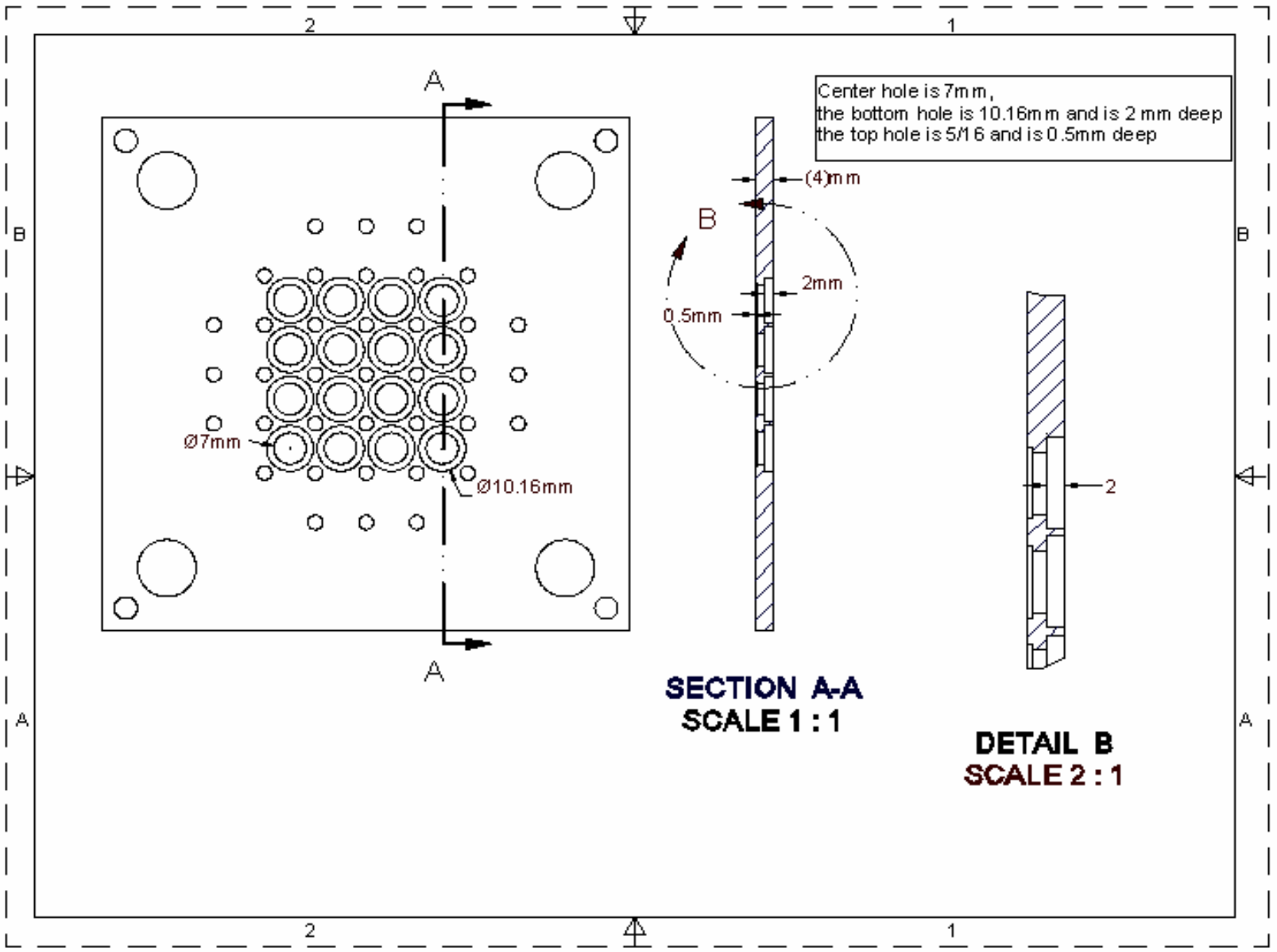
Center hole is 7mm,
the bottom hole is 10.16mm and is 2 mm deep
the top hole is 5/16 and is 0.5mm deep
A
A
B
Ø7mm
Ø10.16mm
(4)mm
2mm
0.5mm
2
SECTION A-A
SCALE 1 : 1
DETAIL B
SCALE 2 : 1

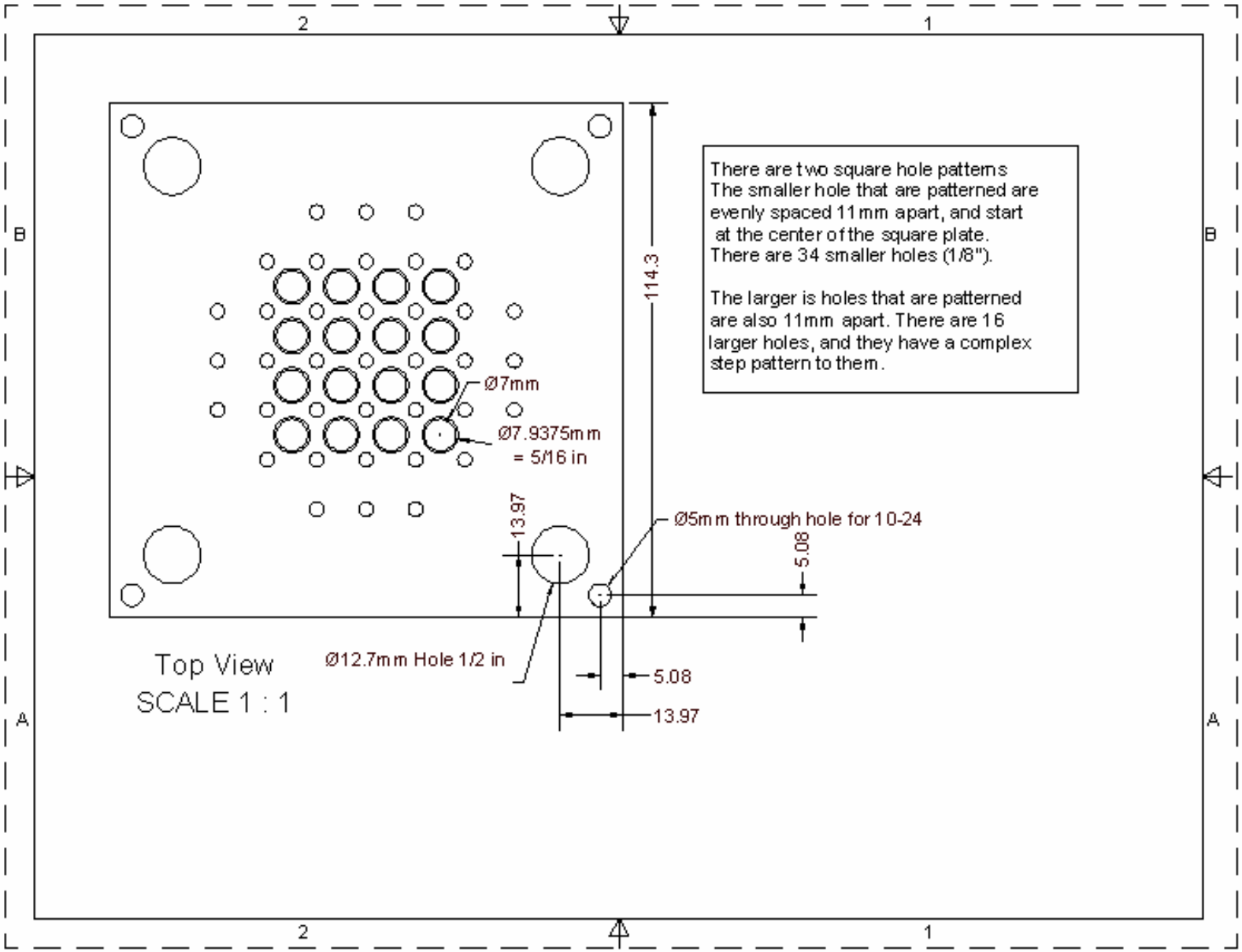
2
1
B
A
There are two square hole patterns
The smaller hole that are patterned are
evenly spaced 11mm apart, and start
at the center of the square plate.
There are 34 smaller holes (1/8").
The larger is holes that are patterned
are also 11mm apart. There are 16
larger holes, and they have a complex
step pattern to them.
114.3
Ø7mm
Ø7.9375mm
= 5/16 in
13.97
Ø5mm through hole for 10-24
5.08
Ø12.7mm Hole 1/2 in
5.08
13.97
Top View
SCALE 1 : 1

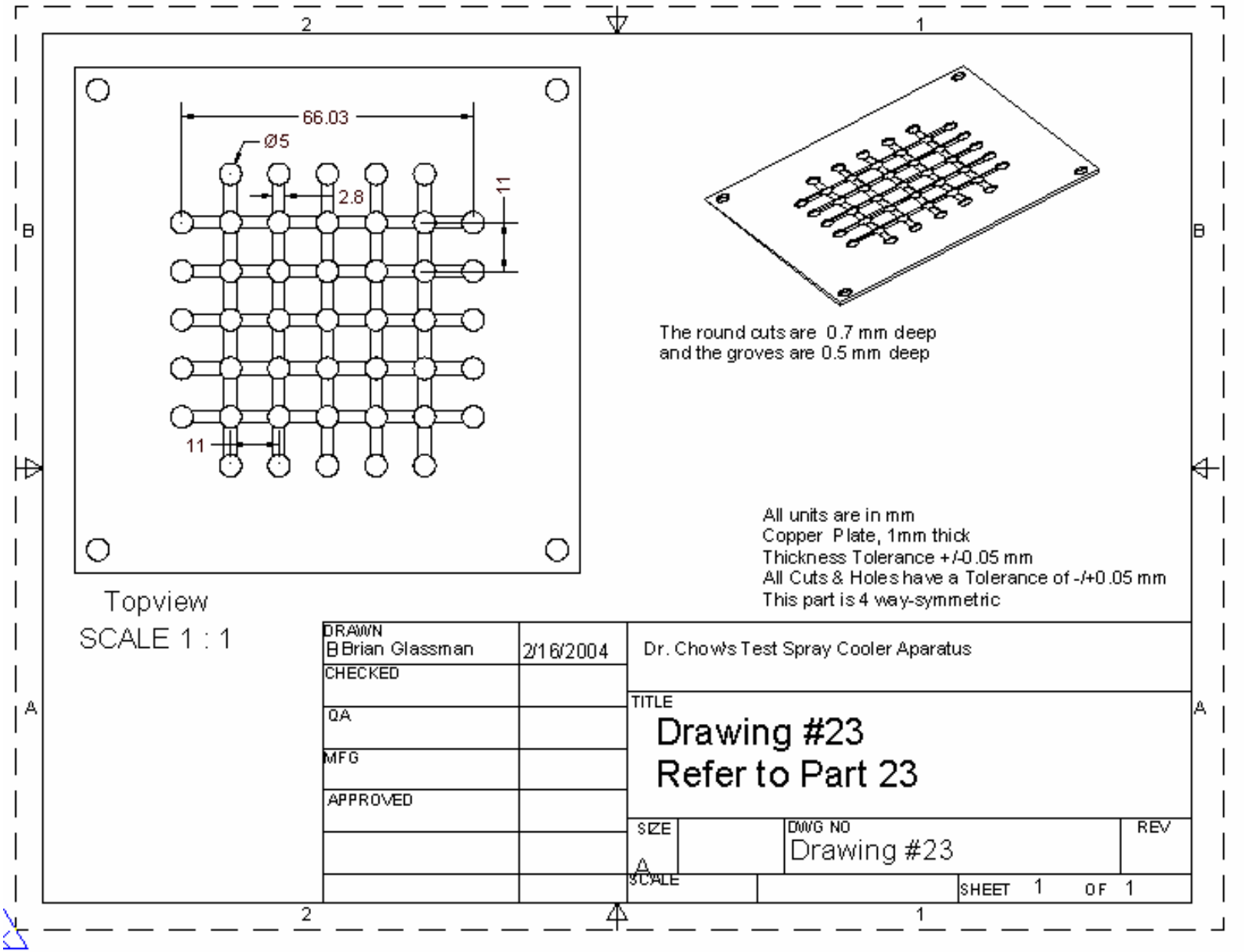
66.03
Ø5
2.8
11
11
Topview
SCALE 1 : 1
The round cuts are 0.7 mm deep
and the groves are 0.5 mm deep
All units are in mm
Copper Plate, 1mm thick
Thickness Tolerance +/-0.05 mm
All Cuts & Holes have a Tolerance of -/+0.05 mm
This part is 4 way-symmetric
DRAWN
Brian Glassman
2/16/2004
CHECKED
QA
MFG
APPROVED
Dr. Chow's Test Spray Cooler Aparatus
TITLE
Drawing #23
Refer to Part 23
SIZE
A
DWG NO
Drawing #23
REV
SCALE
SHEET 1 OF 1

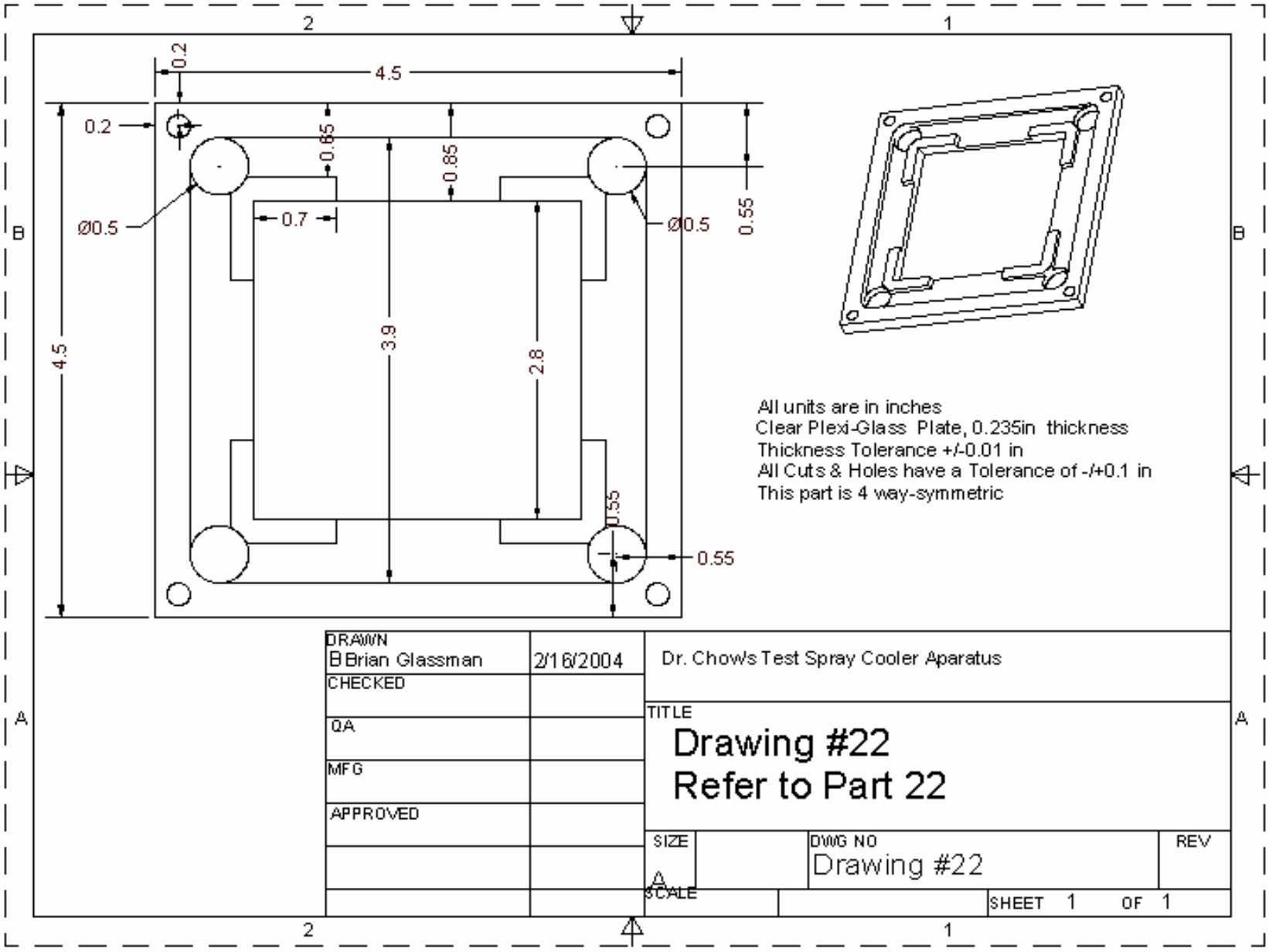
2
1
0.2
4.5
0.2
0.85
0.85
0.7
Ø0.5
Ø0.5
0.55
4.5
3.9
2.8
0.55
0.55
B
A
All units are in inches
Clear Plexi-Glass Plate, 0.235in thickness
Thickness Tolerance +/-0.01 in
All Cuts & Holes have a Tolerance of -/+0.1 in
This part is 4 way-symmetric
DRAWN
Brian Glassman
2/16/2004
CHECKED
QA
MFG
APPROVED
Dr. Chow's Test Spray Cooler Aparatus
TITLE
Drawing #22
Refer to Part 22
SIZE
A
DWG NO
Drawing #22
REV
SCALE
SHEET 1 OF 1

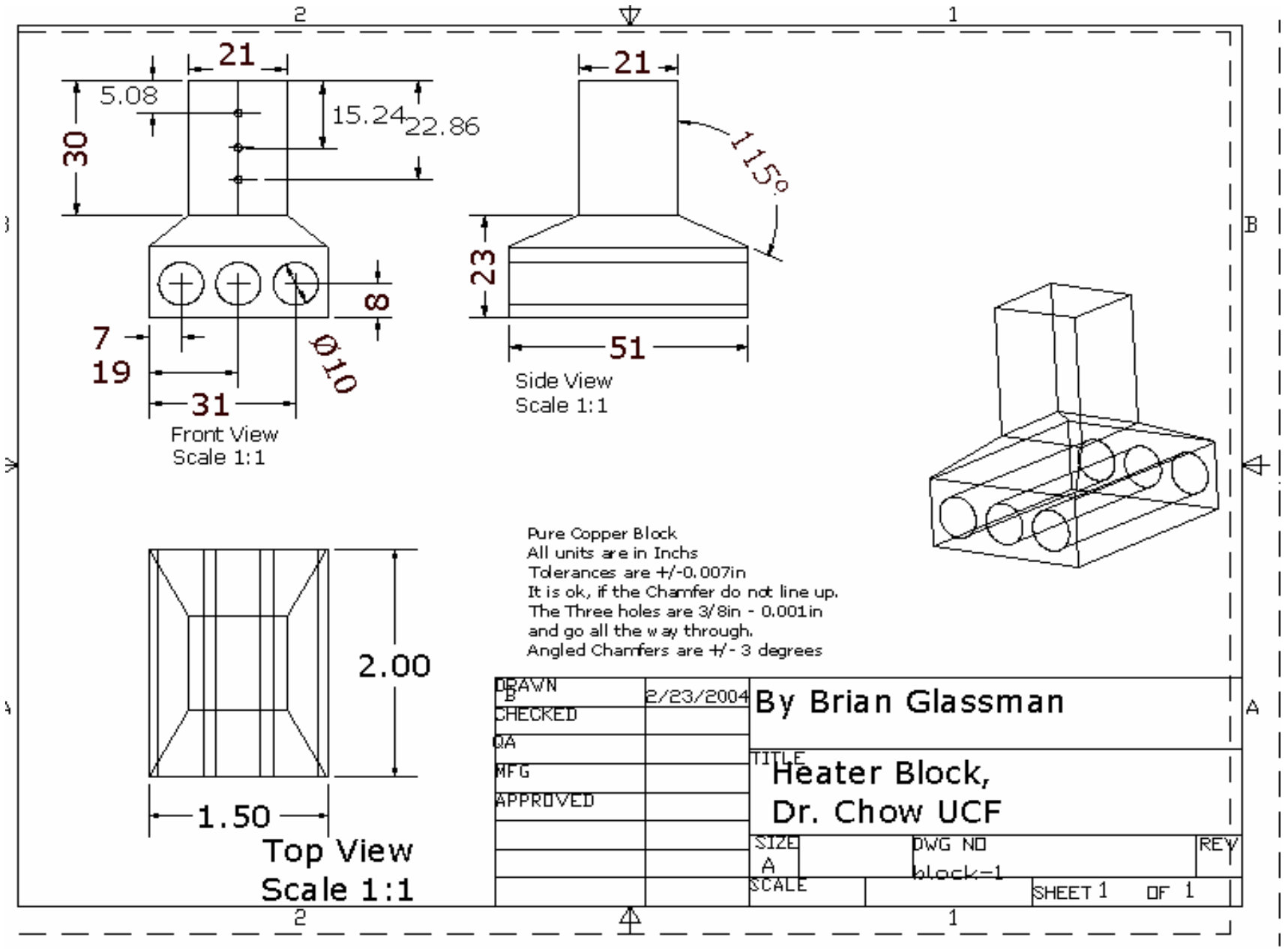
21
5.08
15.24
22.86
30
8
7
19
31
Ø10
Front View
Scale 1:1
21
115°
23
51
Side View
Scale 1:1
2.00
1.50
Top View
Scale 1:1
Pure Copper Block
All units are in Inchs
Tolerances are +/-0.007in
It is ok, if the Chamfer do not line up.
The Three holes are 3/8in - 0.001in
and go all the way through.
Angled Chamfers are +/- 3 degrees
DRAWN
B
2/23/2004
CHECKED
QA
MFG
APPROVED
By Brian Glassman
TITLE
Heater Block,
Dr. Chow UCF
SIZE
A
DWG NO
block-1
REV
SCALE
SHEET 1 OF 1

APPENDIX C: SUBCOOLED FLOW BOILING AND SPRAY COOLING CACLUATIONS

Sub-Cooled Flow Boiling Utilizing Water

Book Values

C_p= 4.18 kJ/ kg-k

Calculations

Win = $\dot{m}(\Delta h) = \dot{m} * C_p(T_{out} - T_{in})$ Solving for $\dot{m}$ one gets

$$\dot{m} = \frac{\dot{Q}}{C_p(T_{out} - T_{in})} = \frac{\dot{Q}}{C_p(\Delta T)}$$

Assume an input 20°C of and an outlet 30°C of which gives a Δ10°C then the flow rate can be calculated as follows: Where ΔT is the temperature difference between the inlet and outlet of the cooling jacket

For ΔT = 10°C one gets

$$\dot{V} = \frac{2{,}500 kJ/s * (1 liter/1 kg)}{4.18 kJ/kg * C(10^{\circ} C)} = 59.8 \text{ L/s} \qquad 60 \text{ L/s} \approx 951 \text{ gallon/min}$$

For ΔT = 20℃ one gets *30 L/s ≈ 475 gallon/min*

For ΔT = 40°C one gets 14L/s ≈ 221 gallons/min

For open loop cooling of a 50KW heat source and a ΔT of 40°C the flow rate would be 0.3 Liters/s or 4.76 gallons/min. That means open loop subcooled flow boiling would have to reject *48.27 lbs/min* of water. This makes an open loop SCFB system extremely unreasonable and thus not applicable to smaller mobile cooling systems.

Spray Cooling Utilizing Water

Book Values for Water

h_{fg} = 2257.0 kJ/kg

The amount of water need to dissipate the heat loading is found by the following formula for spray cooling sub-cooled fluids

$\dot{Q} = \dot{m}(h_f + h_g)$ Solving for $\dot{m}$

$$\dot{m} = \frac{W_{in}}{(\Delta u + h_{fg})}$$

$$\dot{m} = \frac{\dot{Q}}{(h_f - h_g)}$$ Substituting in the values for water at 25°C & 100°C one gets

$$\dot{m} = \frac{2{,}500 kJ/s}{(2676.05 - 104.87) kJ/kg} = 0.97 \text{kg/s}$$

$\dot{m} = 0.97$ kg/s Convert with (1 Liter = 1 kg)

If this was and open loop system, this mass of water needed to operate at this heat load. Remember, excess liquid use during spray cooling can be recaptured and re-used

$\dot{V} = 0.97 Liter/s$ Converting this to gallons/mi

$\dot{V} = 0.266 gallon/s$ Multiply by 10.142 lbs/gallon

This is the amount liquid needed to vaporize to cool the required heat load, however spray cooling has vapor creation rate 20% to 40%. So taking the worst case at 20% vapor creation the required flow rate to the pumps will be

$\dot{V} = \frac{0.97 Liter/s}{0.2}$ =5 Liter/s Converting this to gallons/min one gets

$\dot{V} = 80 \frac{Gallons}{\min}$ *This is the required flow rate supplied by the pumps*

$\dot{V}_{vapor} = \dot{m} * v_{vapor}$ Given the specific volume of steam is 1.673 m^3/kg

$\dot{V}_{vapor} = 1.6228 m^3/s$ This is the volume of vapor created per second

In such case where the heat loads are 250W instead of 2.5MW, the flowrates would be scaled down by a factor $10E^4$.

APPENDIX D: UNCERTAINTY CALCULATIONS FOR HEAT FLUX

$\dot{Q} = k\frac{\Delta T}{\Delta X}$ Partial differentiation and substitution gives

$$\partial\dot{Q} = \partial k\left(\frac{\Delta T}{\Delta X}\right) + \partial\Delta T\left(\frac{k}{\Delta X}\right) + \frac{\partial\Delta X}{\Delta X^2}\left(k * \Delta T\right)$$

Substituting in $\dot{Q} = k\frac{\Delta T}{\Delta X}$

$$\partial\dot{Q} = \dot{Q} * \left(\frac{\partial k}{k}\right) + \dot{Q} * \left(\frac{\partial T}{\Delta T}\right) + \dot{Q} * \left(\frac{\partial X}{X}\right)$$

For the temperature and the position the difference of squares is required

$$\partial\dot{Q} = \dot{Q} * \left(\left(\frac{\partial k}{k}\right) + \left(\frac{\sqrt{2(\partial T)^2}}{\Delta T}\right) + \left(\frac{\sqrt{2(\partial X)^2}}{\Delta X}\right)\right)$$

For example assume the following reasonable values

$\dot{Q} = 500\frac{W}{Cm^2}$ $k = 393\frac{W}{m-K}$ $\Delta T = 382°C$ $\Delta X = 3cm$

$\partial k = 1\frac{W}{m-K}$ $\partial T = 0.5^{\circ}C$ $\partial X = 0.0127cm$

$$\partial\dot{Q} = \left(500\frac{W}{Cm^2}\left(\frac{1\frac{W}{m-K}}{393\frac{W}{m-K}}\right) + 500\frac{W}{Cm^2}\left(\frac{\sqrt{2(\partial 0.5C)^2}}{382C}\right) + 500\frac{W}{Cm^2}\left(\frac{\sqrt{2(0.0127cm)^2}}{3cm}\right)\right)$$

$\partial\dot{Q} = \left(1.3\frac{W}{Cm^2} + 1\frac{W}{Cm^2} + 3\frac{W}{Cm^2}\right)$ = (Error due to k + Error due to T + Error due to X)

The error in heat flux in this example is $\partial\dot{Q} = +/-5.3\frac{W}{Cm^2}$

APPENDIX E: SAMPLE HEAT FLUX AND TEMPERATURE GRAPHS

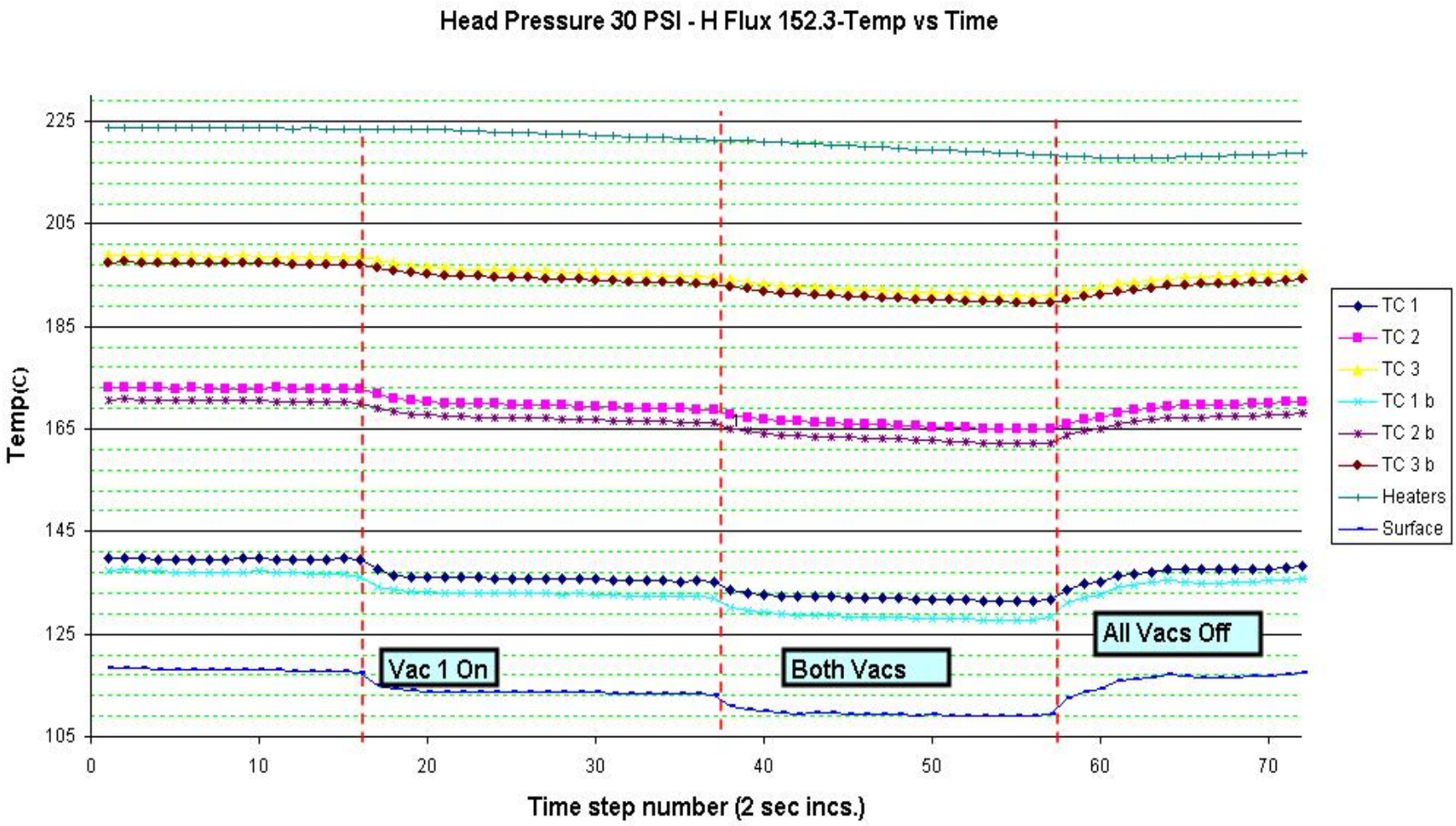

Temperature vs. Time Graph for Multiple Nozzle Experiment showing the effects one & two vacuums at 30 Psi Head Pressure

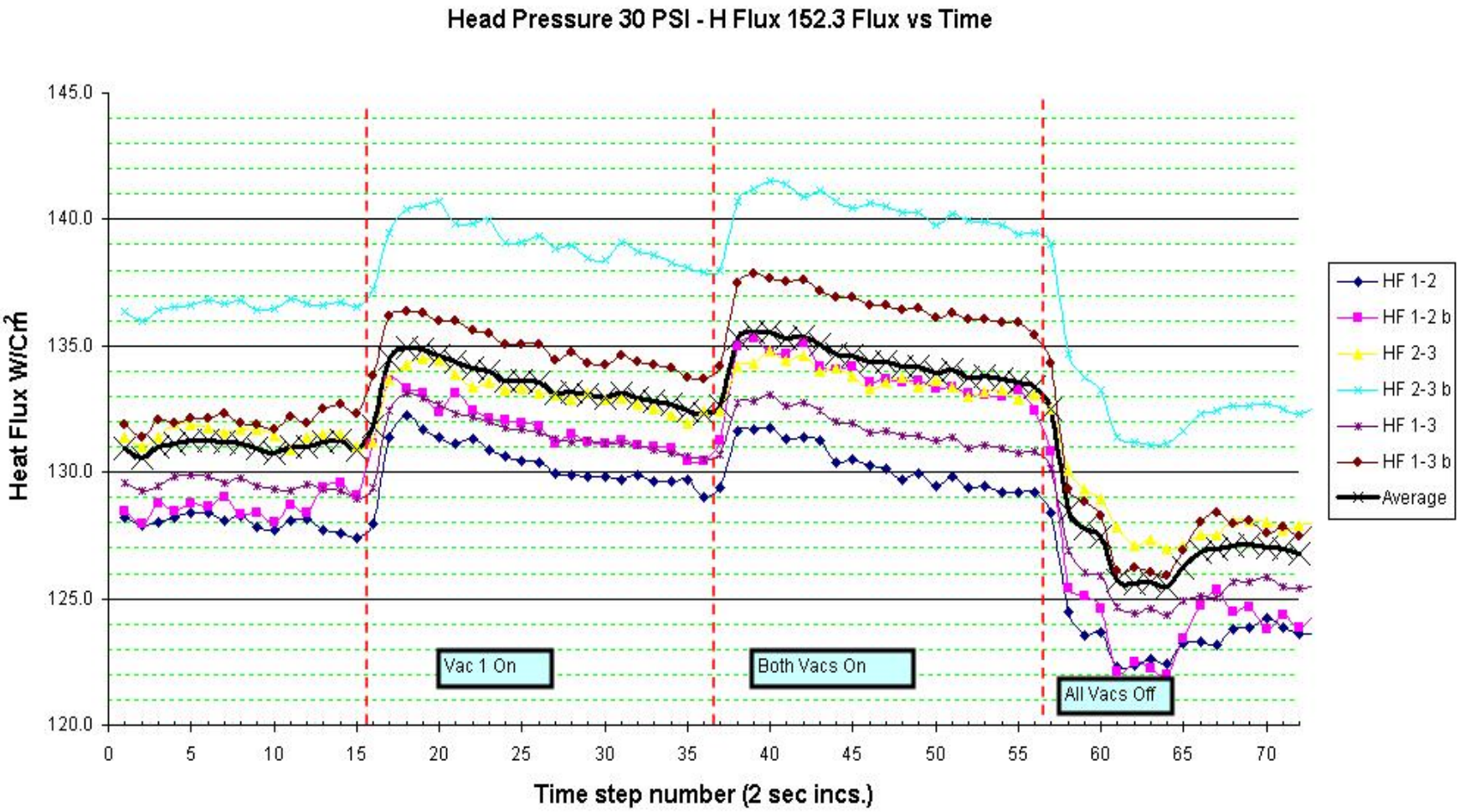

Heat Flux vs. Time Graph for Multiple Nozzle Experiment Showing the Effects One & Two Vacuums at Spray 30 Psi Head Pressure

APPENDIX F: SBIR AND STTR SPRAY COOLING AWARDS

#	PROGRAM	AGENCY	TOPIC NO & YEAR	FIRM	STATE	PHASE	AWARD AMT
1	SBIR	AF	AF 2003-175	CFD RESEARCH CORP.	AL	1	$99,972
2	SBIR	AF	AF 1995-176	CUDO TECHNOLOGIES, LTD.	KY	1	$54,887
3	SBIR	BMDO	BMDO1993-007	CUDO TECHNOLOGIES, LTD.	KY	1	$58,367
4	SBIR	BMDO	BMDO1992-007	CUDO TECHNOLOGIES, LTD.	KY	1	$57,332
5	SBIR	NAVY	NAVY1999-095	FERN ENGINEERING, INC.	MA	1	$67,234
6	SBIR	NAVY	NAVY2003-055	INNOVATIVE FLUIDICS, INC.	GA	1	$70,000
7	STTR	NAVY	NAVY2003-022	INNOVATIVE FLUIDICS, INC.	GA	1	$70,000
8	SBIR	AF	AF 1988-121	ISOTHERMAL SYSTEMS RESEARCH	KY	2	$399,884
9	SBIR	AF	AF 1988-121	ISOTHERMAL SYSTEMS RESEARCH	KY	1	$49,321
10	SBIR	OSD	OSD 2002-P04	ISOTHERMAL SYSTEMS RESEARCH	WA	1	$98,782
11	SBIR	AF	AF 2003-175	ISOTHERMAL SYSTEMS RESEARCH	WA	1	$99,449
12	SBIR	NAVY	NAVY1992-136	ISOTHERMAL SYSTEMS RESEARCH, INC.	WA	2	$790,121
13	SBIR	AF	AF 1995-179	ISOTHERMAL SYSTEMS RESEARCH, INC.	WA	1	$76,022
14	SBIR	MDA	MDA 2002-007	MAINSTREAM ENGINEERING CORP.	FL	1	$70,000
15	SBIR	MDA	MDA 2002-007	MAINSTREAM ENGINEERING CORP.	FL	1	$69,998
16	SBIR	BMDO	BMDO2001-007	MAINSTREAM ENGINEERING CORP.	FL	1	$64,999
17	SBIR	BMDO	BMDO2000-007	MAINSTREAM ENGINEERING CORP.	FL	1	$64,664
18	SBIR	MDA	MDA 2002-007	MAINSTREAM ENGINEERING CORP.	FL	2	$749,956
19	SBIR	NAVY	NAVY2003-055	OMEGA PIEZO TECHNOLOGIES	PA	1	$69,798
20	STTR	NAVY	NAVY2003-022	RINI TECHNOLOGIES, INC.	FL	1	$69,964
21	SBIR	MDA	MDA 2000-007	RINI TECHNOLOGIES, INC.	FL	2	$974,097
					Total Expenditures		$4,124,847

Taken from - http://www.dodsbir.net/Awards/Default.asp

LIST OF REFERANCES

1. F.P. Incropera, D.P Dewitt. *Fundamentals of Heat & Mass Transfer*. 5th ed. New York: John Wley & Sons, 2002.
2. R.A. Hardin, K Liu, A. Kapoor. "A Transient Simulation and Dynamic Spray Cooling Control Model for Continuous Steel Casting." *METALLURGICALAND MATERIALS TRANSACTIONS* 34B June 2003. Un. Iowa. 2/15/2005 <http://www.engineering.uiowa.edu/~becker/documents.dir/Hardin_CCTransient.pdf>
3. R.E Sonntag, C Borgnakke, G J. W. Wylen. *Fundementals of Thermodynamics*. New York: John Wiley & Sons, Inc., 1998.
4. L.C. Chow, M.S. Sehmbey, M.R. Pais. "High Heat Flux Spray Cooling." *Annual Review of Heat Transfer*. Vol. 8, 1997. 291-318.
5. Kaveh Azar. "Advanced Cooling Concepts and Their Challenges." Ed. www.qats.com. 2002. Advanced Thermal Solutions, Inc. <http://tima.imag.fr/Conferences/therminic/Therminic02/Posters/KAzar.pdf>.
6. Daniel P. Rini. "Advanced Liquid Cooling Workshop." 2003. 2/4/2005 <www.vita.com/cool/pres/1400-RTI.ppt>.
7. Kaveh Azar. *Thermal Measurements in Electronics Cooling*. Boca Raton, FL: CRC Press LLC, 1997.
8. M.R. Pais, M.J. Chang, M.J. Morgan and L.C. Chow. "Spray Cooling of High Power Laser Diodes." Paper presented at the 1994 SAE Aerospace Atlanta Conference & Exposition. Dayton, Ohio,: SAE, 1994. SAE Paper 941183.
9. Te-Yuan Chung. "Thermal Management, Beam Control, and Packaging Designs for High Power Diode Laser Arrays and Pump Cavity Designs for Diode Laser Array

Pumped Rod Shaped Lasers." Diss. <http://purl.fcla.edu.ucfproxy.fcla.edu/fcla/etd/CFE0000259>, University of Central Florida.

10. R.K. Sharma, C.E Bash, C.D. Patel. "Experimental Investigation of Heat Transfer Characteristics of Inkjet Assisted Spray Cooling." *ASME Heat Transfer/Fluid Eng. Summer Conf*. HT-FED04-56183. Ed. Hp labs. Charlotte, NC, US: ASME, 2004.
11. Bin He. "Spray Cooling with Ammonium Hydroxide." Masters Thesis. University of Central Florida, 2002.
12. Kelly Michael. "New Power Technologies Clear Path to Tactical Directed Energy Weapons." AFMC News Service Release. 8/July 2003. 2/4/2005 <http://www.afmc-pub.wpafb.af.mil/HQ-AFMC/PA/news/archive/2003/Jul/0709-03.htm>.
13. Rini. "Design and Fabrication of an Apparatus to Measure the Effects of Large Accelerations on Two-Phase Spray Cooling." Masters Thesis. UCF, 1997.
14. Guillermo Aguilar. *Personal Journal Publictions*. University of California, Riverside. 2/16/2005 <http://www.engr.ucr.edu/~gaguilar/PUBLICATIONS.htm>.
15. Karl Pope. *Epidermal Protection Factor - Candela's Dynamic Cooling DeviceTM*. March 1999. Candela Corporation. 2/15/2005 <http://www.lasertraining.com/med-30.htm>.
16. M.C. Shaw, J.R. Waldrop, E.R. Brown. "Enhanced Thermal Management by Direct Water Spray of High-Voltage, High Power Devices in a Three-Phase, 18-Hp AC Motor Drive Demonstration." May 29 - June 1 2002. ITHERM Conference Proceedings 8th. 2/4/2005 <http://www.ee.ucla.edu/xyz/thermal_select/ITHERM_Spray-2002-vf.pdf>. 2. 2002.

17. R. Mahajan, R. Nair, V. Wakharkar. "Emerging Directions For Packaging Technologies." *Intel Technology Journal Vol.6 Issue 2.* 6.2 May 16 2002. Intel Corp <http://developer.intel.com/technology/itj/2002/volume06issue02/art07_emergingdirections/vol6iss2_art07.pdf>.

18. K. Sienski, C. Culhane. "Advanced System Packaging for Embedded High Performance Computing." http://Www.Red-River.Com/. Ken_sienski@qmailgw.Esy.Com, Csculha@afterlife.Ncsc.Mil.

19. Loring Wirbel. "Supercomputer Project Funding Shifts Back to the Government." Cray Supercomputers & Spray Cooling. Nov 15 2001. EETimes Network. 2/4/2005 <http://www.eetimes.com/story/OEG20011115S0058>.

20. Steven Adams. "Electrical Power and Thermal Management for Airborne Directed Energy Weapons." 1/Sep 2001. *AFRL Technology Horizons*. AFRL. 2/4/2005 <http://www.afrlhorizons.com/Briefs/Sept01/PR0101.html>.

21. Steven G. Leonard, Major. "Laser Options for National Missle Defense." Maxwell Air Force Base, Alabama. Masters Thesis. April 1998. 2/4/2005 <www.fas.org/spp/starwars/program/docs/98-165.pdf>.

22. Peter Pae. *Homing In on Laser Weapons*. 20/Oct 2002. Los Angeles Times. 2/4/2005 <http://www.globalsecurity.org/org/news/2002/021020-laser1.htm>.

23. Elihu Zimet. "High-Energy Lasers: Technical, Operational, and Policy Issues." October 2002. Center for Tech. & National Security Policy. 2/5/2005 <http://www.ndu.edu/inss/DefHor/DH18/DH_18.htm>.

24. Compoundsemiconductor.net. "Alfalight Funding Will Boost Diode Laser Efficiency." 7/Oct 2003. 2/13/2005.

25. William H. Possel, Lt Col. "Lasers and Missle Defense: New Concepts for Space-Based & Ground-Based Laser Weapons." Air War College, Montgomery, Alabama. Occasional Paper No. 5. July 1998. 2/4/2005 <http://www.fas.org/spp/starwars/program/docs/occppr05.htm>.

26. High-Energy Laser Destroys Large-Caliber Rocket. "High-Energy Laser Destroys Large-Caliber Rocket." 11/May 2004. www.spacedaily.com. 2/5/2005 <http://www.spacedaily.com/news/laser-04g.html>.

27. MissileThreat.com. "Tactical High Energy Laser (THEL)." *Claremont Institute*. 5/Feb 2005. 2/5/2005 <http://www.missilethreat.com/systems/thel.html>.

28. US Army Space & Missle Defense Command. "ZEUS-HLONS HMMWV Laser Ordnance Neutralization System." March 2003. US Army. 2/5/2005 <http://www.smdc.army.mil/SMDC2004/Factsheets.html>.

http://www.llnl.gov/str/October04/Rotter.html.

29. Lawrence Livermore Labs. "Bright Future for Tactical Laser Weapons." *Www.Llnl.Gov*. April 2002. Lawrence Livermore Labs. 2/5/2005 <http://www.llnl.gov/str/April02/Dane.html>.

http://www.smdc.army.mil/FactSheets/SSL.pdf.

30. Vasileios Bouras Lt. "High Energy Lasers for Ship-Defense and Maritime Propagation." Storming Media. 2002. 2/4/2005 <http://www.stormingmedia.us/keywords/high_energy_lasers.html>.

31. NOAA. Ocean Surface Temperatures. Feb 2005. National Ocean & Atmospheric Administration. 2/5/2005 <http://www.nodc.noaa.gov/dsdt/sst_ani.htm>.

32. Boeing Corp. Home Page. 2005. Boeing Airborne Laser System Home Page. 2/5/2005 <http://www.boeing.com/defense-space/military/abl/overview.html>.

33. Raytheon Company. . 2005. 2/12/2005 <http://www.raytheon.com>.

34. Intelgurl. See for Additional Referances. 8/March 2004. 2/12/2005 <http://www.atsnn.com/story/36894.html>.

35. Jeff Hecht. . 24/July 2002. New Scientist.Com. 2/12/2005 <http://www.newscientist.com/article.ns?id=dn2585>.

36. S.M. Iden, M. S. Sehmbey, D.P. Borger. "MW Class Power System Intergration in Aircraft." *Society of Automotice Engineers* (2004).

37. Tom Benson. *Interactive Atmosphere Simulator*. 04/Mar 2004. NASA Glenn Research Center. 2/6/2005 <http://www.grc.nasa.gov/WWW/K-12/airplane/atmosi.html>.

38. Ray Preston. *Supersonic Engine Inlets*. 2004. 2/12/2005 <http://selair.selkirk.bc.ca/aerodynamics1/High-Speed/Page7.html>.

39. Mark E. Rogers, Lt Col. "Lasers in Space Technological Options for Enhancing US Military." Air War College, Montgomery, Alabama. Occasional Paper No. 2. Nov 1997. 2/4/2005 <http://www.fas.org/spp/starwars/program/occppr02.htm>.

40. Committee on Microgravity Research Space Studies Board Commission on Physical Sciences, Mathematics & Applications National Research Council. *Microgravity Research in Support of Technologies for the Human Exploration and Development of Space and Planetary Bodies*. Washington D.C: National Academy Press, 2000.

41. What is the Temperature in Space? Message posted to http://www.faqs.org/faqs/astronomy/faq/part4/section-14.html. Jlazio@patriot.Net <Mailto:Jlazio@patriot.Net>.

42. Martin Donabedian. *Spacecraft Thermal Control Handbook Volume II: Cryogenics*. El Segundo, CA: The Aerospace Press, 2003.

43. V. Shanmugasundaram, J. R. Brown, and K. L. Yerkes. "Thermal Management of High Heat-Flux Sources Using Phase Change Materials - A Design Optimization Procedure." AIAA-1997-2451. Paper presented at the Thermophysics Conference, 32nd. Atlanta, GA,: AIAA, 23-25/June, 1997.

44. NASA. *Cassini-Huygens*. Homepage. 2005. 2/6/2005 <http://saturn.jpl.nasa.gov/operations/index.cfm>.

45. L. Lin, R. Ponnappan, K. Yerkes. "Large Area Spray Cooling." *AIAA-2004-1340*. 42nd AIAA Thermophysics & Heat Transfer Conf. Reno, NV, 2004.

46. R.H. Chen, L.C. Chow, J.E. Navedo. "Effects of Spray Characteristics on Critical Heat Flux in Subcooled Water Spray Cooling." *Int. Journal of Heat Transfer & Mass Transfer* 45 (25/April 2001).

47. X.Q. Chen, L.C. Chow, M.S. Sehmbey. "Thickness of Film Produced by a Pressure Atomizing Nozzle." *30th AIAA Thermophysics & Heat Transfer Conf.* Paper No. AIAA-95-2103. San Diego, CA, 1995.

48. D.F. Young, B.R. Munson, T.H. Okiihi. *A Brief Introduction to Fluid Mechanics*. New York, NY: John Wilsey & Sons, 1997.

49. A.V. Chizhov, K. Takayoma. "The Impact of Compressible Liquid Droplets on Hot Rigid Surface." *Int. Journal Heat & Mass Transfer* 47 (2004): 1391-401.

50. Donald E. Tilton. "Spray Cooling." Diss. University Of Kentucky, 1989.

51. E Martinez, E Venkatapathy, T Oishi. "Current Developments In Future Planetary Probe Sensors For Tps." Nasa. 3/6/2005 <http://thermo-physics.arc.nasa.gov/fact_sheets/aESA_Reentry_Paper.pdf>.

BIO INFORMATION

Mr. Brian Glassman

Contact e-mails as of 2005

Briang1621@gmail.com

Briang1621@hotmail.com

Cell Phone number

USA 321-543-7165

Open to inquiries